Development of Hemocompatible Polymeric Materials for Blood-Contacting Medical Devices

by

Biyun Wu

A dissertation submitted in partial fulfillment
of the requirement for the degree of
Doctor of Philosophy
(Chemistry)
in the University of Michigan
2009

Doctoral Committee:

Professor Mark E. Meyerhoff, Chair
Professor Zhan Chen
Professor E Neil G. Marsh
Associate Professor Joerg Lahann

Grace

Alone

ACKNOWLEGDEMENTS

First and foremost, I would like to express my sincere thanks to Dr. Mark Meyerhoff, my advisor, for giving me the opportunity to be part of this exciting research. I thank him for his guidance through the past 5 years to help me grow from a new graduate student to a young scientist. I thank him for his encouragement and inspiration during the hard times of this research effort. I thank him for not only being a boss in the lab, but also a mentor in my life. All the moments in the proud Meyerhoff Lab will be treasured in my memory.

I want to also take this opportunity to acknowledge all my dissertation committee members, Dr. Zhan Chen, Dr. Joerg Lahann and Dr. Neil Marsh, for their advice and suggestions in my proposal writing, pre-doctoral scholarship application, data meeting presentation as well as this thesis preparation. I would like to give special thanks to Dr. Chen for his guidance during my first research rotation at the University of Michigan.

Sincere thanks need to be given to Ms. Diane Studzinski in Dr. Shanley's surgical research lab at Beaumont Hospital who did all the *in vitro* cell tests in this dissertation. I really appreciate Dr. Yang Wang in Dr. Prabir Roy-Chaudhury's internal medicine research lab at the University of Cincinnati for testing the systemic toxicity of

one of the polymers I synthesized. Dr. John Zhang in MC3 Inc. was very kind to perform the mechanical testing for one of the polymer films I prepared. Special thanks also must be given to Drs. Bruce Gerlitz and Brian Grinnell at Eli Lilly and Company for their preparation of human recombinant thrombomodulin, without which the second chapter of my thesis would be impossible to complete.

I am greatly indebted to Dr. Wei Tang in Dr. Raoul Kopelman's lab in the Chemistry Department at the University of Michigan for her assistance with the confocal fluorescence microscopic testing. I thank Drs. Kai Sun and Haiping Sun in the University of Michigan's Electron Microbeam Analysis Laboratory for their assistance in surface characterization with SEM and EDX. I also wish to thank Mr. Nathan Gray Lafayette and Ms. Candice Marie Hall in the Extracorporeal Membrane Oxygenation Lab at the University of Michigan Medical School for preparing the sheep blood used in my dissertation work. I am also grateful to all the people at the University of Michigan for their technical support**,** including but not limited to Mr. Ted Huston in Geological Sciences Department as well as Ms. Carol Carter and Mr. James Windak in Chemistry Department.

Over the past 5 years, Dr. Zhengrong Zhou has given me great support in my research by teaching me all the techniques required in polymer synthesis and characterization, and by inspiring me with many sparkling conversations and brilliant ideas. I also greatly appreciate his help in reviewing this thesis and previous manuscripts. I thank Dr. Kun Liu who has kindly prepared one batch of sulfonated polyurethane in 2009. I also want to express my gratitude to all the past and present members of the Meyerhoff group, including Dr. Hairong Zhang, Dr. Fenghua Zhang, Dr. Dongxuan Shen,

Dr. Yiduo Wu, Dr. Jason Bennett, Dr. Jeremy Mitchell-Koch, Dr. Wansik Cha, Dr. Sangyeul Hwang, Dr. Youngjea Kang, Dr. Melissa Reynolds, Dr. Megan Frost, Qinyi Yan, Jun Yang, Lin Wang, Laura Zimmerman, Natalie Walker, Maxim Burgman, Wenyi Cai, Teng Xue and Teng Peng. It's my great pleasure working with all these talented people and I want to give thanks to you all for your friendship.

I especially appreciate Dr. Fei Liu in the Department of Biologic and Materials Sciences at the University of Michigan Dental School for his support and encouragement throughout my thesis writing process, including the careful and efficient proof-reading of all six chapters in this dissertation. Last but not the least, special thanks will be given to my dearest mom and dad, Yaohua Shen and Weijia Wu. I thank them for bringing me into this world, for their unconditional love, and for loving me for who I am!

TABLE OF CONTENTS

LIST OF FIGURES

Figure

LIST OF SCHEMES

Scheme

LIST OF TABLES

Table

ABSTRACT

Development of Hemocompatible Polymeric Materials for Blood-Contacting Medical Devices

by

Biyun Wu

Chair: Mark E. Meyerhoff

One of the major problems of cardiovascular and other blood-contacting medical devices remains the lack of hemocompatibility of their surfaces. Hence, the research in this dissertation focuses on the development of novel multifunctional polymeric coatings that incorporate multiple antithrombogenic and/or anti-proliferative bioactive agents. The incorporated bioactive agents, whether endogenous small molecules (nitric oxide (NO)), polysaccharides (heparin), proteins (thrombomodulin (TM)), or drugs (sirolimus), are intended to function synergistically to prevent the formation of thrombus and the proliferation of smooth muscle cells (SMCs), which are considered to be two of the major causes for the failure of various blood-contacting implantable devices.

New multifunctional bilayer polyurethane (PU) coatings were developed that exhibit both controlled NO release (via use embedded diazeniumdiolate NO donors)

and surface-bound active TM or combined TM and heparin. Both TM and heparin's activity were evaluated by chromogenic assays and found to be at clinically significant levels. The NO release rate could be tuned by changing the thickness of top coatings. The duration of NO release at physiologically relevant levels (1×10^{-10} mol min^{-1} cm^{-2}) could be as long as 2 weeks.

To control the rate of NO release of polymers containing diazeniumdiolate NO donors, more stable and less toxic lipophilic tetrapenylborate species were examined to help buffer the pH in the polymeric phase of the coatings. Furthermore, in order to completely eliminate the leaching and possible toxicity issues associated with small molecules, a new sulfonated PU was synthesized with sulfonic anionic sites covalently tethered to the PU backbones as a potential replacement for borate additives. *In vitro* endothelial cell and SMC studies demonstrated that such coatings exhibit much improved biocompatibility compared to films prepared with conventional tetrakis(*p*-chlorophenyl)borate.

In addition to thrombus formation, SMC proliferation is another important cause for medical device failure, especially for stents and small-diameter vascular grafts. The use of NO, in combination with an anti-cell proliferation agent, might provide the ideal solution to reduce both clotting and restenosis risks. Thus, the first dual-functional polymeric coatings that released both sirolimus (rapamycin) and NO were prepared. NO is released at physiologically relevant levels with simultaneous release of sirolimus from 3.00 to 0.10 μg cm^{-2} h^{-1} over a period of 2 weeks. The possibility of combining catalytic NO generation and sirolimus release was also explored by doping a selenium-derivatized PU with sirolimus.

CHAPTER 1

Introduction

1.1. Challenges Inherent to Blood-Contacting Medical Devices

During the past century, the use of cardiovascular and other blood contacting biomedical devices has evolved from a mere dream to a widely adopted practice, including the use of heart valves, vascular grafts, stents, extracorporeal circuits and membrane oxygenators[1,2] (see Figure 1.1). These blood-contacting devices have saved the lives of millions of people.

However, one of the major problems of these devices remains the lack of haemocompatibility of their surafaces[3]. Some examples are the occlusion of small-diameter vascular grafts[4] and failure of blood-contacting biosensors[5, 6] due to thrombus formation on the device surface. Other examples include embolism and thrombocytopenia (platelet consumption[7]) caused by the blood-contacting biomedical devices. Thus, long term, in some cases even life-long, administration of anticoagulant drugs is required[2]. Furthermore, the possibility of hemorrhage will be greatly increased as a side effect of using such drugs[8].

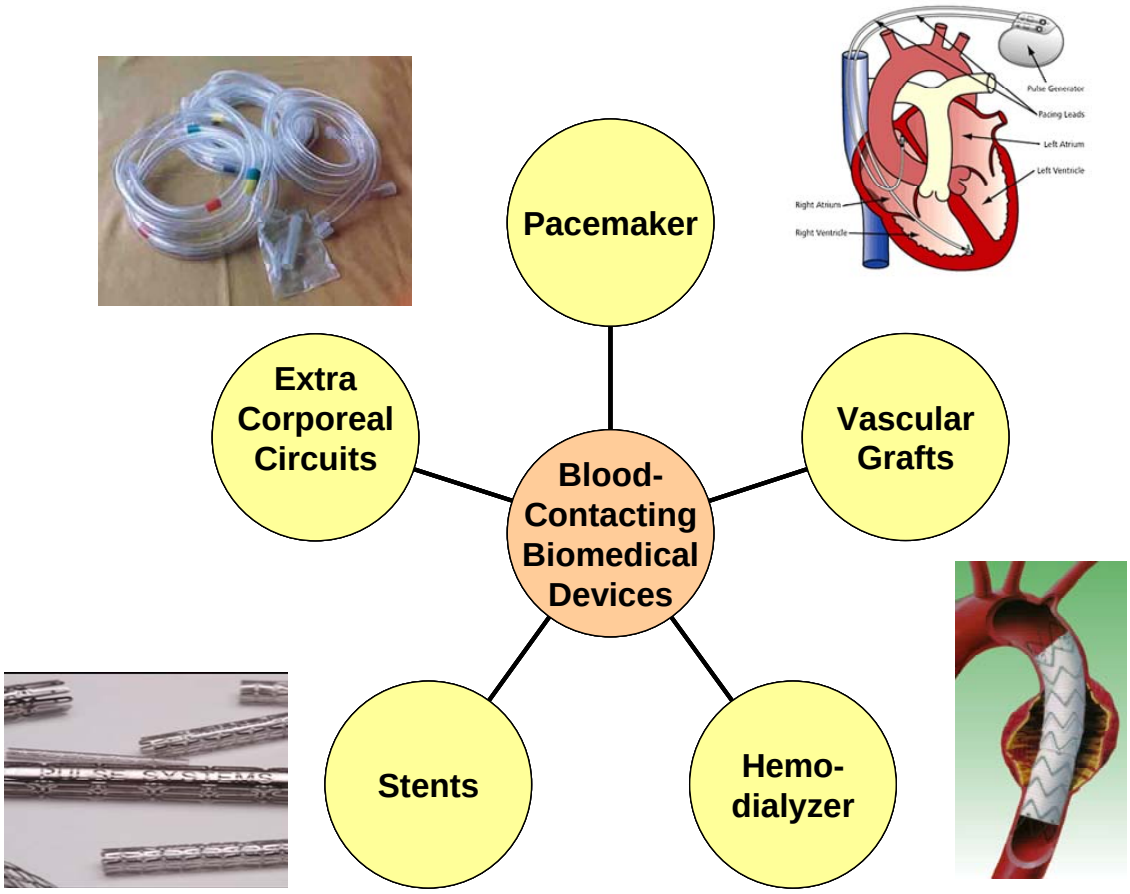

Figure 1.1. Examples of blood-contacting medical devices.

In a review paper published in *J. Biomater. Sci.: Polymer Edn.* in 2000[2], Dr. Ratner clearly expressed his concerns on the significant challenges facing current medical devices:

- Small-diameter vascular grafts fail early due to thrombolic occlusion;
- Embolic complications are noticed with artificial hearts;
- Embolic problems frequently occur with catheters;

- Non-tissue heart valves require lifelong anticoagulation;
- Blood contacting biosensors fail due to thrombus accumulation;
- Long-term implants are seen to be continuously platelet reactive;
- Significant blood damage is observed during hemodialysis and extracorporeal blood oxygenation;
- Venous prostheses cannot be made at all;
- Endoluminal stents are associated with blood interaction problems.

Pader and Schoen have also summarized the major complications of cardiovascular devices, and these are listed in Table 1.1. Indeed, lack of hemocompatibility still remains one of the biggest hurdles associated with blood-contacting medical devices. The focus of this dissertation is to develop polymeric coatings through various approaches that can potentially reduce or even eliminate the adverse effects caused by blood-device interactions.

Table 1.1. Complications of cardiovascular devices (adapted from Padera and Schoen's book chapter 'Carciovascular Medical Devices'[9] in *Biomaterials Sciences – An Introduction to Materials in Medicine, 2nd Ed.*).

Heart Valve Prostheses	**Vascular Grafts**	**Circulatory Assist Devices**
Thrombosis/thromboembolism	Thrombosis/thromboembolism	Thrombosis/thromboembolism
Anticoagulant-related hemorrhage	Infection	Endocarditis
Prosthetic valve endocarditis	Erosion into adjacent structures	Extraluminal Infection
Intrinsic structural deterioration (wear, fracture, popper escape, cuspal tear, calcification)	Perigraft seroma	System component fractures
	(Anastomotic) false aneurysm	Bladder/valve calcification
Nonstructural dysfunction (pannus overgrowth, tissue or suture entrapment, paravalvular leak, inappropriate sizing, hemolytic anemia, noise)	(Anastomotic) intimal fibrous hyperplasia	Hemolysis
	Mechanical failure	Mechanical failure

1.2. Inspiration from Endothelium – the Natural Nonthrombogenic 'Coating'

1.2.1. Thrombus Formation

The formation of thrombus is a complex process that involves the participation of a large number of cells, tissue factors, enzymes and their cofactors[10, 11]. Vascular damage or direct contact between foreign objects and blood initiate the coagulation cascade, the first step of which is the activation of a zymogen, factor IX (FIX), to its active counterpart, factor IXa (FIXa). FIXa then activates factor X (FX) to factor Xa (FXa), which in turn activates prothrombin (FII) to form thrombin (FIIa), the pivotal agent in the process of thrombosis. At the same time, proteins adsorb onto the surface of the injured vessel or the foreign object, which is followed by platelet adhesion. The adhered platelets become activated, and then form platelet aggregates[12]. Thrombin activates fibrinogen to form the insoluble cross-linked fibrin, which, together with activated platelets and red blood cells, ultimately leads to thrombus formation[4]. Scheme 1.1 illustrates how the coagulation cascade (initiated by either intrinsic or extrinsic pathway) and the activation of platelets interact with each other and form thrombi as a result.

Platelet adhesion/activation and thrombus formation do not readily occur on the surface of a healthy endothelium that lines the inner walls of all blood vessels. The excellent thromboresistancy of endothelial cells (ECs) is largely attributed to both secreted agents (nitric oxide (NO)[13], prostacyclin[14], plasminogen[15], antithrombin III (AT III)[16]) and membrane-bound species (heparan sulphate (HS)[17], thrombomodulin (TM)[18]). Both NO and prostacyclin have long been recognized for their anti-platelet activity, while heparin[19] (an HS analogue) and TM are well known for their anticoagulant function.

Scheme 1.1 also shows how NO, HS and TM, as endogenous antiplatelet and anticoagulant agents, check the coagulation cascade and platelet activation/aggregation process so that thrombi do not form on healthy endothelium surfaces.

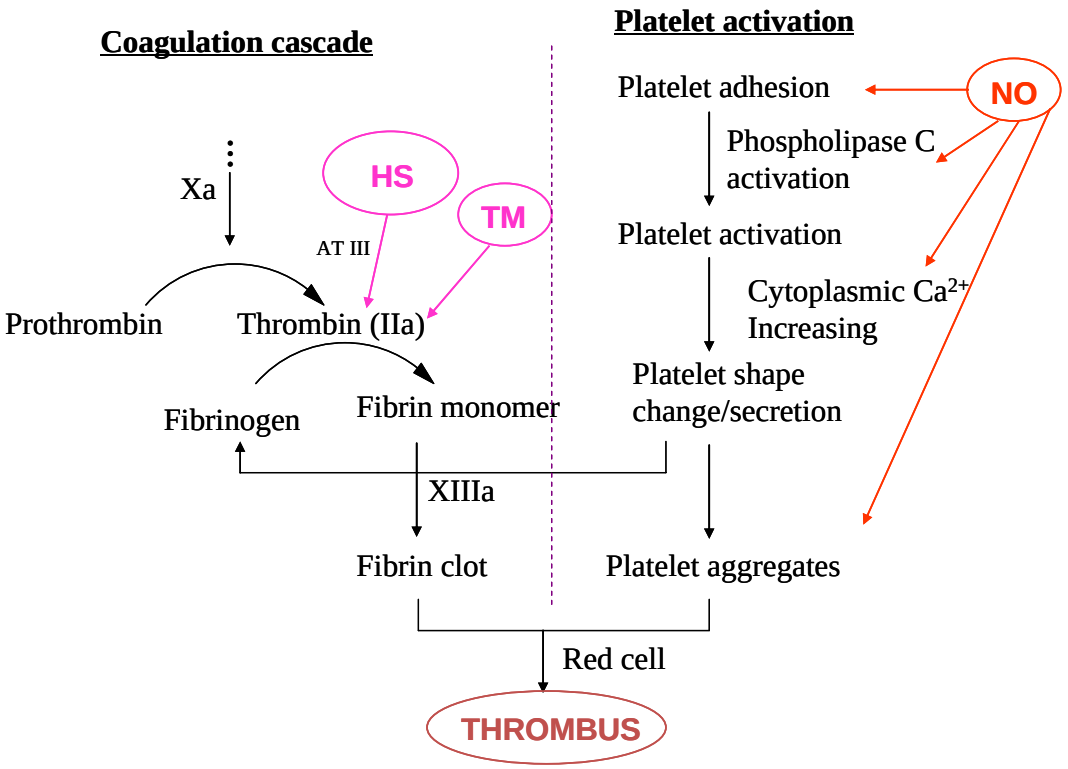

Scheme 1.1. The formation and inhibition (by HS, TM and NO) of thrombus.

1.2.2. Heparan Sulfate and Heparin

Heparan sulfate is a complex and highly active biopolymer that is synthesized as an alternating copolymer of hexuronic acid and glucosamine and modified at various positions with sulfate[20] (Figure 1.2A), which affects and controls its biological activities[21]. Heparin is considered as an oversulfated intracellular variant of the ubiquitous HS. It

was first discovered in 1916 as an inhibitor of coagulation and was further developed to become an anticoagulant drug in the mid 1930s. It has been used as an anticoagulant drug for over 70 years[22]. Indeed, heparin is second only to insulin as a very successful natural therapeutic agent. It received its name, heparin, because hepatic tissue was a common and abundant source from which it was first isolated and studied[17].

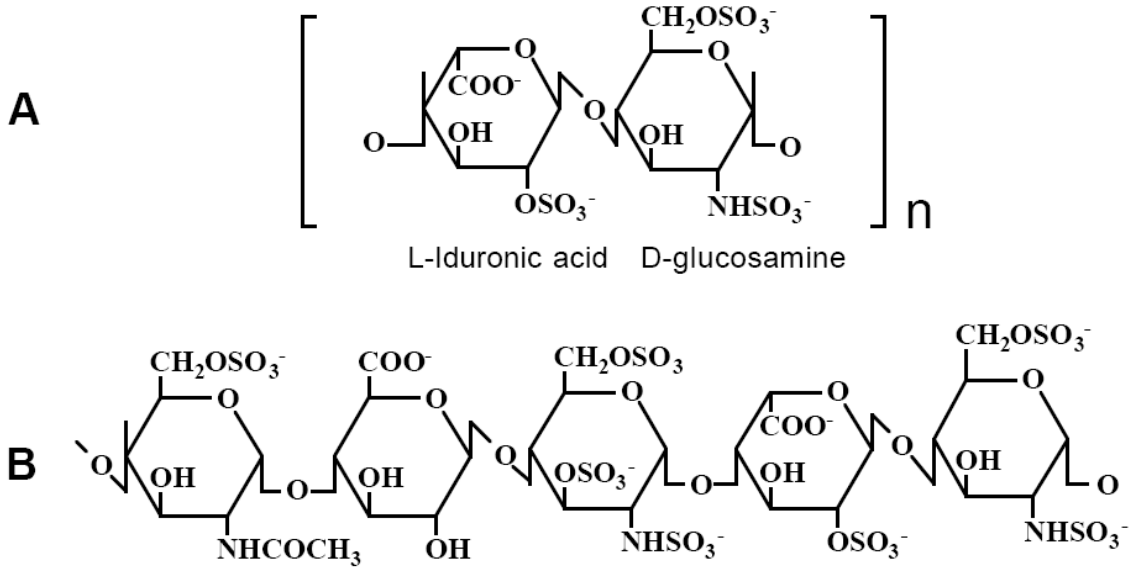

Figure 1.2. Heparin structure (adapted from 'Heparin Momograph'[20] by Chromogenix). Heparin is a heterogenous mixture of polysaccharides, whose chains are made up of alternating 1 to 4 linked, sulfated monosaccharide residues of *L*-iduronic acid and *D*-glucosamine. **A** – the most frequent type of disaccharide unit, representing up to 90 % of the structure of beef-lung heparin, and up to 70% of pig-mucosa heparin; **B** – the unique pentasaccharide binding site for AT III which occurs in about one-third of the heparin chains.

Both heparin and HS act as a cofactor of AT III in the inhibition of various enzymes in the coagulation cascade, but primarily thrombin and FXa (Scheme 1.1). A specific pentasaccharide sequence[20] (Figure 1.2B) of heparin binds to AT III to induce a

conformational change in AT III, which, in turn, accelerates the binding and hence the inhibition of certain proteases by AT III[19, 22] (Figure 1.3).

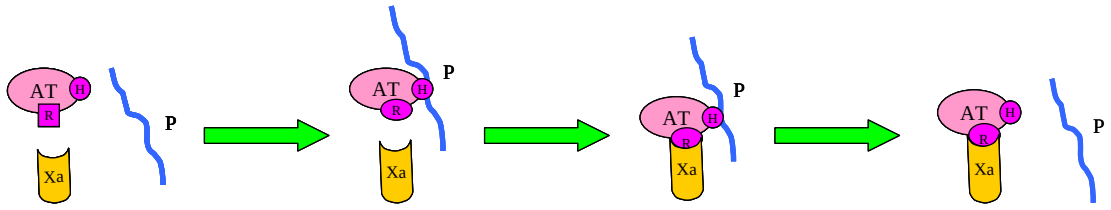

Figure 1.3. Inhibition of FXa by AT III catalyzed by heparin. **[H]** – heparin binding site; **[R]** – reactive site in antithrombin; **[P]** – the unique antithrombin binding sequence of heparin. Binding to this sequence induces a conformational change in antithrombin, shown here by the square changing to a circle, which facilitates its reaction with its target proteases. The end result is a complex of heparin, AT III, and the now inactive FXa.

1.2.3. Thrombomodulin

Thrombomodulin is named after its bioactivity as a 'thrombin modulator'[23]. It is a transmembrane protein with a molecular weight of 74 kDa[24] (Figure 1.4[25]). The mature TM molecule consists of 557 amino acid residues and usually has a chondroitin sulfate moiety attached to its Ser/Thr-rich domain[26]. There are approx. 100,000 TM molecules on the surface of every endothelial cell. Once thrombin, the pivotal protein in the coagulation cascade, binds to TM on the surface of the EC layer, thrombin's fibrinogen-cleaving activity is inhibited. This thrombin-antithrombin reaction is accelerated by the existence of the chondroitin sulfate moiety that is attached to the Ser/Thr-rich domain[26].

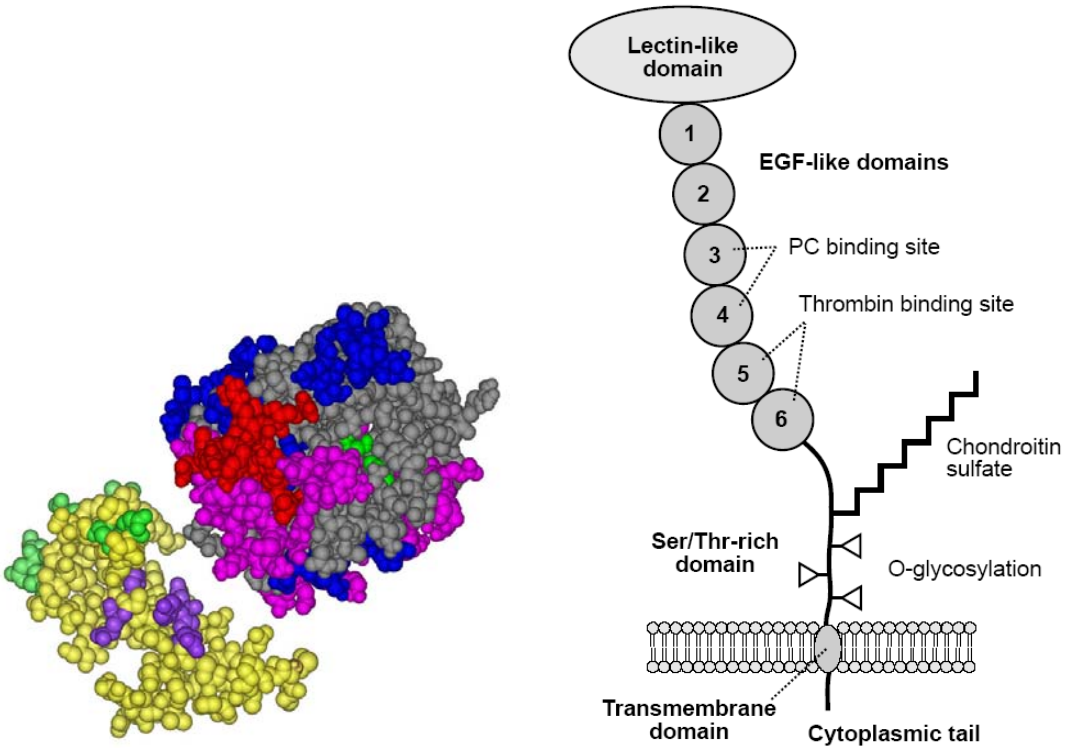

Figure 1.4. Two representations of TM structure. **Left** – Solvent accessible surface representation of TM colored by residue type (red – acidic residues, blue – basic residues, green – polar residues, grey – nonpolar residues) (adapted from Zhengrong Zhou's PhD dissertaion[25]); **Right** – domain representaion of TM: The mature TM molecule consists of 557 amino acids residues arranged in a lectin-like domain, six EGF-like domains, a Ser/Thr-rich domain (usually with an attached chondritin sulfate moiety), a transmembrane domain, and a short cytoplasmic tail (adapted from Chromogenix 'Protein C Product Monograph.'[26]).

In addition, this binding will also alter thrombin from a procoagulant to an anticoagulant by activating protein C (PC) to initiate the PC anticoagulation pathway[15]. Activation of PC by thrombin alone is slow and has no physiological function. However, when thrombin binds to TM, a 20,000-fold increase in the PC activation rate can be observed (Figure 1.5). In summary, the three anticoagulant activities of TM are listed as follows[27]:

- Direct anticoagulant activity by preventing the cleavage of fibrinogen by thrombin;
- AT III-dependent anticoagulant activity by promoting the inactivation of thrombin via AT III;
- PC activation cofactor activity by promoting the activation of PC via thrombin (see Figure 1.5).

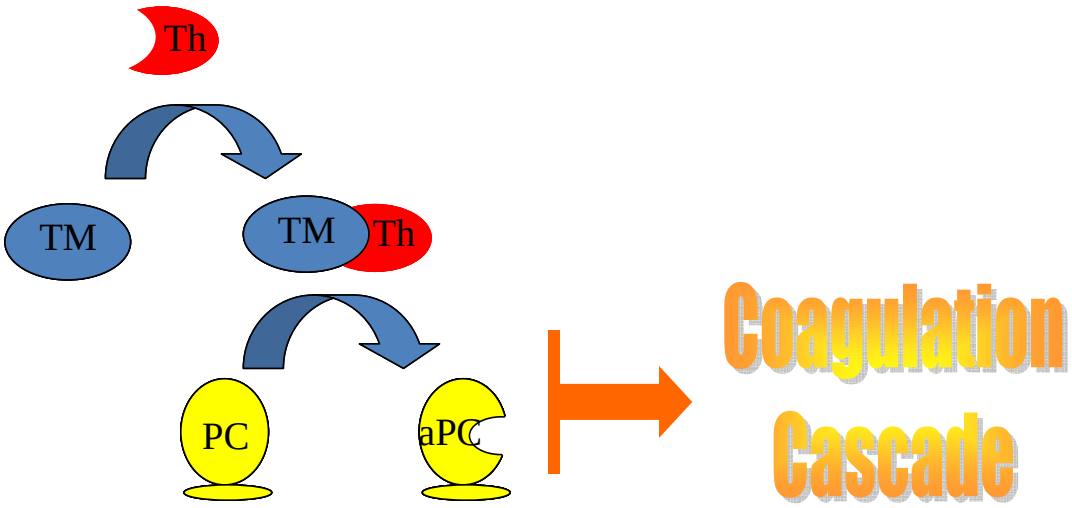

Figure 1.5. TM binds to thrombin and greatly enhances its PC activation activity.

1.2.4. Nitric Oxide

Until the mid 1980s, NO was regarded as an atmospheric pollutant and bacterial metabolite. Twenty years later, NO is highly recognized for its indispensable functions in various biological processes including neurotransmission[28,29], vasodilation[30], bronchodilation, modulation of intestinal motility, as well as contraction of heart and skeletal muscle[31].

Nitric oxide is endogenously produced in many cells in the body. In mammalian ECs, NO is synthesized from *L*-arginine by NO synthase, a calcium dependent enzyme[32, 33]. Its basal flux level from the EC surface[34] is estimated to be 1×10^{-10} mol cm^{-2} min^{-1} (see Figure 1.6). It is an extremely reactive free radical (•N=O) with a less-than-one-second lifetime in blood owing to its rapid reaction with oxyhemoglobin[13].

Nitric oxide can diffuse to the adjacent blood and the nearby platelets to inhibit both platelet adhesion to endothelium as well as platelet activation[13] (see Figure 1.6). Once NO diffuses into platelets, particularly as they approach the surface of the EC lining of the vessel, it activates guanalate cyclase, which, in turn, increases the intracellular level of cyclic guanosine monophosphate (cGMP). Cyclic guanosine monophosphate further decreases the intracellular Ca^{2+} level and inhibits the activity of phospholipase C, the two key substances required for platelet activation[35-37] (see Scheme 1.1). Nitric oxide can also down-regulate the functions of some platelet receptors, which in turn prevents platelet aggregation and adhesion onto blood vessel walls. Beyond binding to hemoproteins, NO also reacts with thiol species (RSHs) in the blood, resulting in the formation of *S*-nitrosothiols (RSNO). This formation prolongs the half-life and biologic activity of NO and allows for further platelet inhibition by RSNOs.

Nitric oxide can also diffuse into and relax the underlying smooth muscle cells (SMCs) which, in turn, dilates the artery and increases the blood flow (Figure 1.6). When NO reaches the underlying vascular SMCs, it binds to the heme groups of the enzyme guanylate cyclase. This results in an increased production of cGMP. The increased level of cGMP leads to vascular relaxation that allows the vessel to dilate and thereby lowers blood pressure[38].

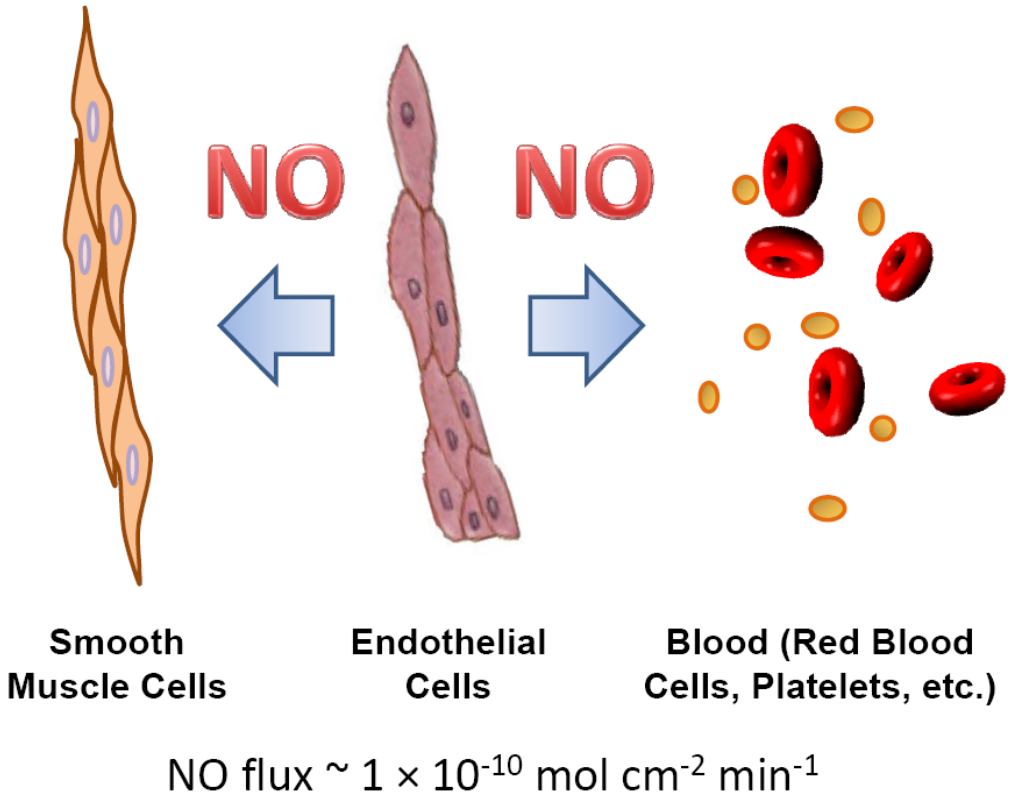

Figure 1.6. NO is synthesized in ECs by NOS. It then diffuses toward platelets and red blood cells in adjacent blood stream, as well as to the underlying SMCs to dilate the walls of the blood vessels. The gap between SMC layer and EC layer is exaggerated.

In addition to its anti-platelet and vasodilation activities, NO is also known to effectively inhibit SMC proliferation[39] and reduce restenosis, which are caused by the damage of the fragile EC layer during the process of implantation of certain medical devices[40] (e.g., stents, vascular grafts). Furthermore, it is known that NO plays a crucial role in wound healing, and down regulates mediators of inflammatory response such as cytokines, chemokines, and growth factors that signal the recruitment of neutrophils and macrophages to the implant site[41-43]. NO also promotes angiogenesis, an important component of the normal wound healing process[44, 45].

1.2.5. Strategies to Prepare Bioactive Nonthrombogenic Polymeric Surfaces

In addition to heparin, TM and NO, there exist many other anticoagulant and antiplatelet agents that work synergistically to prevent the formation of blood clots. The following is a list of representative, not exhaustive, approaches that have been adopted to improve the nonthrombogenicity of device surfaces:

- Phospholiplid-mimicking surfaces[46];
- Ionically-bound heparin and controlled release systems[47];
- Surfaces with covalently-bound heparin[48] (see Figure 1.7);
- Hirudin-immobilized surfaces[49];
- Thrombomodulin-immobilized surfaces[50, 51];
- Incorporate prostacyclin into polymer matrices for controlled release[52];
- Aspirin-releasing polymer membranes[53];
- Immobilization of fibrinolytic agents – urokinase[54], plasminogen[55] and lysine[56];

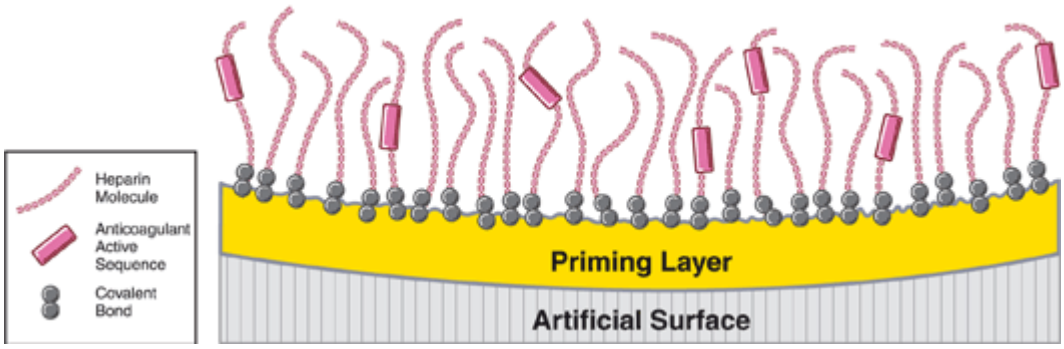

Figure 1.7. Medtronic Carmeda® BioActive Surface with heparin molecules that are covalently bonded into the surface using an end-point attached method (adapted from product website[48]).

As has been stated by Sefton and Gemmell[56], it is impossible to predict which approach will ultimately be successful. However, combining approaches to address thrombin production and platelet activation may lead to new opportunities. Indeed, it is impossible for each of the individual agents to perform the whole spectrum of the thromboresistant functionalities of the healthy endothelium. Such a surface lined with ECs presents all the anticoagulant agents not only simultaneously but also in a well regulated way. Thus, the first part of this dissertation focuses on preparing EC-mimicking polymeric coatings combining two or more anticoagulant agents (NO, heparin, TM) that possess desirable thromboresistance properties.

1.3. Combining Antithrombogenicity and Anti-SMC Proliferation

1.3.1. Drug-Eluting Stent

Thrombosis is not the only problem associated with blood-contacting medical devices. In many cases, SMC activation can be the problem as well. In the treatment of coronary artery disease, balloon angioplasty and stenting have become common procedures for the relief of arterial stenosis and to restore normal blood flow. Over time, this traditional bare-metal stent (BMS) used in the procedure is fully endothelialized. In roughly a third of bare-metal stenting cases, however, restenosis occurs. Tissue engulfs the stent, once more reducing the blood flow in the stented vessel, which can lead to subsequent coronary symptoms (see Figure 1.8). This type of restenosis is believed to be the result of an inflammatory response to injury from the initial angioplasty procedure and to the BMS itself[57].

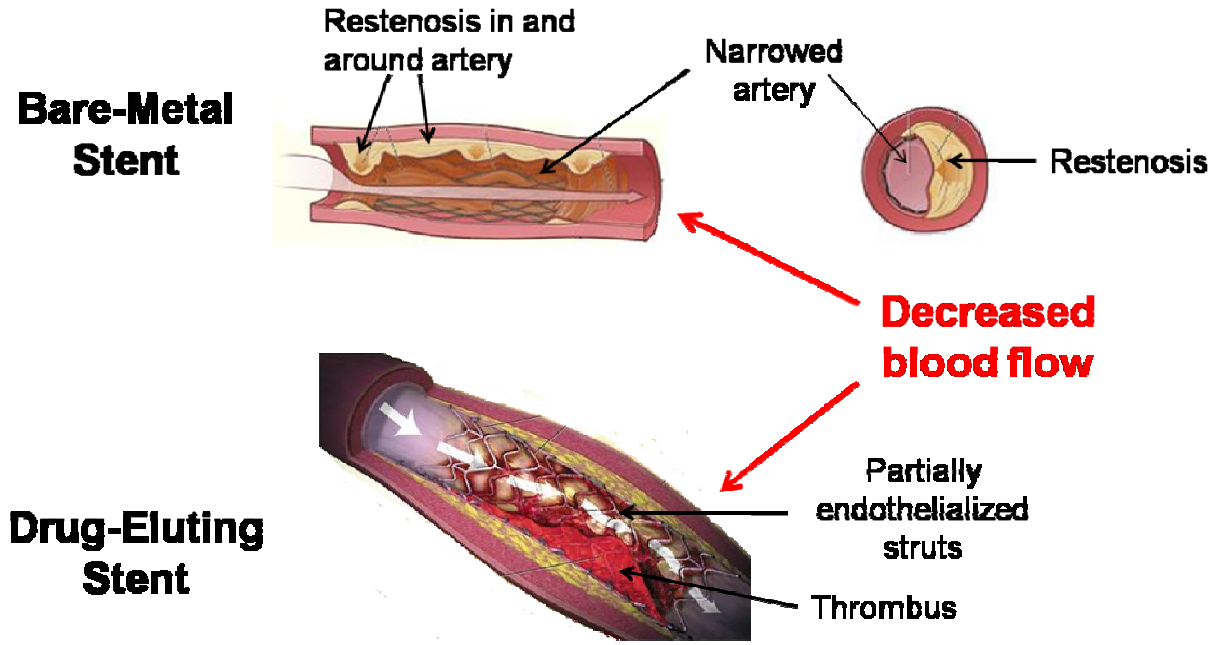

Figure 1.8. Restenosis in traditional BMSs vs. late thrombosis in DESs.

Drug-eluting stents (DESs) were developed to prevent the kind of restenosis seen with BMSs. Drug eluting stents differ from BMSs mainly in that they are coated with a polymer containing a drug meant to interfere with the process of restenosis. Sirolimus (rapamycin) and paclitaxel (Figure 1.9) are the most widely used drugs on DESs. The drugs are released from the polymeric matrices that cover the stainless-steel stents in a controlled way to address the in-stent restenosis problem caused by stenting-induced biological responses to the vessel wall injury[58-62]. Over time, these drugs inhibit the proliferation and migration of SMCs and inflammatory cells responsible for restenosis. Table 1.2 lists some of the representative DESs that have been clinically approved and are commercially available.

Table 1.2. Information of some representative clinically approved DESs that are currently commercially available.

DES	Manufacturer	Delivery Platform	Polymer Coating	Drug
Cypher[63]	Cordis, Johnson & Johnson	316L Stainless Steel BX Velocity Stent	Three-layer coating (base coat – Parylene C; main coat – PEVA (polyethylene-co-vinyl acetate) & PBMA (poly n-butyl methacrylate); top coat – drug free PBMA)	Sirolumus
Promus[64, 65]	Distributed by Boston Scientific/Manufactured by Abbott (Xience V)	L605 cobalt chrome alloy Multi-Link Vision stent	Mixture of PBMA and PVDF-HFP (a copolymer of vinylidene fluoride and hexafluoropropylene)	Everolimus
Taxus Express[2]/Liberte /Liberte Atom[66-68]	Boston Scientific	316L Stainless Steel Express/Liberte stent	Single-layer Translute polymer (poly(styrene-b-isobutylene-b-styrene) coating	Paclitaxel
Endeavor[69]	Medtronic	Cobalt alloy Driver stent	Phosphorylcholine polymer	Zotarolimus

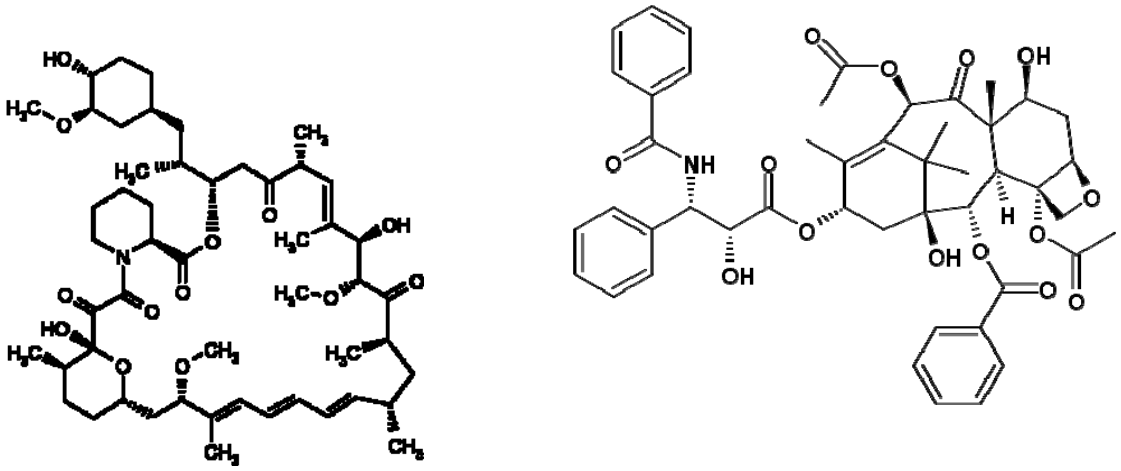

Figure 1.9. Structures of Sirolimus (**Left**) and Paclitaxel (**Right**).

1.3.2. Problems with DES

Unfortunately, DESs do not provide a benefit relative to BMSs in reducing/preventing sub-acute thrombosis (SAT). Therefore, patients must be placed on anticoagulation therapy after stent implantation, by taking antiplatelet drug for up to six months[70]. Recent findings have suggested an increased risk of late stage thrombosis associated with drug-eluting stents due to the incomplete endothelialization on the surface of the struts of the stents since these drugs can also retard the migration and proliferation of ECs[71]. For example, after reviewing 4-year follow-up data on its sirolimus-eluting Cypher stents, Cordis Corporation (Johnson & Johnson) found a higher incidence of thrombosis (which may increase the risk of myocardial infarction and death) in the Cypher group compared to the BMS control group[71]. More and more evidence indicates that the drugs can prevent or delay full endothelialization of the stent, allowing platelets, red blood cells, fibrin and white blood cells to adhere to the exposed struts of

the stents, leading to late-stage thrombosis in a small fraction of patients[57]. The resulting thrombi can lead to narrowing or complete occlusion of the lumin which may then lead to myocardioinfarction. Hence, it is now recognized that using anti-restenotic drugs alone may only solve part of the issues associated with stent placement. Furthermore, similar thrombosis and SMC proliferation problems exist in the case of implanted vascular grafts as well.

1.3.3. Combining NO and Anti-SMC Proliferation Drug – A Possible Solution

As has been stated before, in addition to its anti-platelet and vasodilation activities, NO is also known to effectively inhibit SMC proliferation[39,40] and reduce restenosis. Furthermore, it is known that NO plays a crucial role in wound healing, and down regulates mediators of inflammatory response[41-43]. Some researchers have also found that NO release can enhance EC growth on surfaces. In two studies reported by Dr. West's group in Rice University, NO releasing PUs promoted endothlialization and suppressed platelet adhesion[72,73]. Hence, NO release coatings may reduce the possibility of stent thrombosis. If this is true, then the presence of NO release would prevent thrombosis early on, and if EC growth is in fact promoted, it would help solve the fundamental problem associated with drug eluting stents!

Hence, the use of NO, a naturally occurring anti-thrombotic/anti-platelet/pro-endothelialization agent, in combination with sirolimus, an anti-cell proliferation agent, may provide the ideal solution to reduce both clotting and restenosis risk for stents as well as vascular grafts and other implanted medical devices. To prepare polymeric coatings based on this multivalent functionality is the second focus of this dissertation.

The new coatings can potentially suppress the migration and proliferation of SMC and at the same time, exhibit decreased thrombus formation and enhanced endothelialization.

1.4. Statement of Dissertation Research

The primary goal of the research described in this dissertation is to develop and investigate novel multifunctional polymeric coatings that incorporate multiple antithrombogenic and/or anti-proliferative bioactive agents. These bioactive agents, whether endogenous small molecules (NO), polysaccharides (heparin), proteins (TM), or drugs (sirolimus), are intended to function synergistically to prevent the formation of thrombus and the proliferation of SMCs.

In Chapter 2, new polymeric coatings are reported that exhibit both controlled NO release and surface-bound active TM or combined TM and heparin. These multifunctional bilayer polymeric coatings were prepared to more closely mimic the nonthrombogenic properties of the endothelium by multiple complementary anti-thrombotic mechanisms based on the anti-platelet activity of NO and the anticoagulant ability of immobilized heparin and TM. This work has been published in *Biomaterials* in 2007[74]. It has also been presented at 3 local and national conferences[75-77].

Chapter 3 describes the first dual-functional polymeric coating that releases both sirolimus and NO. The use of NO, in combination with an anti-cell proliferation agent may provide the ideal solution to reduce both clotting and restenosis risk for stents as well as vascular grafts and other implanted medical devices. This work has been presented at 3 local and national conferences[78-80].

As we moved forward with *in vitro* cell testings of some of the NO release coatings, the toxicity of the borate additive (lipophilic anionic species used to sustain the NO flux) was discovered and as a result, efforts were undertaken to find a more stable and lipophilic borate species to greatly reduce the problems of degradation and leaching. This is reported in Chapter 4. Furthermore, also described in Chapter 4, a sulfonated polyurethane was synthesized with sulfonic anionic sites chemically tethered to the polymer backbones to completely eliminate the leaching and possible toxicity issue associated with using small borate derivatives. *In vitro* EC and SMC studies have proved that such coatings indeed show much improved biocompatibility. This work has been presented at 3 local and national conferences[81-83].

Another approach to achieve sustained NO release is to use endogenous NO donors (RSNO species) that are circulating in our blood stream. In Chapter 5, the synthesis of selenium-derivatized polyurethanes is described, and coatings made from such polymers are shown to exhibit prolonged NO-generating capability in the presence of RSNO species that are constantly generated *in vivo*. The thickness of such coatings could ultimately be decreased significantly which would make them more applicable to the polymeric coating matrices of DESs and other medical devices in which thinner coatings are preferred. Indeed, this chapter reports the first dual-functional polymeric coating that can both generate NO from endogeneous RSNO species and simultaneously release sirolimus at a controlled rate. The new coatings can potentially suppress SMC proliferation and thrombosis, as well as facilitate endothelialization at a given implant site. This work has been presented at 2 national conferences[84,85].

1.5. References

1. Peppas, N.A.; Langer, R. 'New challenges in biomaterials.' *Science* **1994,** 263, 1715-1720.

2. Ratner, B.D. 'Blood compatibility - a perspective.' *J. Biomater. Sci-Polym. E* **2000,** 11, 1107-1119.

3. Xue, L.; Greisler, H.P. 'Biomaterials in the development and future of vascular grafts.' *J. Vasc. Surg.* **2003,** 37, 472-480.

4. Brash, J.L. 'Exploiting the current paradigm of blood–material interactions for the rational design of blood-compatible materials.' *J. Biomater. Sci. Polymer Edn.* **2000,** 11, 1135–1146.

5. Frost, M.C.; Meyerhoff, M.E. 'Implantable chemical sensors for real-time clinical monitoring: Progress and challenges.' *Curr. Opin. Chem. Biol.* **2002,** 6, 633–641.

6. Frost, M.C.; Batchelor, M.M.; Lee, Y.; Zhang, H.; Kang, Y.; Oh, B.; Wilson, G.S.; Gifford, R.; Rudich, S.M.; Meyerhoff M.E. 'Preparation and characterization of implantable sensors with nitric oxide release coatings.' *Microchem. J.* **2003**, 74, 277–288.

7. Cholakis, C.H.; Zingg, W.; Sefton, M.V. **'**Effect of heparin-pva hydrogel on platelets in a chronic canine arterio-venous shunt.' *J. Biomed. Mater. Res.* **1989**, 23, 417-441.

8. Kidane, A.G.; Salacinski, H.; Tiwari, K.A.; Bruckdorfer, R.; Seifalian, A.M. 'Anticoagulant and antiplatelet agents: Their clinical and device application(s) together with usages to engineer surfaces.' *Biomacromolecules* **2004**, 5, 798-813.

9. Padera, R.F.; Schoen, F.J. 'Chapter 7.3 – Cardiovascular Medical Devices.' *Biomaterials Sciences – An Introduction to Materials in Medicine (2nd Ed.)* Elsevier, **2004.**

10. Adcock, D.M. 'The revised model of blood coagulation.' *Clin. Hemostasis Rev.* **2002**, 16, 1-5.

11. Furie, B.; Furie B.C. 'Mechanisms of thrombus formation.' *N. Eng. J. Med.* **2008,** 359, 938-949.

12. Sefton, M.V.; Gemmell, C.H.; Gorbet, M.B. 'What really is blood compatibility?' *J. Biomater. Sci. Polymer Ed.* **2000**, 11, 1165-1182.

13. Moncada, S.; Palmer, R.M.J.; Higgs, E.A. 'Nitric-oxide – physiology, pathophysiology, and pharmacology.' *Pharmacol. Rev.* **1991,** 43, 109-142.

14. Vane, J.R.; Botting, R.M. 'Pharmacodynamic profile of prostacyclin.' *Am. J. Cardiol.* **1995,** 75, A3-A10.

15. Woodhouse, K.A.; Weitz, J.I.; Brash, J.L. 'Lysis of surface-localized fibrin clots by adsorbed plasminogen in the presence of tissue plasminogen activator.' *Biomaterials* **1996,** 17, 75-77.

16. Hoylaerts, M.; Owen, W.G.; Collen, D. 'Involvement of heparin chain-length in the heparin-catalyzed inhibition of thrombin by antithrombin-III.' *J. Biol. Chem.* **1984**, 259, 5670-5677.

17. Whitelock, J.M.; Iozzo, R.V. 'Heparan sulfate: A complex polymer charged with biological activity.' *Chem. Rev.* **2005,** 105, 2745-2764.

18. Esmon, C.T. 'The roles of protein-C and thrombomodulin in the regulation of blood-coagulation.' *J. Biol. Chem.* **1989**, 264, 4743-4746.

19. Munoz, E.M.; Linhardt, R.J. 'Heparin-binding domains in vascular biology.' *Arterioscl. Throm. Vas.* **2004,** 24, 1549-1557.

20. Chromogenix 'Heparin Product Monograph.'

21. Lindahl, U.; Kusche-Gullberg, M.; Kjelle´n, L. **'**Regulated diversity of heparan sulfate.' *J. Biol. Chem.* **1998,** 273, 24979-24982.

22. Monien, B.H.; Cheang, K.I.; Desai, U.R. 'Mechanism of poly(acrylic acid) acceleration of antithrombin inhibition of thrombin: Implications for the design of novel heparin mimics.' *J. Med. Chem.* **2005**, 48, 5360-5368.

23. Esmon, N.L.; Owen, W.G.; Esmon, C.T. 'Isolation of a membrane-bound cofactor for thrombin-catalyzed activation of protein-C.' *J. Biol. Chem.* **1982,** 257, 859-864.

24. Marconi, W.; Piozzi, A.; Romoli, D. 'Preparation and evlauation of polyurethane surfaces containing plasminogen.' *J. Biomater. Sci.: Polymer Ed.* **1996**, 8, 237-249.

25. Zhou, Z. 'Development of Novel Nitric Oxide Releasing Materials and Polymeric Coatings for Blood Contacting Biomedical Applications.' *Ph.D. Dissertation*, **2006**, University of Michigan, Ann Arbor, MI.

26. Chromogenix 'Protein C Product Monograph**' 1995.**

27. Bourin, M.C.; Ohlin, A.K.; Lane, D.A.; Stenflo, J.; Lindahl, U**. '**Relationship between anticoagulant activities and polyanionic properties of rabbit thrombomodulin.' *J. Biol. Chem.* **1988,** 263, 8044-8052.

28. Bredt, D.S.; Snyder, S.H. 'Nitric oxide, a novel neuronal messenger.' *Neuron* **1992**, 8, 3-11.

29. Bredt, D.S.; Hwang, P.M.; Snyder, S.H. 'Localization of nitric oxide synthase indicating a neural role for nitric oxide.' *Nature* **1990**, 347, 768-770.

30. Maragos, C.M.; Morley, D.; Wink, D.A.; Dunams, T.M.; Saavedra, J.E.; Hoffman, A.; Bove, A.A.; Isaac, L.; Hrabie, J.A.; Keefer, L.K. 'Complexes of ·NO with nucleophiles as agents for the controlled biological release of nitric oxide. Vasorelaxant effects.' *J. Med. Chem.* **1991,** 34, 3242-3247.

31. Feelisch, M.; Stamler, J. S. *Methods in Nitric Oxide Research* John Willey and Sons Ltd.: West Sussex, **1996**.

32. Ignarro, L.J.; Buga, G.M.; Wood, K.S.; Byrns, R.E.; Chaudhuri, G. 'Endothelium-derived relaxing factor produced and released from artery and vein is nitric oxide.' *Proc. Natl. Acad. Sci. U. S. A.* **1987**, 84, 9265-9269.

33. Palmer, R.M.J.; Ferrige, A.G.; Moncada, S. 'Nitric oxide release accounts for the biological activity of endothelium-derived relaxing factor.' *Nature* **1987**, 327, 524-526.

34. Vaughn, M.W.; Kuo, L.; Liao, J.C. 'Estimation of nitric oxide production and reaction rates in tissue by use of a mathematical model.' *Am. J. Physiol.* **1998,** 274, H2163-H2176.

35. Colman, R.W. 'Chapter 3 Mechanisms of thrombus formation and dissolution.' *Cardiovasc. Path.* **1993**, 2, S23-S31.

36. Missirlis, Y.F.; Wautier, J.L. *The Role of Platelets in Blood-Biomaterial Interactions* Kluwer Academic Publishers: Boston, **1993.**

37. Kroll, M.H.; Sullivan, R. In *Thrombosis and Hemorrhage* Loscalzo, J.; Schafer, A. I. Eds. Williams & Wilkins: Baltimore, **1998**, 261-291.

38. Moncada, S.; Radomski, M.W.; Palmer, R.M.J. 'Endothelium-derived relaxing factor: Identification as nitric oxide and role in the control of vascular tone and platelet function.' *Biochem. Pharmacol.* **1988**, 37, 2495-2501.

39. Chen, C.Y.; Hanson, S.R.; Keefer, L.K.; Saavedra, J.E.; Davies, K.M.; Hutsell, T.C.; Hughes, J.D.; Ku, D.N.; Lumsden, A.B. 'Boundary Layer Infusion of Nitric Oxide Reduces Early Smooth Muscle Cell Proliferation in the Endarterectomized Canine Artery.' *J. Surg. Res.* **1997**, 67, 26-32.

40. Groves, P.H.; Banning, A.P.; Penny, W.J.; Newby, A.C.; Cheadle, H.A.; Lewis, M.J. 'The effects of exogenous nitric oxide on smooth muscle cell proliferation following porcine carotid angioplasty.' *Cardiovasc. Res.,* **1995**, 30, 87-96.

41. Schwentker, A.; Vodovotz, Y.; Weller, R.; Billiar, T.R. 'Nitric oxide and wound repair: Role of cytokines?' *Nitric Oxide*, **2002**, 7, 1-10.

42. Witte, M.B; Barbul, A. 'Role of nitric oxide in wound repair.' *Am. J. Surg.*, **2002**, 183, 406–412.

43. Anderson, J.M. 'Mechanism of inflammation and infection with implanted devices.' *Cardiovasc. Path.* **1993**, 2, 33S-41S.

44. Cooke, J.P. 'NO and angiogenesis.' *Atherosclerosis,* **2003,** suppl. 4, 53–60.

45. Ziche, M.; Morbidelli, L. "Nitric oxide and angiogenesis." *J. Neuro-Oncology*, **2000**, 50, 139-48.

46. Campbell, E.J.; O'Byrne V.; Stratford, P.W.; Quirk, I.; Vick, T.A.; Wiles, M.C.; Yianni, Y.P. 'Biocompatible surfaces using methacryloylphosphorylcholine laurylmethacrylate copolymer.' *ASAIO J.* **1994**, 47, 193-199.

47. Kim, S.W.; Jacobs, J. 'Design of nonthrombogenic polymer surfaces for blood-contacting medical devices.' *Blood Purif,* **1996**, 14, 357-372.

48. http://www.medtronic.com/cardsurgery/arrested_heart/carmeda_bioactive.html.

49. Seifert, B.; Romaniuk, P.; Groth, T. 'Covalent immobilization of hirudin improves the haemocompatibility of polylactidepolyglycolide in vitro.' *Biomaterials* **1997**, 8, 1495-1502.

50. Akashi, M.; Maruyama, I.; Fukudome, N.; Yashima, E. 'Immobilization of human thrombomodulin on glass-beads and its anticoagulant activity.' *Bioconjugate Chem.* **1992,** 3, 363-365.

51. Han, H.S.; Yang, S.L.; Yeh, H.Y.; Lin, J.C.; Wu, H.L.; Shi, G.Y. 'Studies of a novel human thrombomodulin immobilized substrate: surface characterization and anticoagulation activity evaluation.' *J. Biomater. Sci-Polym. E* **2001,** 12, 1075-1089.

52. McRea, J.C.; Kim, S.W. 'Characterization of controlled release of prostaglandin from polymer matrices for thrombus prevention.' *Trans. Am. Soc. Artif. Internal Organs J.* **1983**, 6, 60-64.

53. Paul, W.; Sharma, C.P. 'Acetylsalicylic acid loaded poly(vinyl alcohol) hemodialysis membranes: effect of drug release on blood compatibility and permeability.' *J. Biomater. Sci.: Polymer Ed.* **1997**, 8, 755-764.

54. Sugitachi, A.; Takagi, K. 'Antithrombogenicity of immobilized urokinase – clinical applications.' *Int. J. Artif. Organs* **1978**, 1, 88-92.

55. Woodhouse, K.A.; Brash, J.L. 'Adsorption of plasminogen from plasma to lysine-derivatized polyurethane surfaces.' *Biomaterials,* **1992**, 13, 1103-1108.

56. Sefton, M.V.; Gemmell, C.H. 'Chapter 7.2 – Nonthrombogenic treatment and strategies.' *Biomaterials Sciences – An Introduction to Materials in Medicine, 2nd Ed.* Elsevier, **2004**.

57. http://www.nhlbi.nih.gov/health/dci/Diseases/Angioplasty/Angioplasty_Risks.html.

58. Windecker, S.; Remondino, A.; Eberli, F.R.; Juni, P.; Raber, L.; Wenaweser, P.; Togni, M.; Billinger, M.; Tuller, D.; Seiler, C.; Roffi, M.; Corti, R.; Sutsch, G.; Maier, W.; Luscher, T.; Hess, O.M.; Egger, M.; Meier, B. 'Sirolimus-eluting and paclitaxel-eluting stents for coronary revascularization.' *N. Engl. J. Med.* **2005**, 353, 653-662.

59. Dibra, A.; Kastrati, A.; Mehilli, J.; Pache, J.; Schuhlen, H.; von Beckerath, N.; Ulm, K.; Wessely, R.; Dirschinger, J.; Schomig, A. 'Paclitaxel-eluting or sirolimus-eluting stents to prevent restenosis in diabetic patients.' *N. Engl. J. Med*. **2005,** 353, 663-670.

60. Moses, J.W.; Leon, M.B.; Popma, J.J.; Fitzgerald, P.J.; Holmes, D.R.; O'Shaughnessy, C.; Caputo, R.P.; Kereiakes, D.J.; Williams, D.O.; Teirstein, P.S.; Jaeger, J.L.; Kuntz, R.E. 'Sirolimus-eluting stents versus standard stents in patients with stenosis in a native coronary artery.' *N. Engl. J. Med*. **2003**, 349, 1315-1323.

61. Schofer, J.; Schluter, M.; Gershlick, A.H.; Wijns, W.; Garcia, E.; Schampaert, E.; Breithardt, G. 'Sirolimus-eluting stents for treatment of patients with long atherosclerotic lesions in small coronary arteries: double-blind, randomised controlled trial (E-SIRIUS).' *Lancet* **2003,** 362, 1093-1099.

62. Morice, M.; Serruys, P.W.; Sousa, J.E.; Fajadet, J.; Hayashi, E.B.; Perin, M.; Colombo, A.; Schuler, G.; Barragan, P.; Guagliumi, G.; Molnar, F.; Falotico, R. 'A randomized comparison of a sirolimus-eluting stnet with a standard stent for coronary revascularization.' *N. Engl. J. Med.* **2002**, 346, 1773-1780.

63. http://www.cypherstent.com/cypher-stent/specifications/pages/index.aspx.

64. http://www.stent.com/DisplayPage.bsci/id/4/1a1/m/IC/heart-stent-products/promus/promus-stent.html/page.bsc.

65. Abbott Laboratories 'The XIENCE™ V Everolimus Eluting Coronary Stent System Instructions for Use.'

66. http://www.stent.com/DisplayPage.bsci/id/3/1a1/m/IC/heart-stent-products/landing.html/page.bsc

67. Boston Scientific 'Express^2 Monorail Coronay Stent Delivery System and Over-the-Wire Stent Delivery System – Instructions for Use.'

68. Boston Scientific 'Liberte Monorail Over-the-Wire Coronary Stent System – Instructions for Use.'

69. http://www.endeavorstent.com/html/us/hcp_end_differentbydesign.html

70. Gurbel, P.A.; Cummings, C.C.; Bell, C.R.; Alford, A.B.; Meister, A.F.; Serebruany, V.L. 'Onset and extent of platelet inhibition by clopidogrel loading in patients undergoing elective coronary stenting: The Plavix Reduction Of New Thrombus Occurrence (PRONTO) trial.' *Am. Heart J.* **2003,** 145, 239-247.

71. Shuchman, M. 'Trading restenosis for thrombosis? New questions about drug-eluting stents.' *N. Engl. J. Med*. **2006**, 355, 1949-1952.

72. Jun, H.W.; Taite, L.J.; West, J.L. 'Nitric oxide-producing polyurethanes.' *Biomacromolecules* **2005**, 838-844.

73. Taite, L.J.; Jun H.W.; Yang, P.; West J.L. 'Nitric oxide-releasing polyurethane-PEG copolymer containing the YIGSR peptide promotes endothelialization with decreased platelet adhesion.' *J. Biomed. Mater. Res. B* **2007**, 108-116.

74. Wu B.; Gerlitz, B.; Grinnel, B.W. and Meyerhoff, M.E. 'Polymeric coatings that mimic the endothelium: combining nitric oxide release with surface-bound active thrombomodulin and heparin.' *Biomateirals* **2007**, 28, 4047-4055.

75. Wu, B.; Zhou, Z. and Meyerhoff, M.E. 'Dual-acting biomimetic polymeric coatings: Combining nitric oxide release with surface-bound active thrombomodulin.' *232nd American Chemical Society National Meeting & Exposition*, Sept 10, **2006**; San Francisco, CA.

76. Wu, B. and Meyerhoff, M.E. 'Combining nitric oxide release with surface-bound active thrombomodulin.' 1st *Annual Meeting of Methods in Bioengineering Conference*, Jul 17, **2006**, Boston, MA.

77. Zhou, Z.; Wu, Y.; Wu, B. and Meyerhoff, M.E. 'Multifunctional biomimetic coatings for medical devices.' *29th Macromolecular Science and Engineering Annual Symposium*, Oct 27, **2005**, Ann Arbor, MI.

78. Wu, B. and Meyerhoff, M.E. 'A dual functional polymer coating combining rapamycin and nitric oxide release.' *34th Annual Spring Symposium: Smart Functional Materials and Thin Films for Biomedical Applications*, May 9, **2007**, Ann Arbor, MI.

79. Wu, B. and Meyerhoff, M.E. 'A dual-functional polymeric coating combining rapamycin and nitric oxide release.' *2007 Society of Materials Annual Meeting*, Apr 18, **2007,** Chicago, IL.

80. Wu, B. and Meyerhoff, M.E. 'A dual-functional polymeric coating combining rapamycin and nitric oxide release.' *The 27th Annual Graduate Student Symposium in the Pharmacological Sciences and Biorelated Chemistry*, Mar 30, **2007**, Ann Arbor, MI.

81. Wu, B.; Studzinski, D.; Shanley, C.J. and Meyerhoff, M.E. 'Hemocompatible polymeric coatings with sulfonated polyurethanes as matrix for sustained nitric oxide release.' *2009 Society of Materials Annual Meeting*, Apr 22, **2009,** San Antonio, TX.

82. Wu, B.; Studzinski, D.; Shanley, C.J. and Meyerhoff, M.E. 'Combining antiplatelet and antiproliferation agents: Polymeric coatings that release both nitric oxide and sirolimus.' *236th American Chemical Society National Meeting & Exposition*, Aug 17, **2008**, Philadelphia, PA.

83. Wu, B.; Studzinski, D.; Shanley, C.J. and Meyerhoff, M.E. 'Polymeric coatings that release both nitric oxide and sirolimus – Towards the elimination of smooth muscle cell proliferation and late-stent thrombosis.' *Perspectives in Chemistry Research at The University of Michigan*, Aug 1, **2008**, Ann Arbor, MI.

84. Wu, B.; Wang, Y.; Roy-Chaudhury, P. and Meyerhoff, M.E. 'Combining nitric oxide generation and sirolimus release in polymeric films – Potential coatings for stents and other biomedical devices.' *237th American Chemical Society National Meeting & Exposition*, Mar 22, **2009,** Salt Lake City, UT.

85. Wu, B. and Meyerhoff, M.E. 'Selenium-derivatized polyurethanes – Potential nitric oxide generating coatings for stents and other biomedical devices.' *The Society for Biomaterials 2008 Translational Biomaterial Research Symposium,* Sept 11, **2008**, Atlanta, GA.

CHAPTER 2

Polymeric Coatings That Mimic the Endothelium: Combining Nitric Oxide Release with Surface-Bound Active Thrombomodulin and Heparin

2.1. Introduction

During the past century, the use of cardiovascular and other blood contacting biomedical devices has evolved from a mere dream to a widely adopted practice, including the use of heart valves, vascular grafts, stents, extracorporeal circuits and membrane oxygenators[1,2]. However, a lingering issue is the potential of thrombus formation and/or platelet activation at the blood/device interface owing to the lack of hemocompatibility of the polymeric materials employed to fabricate such devices[3].

Platelet adhesion/activation and thrombus formation do not readily occur on the surface of a healthy endothelium that lines the inner walls of all blood vessels. The excellent thromboresistancy of endothelial cells (ECs) is largely attributed to both secreted agents such as nitric oxide (NO)[4], prostacyclin (PGI_2)[5], plasminogen[6] and antithrombin III (AT III)[7] as well as membrane-bound species including heparan sulphate (HS)[8] and thrombomodulin (TM)[9]. Both NO and PGI_2 have long been recognized for

their anti-platelet activity, while heparin[10] (an HS analogue) and TM are well known for their anticoagulant function.

Based on the knowledge of which species contribute to the exceptional biocompatibility of the ECs, efforts have been made to utilize such agents to create more hemocompatible surfaces. Some examples include NO-release[11], heparin-bound[12] and TM-immobilized[2] polymeric coatings. However, their potency in preventing blood clot formation may be limited by the fact that such surfaces only possess partial thromboresistancy (i.e., either only anti-platelet or only anticoagulant activity). A surface that integrates both anti-platelet and anticoagulant agents would seem more promising in that these agents can work synergistically to achieve true thromboresistancy. Recently, the first polymeric coating that combines both NO release and surface-bound biologically active heparin was reported as an initial effort toward this goal[13].

Thrombomodulin is named after its bioactivity as a 'thrombin modulator'[14]. It is a transmembrane protein with a molecular weight of 74 kDa. The mature human TM molecule consists of 557 amino acid residues and usually has a chondroitin sulfate moiety attached to its Ser/Thr-rich domain[15]. Once thrombin, a pivotal protein in the coagulation cascade, binds to TM on the surface of the EC layer, thrombin's fibrinogen-cleaving activity is inhibited. In addition, this binding will also alter thrombin from a procoagulant to an anticoagulant by activating protein C (PC) to initiate the PC anticoagulation pathway[15].

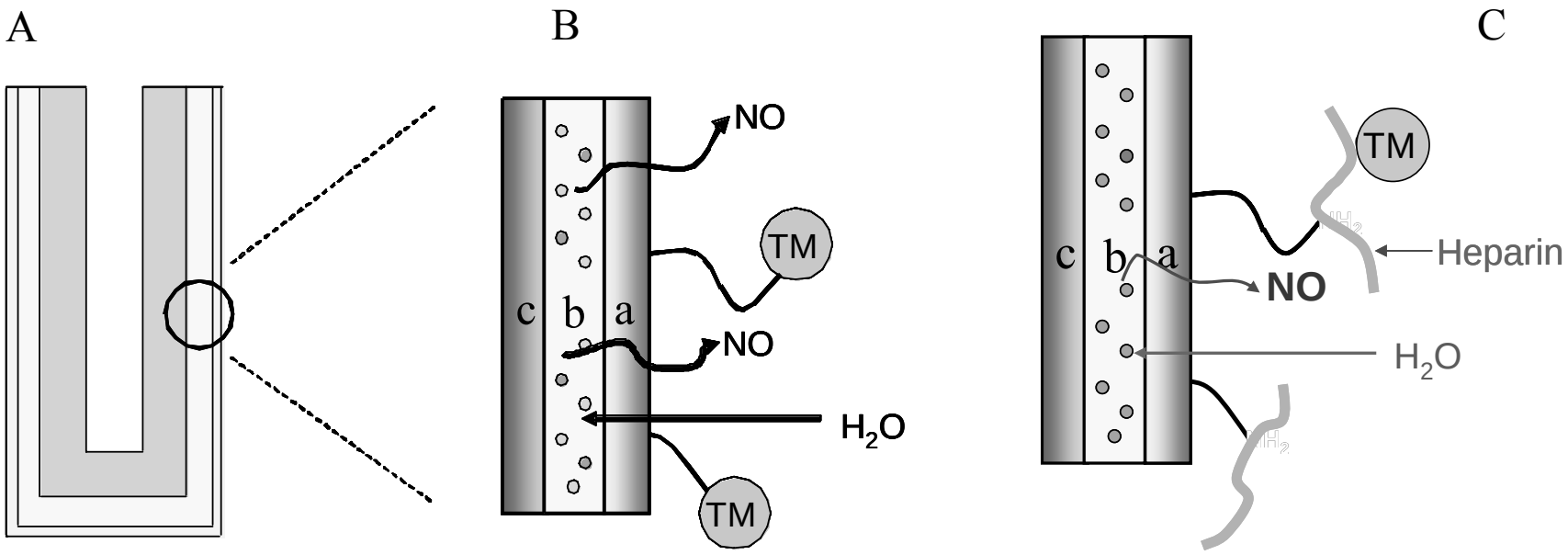

Scheme 2.1. A) Schematic of silicone rubber (SR) catheter sleeve (made with SR tube (OD = 1.19 mm, ID = 0.64 mm, L = 1.5 cm) sealed at one end with Dow Corning RTV 3140 silicone coating) with biomimetic bilayer coating. **B)** Illustration of this bilayer polymeric coating with combined NO release and surface-bound TM: **a)** top layer: carboxylated CarboSil with surface-bound TM; **b)** underlying layer: PurSil matrix doped with DBHD/N_2O_2 (structure shown in Figure 2.2 below) and potassium tetrakis(*p*-chlorophenyl)borate (KTpClPB); **c)** SR substrate. **C)** Illustration of this bilayer polymeric coating with combined NO release and surface-bound heparin and TM: **a)** top layer: aminated CarboSil with TM attached onto the surface-bound heparin; **b)** underlying layer: PurSil matrix doped with DBHD/N_2O_2 and KTpClPB; **c)** SR substrate.

Herein, polymeric coatings with controlled NO release and surface-bound active TM alone or along with heparin were prepared and characterized (see Scheme 2.1). Two approaches were examined. In both cases, an underlying NO release polymer film was employed in which a lipophilic diazeniumdiolated NO donor molecule was incorporated (see Scheme 2.1A). This layer provided the NO release once water partitions into the film. In the first scheme in which TM was immobilized alone, an outer polymer coating (over the inner NO release film) was modified with free carboxyl groups (see Scheme 2.1B) so that TM could be covalently linked via amide bonds. In the second approach, heparin was first immobilized to an outer layer possessing free amine groups, and then TM was coupled to heparin using the excess carboxyl groups on heparin to create amide bond with amine groups on TM (see Scheme 2.1C). The effect of TM immobilization chemistry on the NO release properties of the underlying film was examined. Further, it was shown that in addition to releasing NO at physiologically relevant fluxes, the resulting polymer coatings possessed significant amounts of immobilized TM or TM plus heparin with biological activities, as determined by activated PC (APC) and anti-Factor Xa (anti-FXa) chromogenic assays.

2.2. Experimental

2.2.1. Materials and Instrumentation

Recombinant soluble human TM (TM (CS+), with a chondriotin sulfate moiety attached to TM's Ser-Thr rich domain) was a generous gift from Dr. Bruce Gerlitz and Dr. Brian Grinnell in Eli Lilly and Company (Indianapolis, IN). It was produced by a high-

producing AV12-664 cell line and was purified as described previously[16]. Human PC, as well as the chromogenic substrates S-2366 and S-2222, were generous gifts from Instrumentation Laboratory Inc. (Lexington, MA). Human APC, human α-thrombin and human AT III were purchased from Haematologic Technologies Inc. (Essex Junction, VT). Hirudin (from leeches), porcine heparin (171 USP units/mg), glutaraldehyde (25 % aqueous solution), Triton X-100, Trizma® Pre-set crystals (for preparing Tris buffer), 2-(*N*-morpholino)ethanesulfonic acid hydrate (for preparing MES buffer), phosphate buffered saline (PBS, pH 7.4), PBS (containing Tween 20, pH 7.4), bromophenol blue and dibutylamine (DBA) were all purchased from Sigma (St. Louis, MO). Bovine serum albumin (BSA) solution was obtained from Invitrogen (Carlsbad, CA). Potassium tetrakis(*p*-chlorophenyl) borate (KTpClPB) and triglycine (glycyl-glycyl-glycine, TG) were obtained from Fluka (Ronkonkoma, NY). Glycine (Gly), 0.6 mL Fisherbrand low retention microcentrifuge tubes and 96-well polystyrene (PS) microtiter plates were obtained from Fisher Scientific (Fair Lawn, NJ). Diprimary amine terminated poly(ethylene oxide) (DPA-PEO, with 10 repeating ethylene oxide units) was generously donated by Tomah Inc. (Milton, WI). PurSil 20 80A and CarboSil 20 90A were from The Polymer Technology Group (Berkeley, CA).

Silicone rubber catheter sleeves were made from silicone tubing (0.64 mm ID/1.19 mm OD), purchased from Helix Medical Inc. (Carpinteria, CA). Polypropylene (PP) 96-well microplates with round 'U' bottom wells were purchased from Evergreen Scientific (Los Angeles, CA). Nanosep centrifugal devices (Mw cut-off = 5K) were purchased from Pall Life Sciences (Ann Arbor, MI). Whatman 13 mm ZC syringe filters were obtained from Whatman (Florham Park, NJ). Hexamethylene diisocyanate (HMDI,

Aldrich (St. Louis, MO)) was distilled at reduced pressure immediately before use. The 3140 RTV SR was purchased from Dow Corning Corporation (Midland, MI). Pyridine (Aldrich) was dried and distilled over 4M molecular sieves right before the reaction. Dibutyltin dilaurate (DBTDL), 1-ethyl-3-(3-dimethylaminopropyl)carbodiimide hydrochloride (EDC), *N*-hydroxysuccinimide (NHS), absolute ethanol and *p*-toluenesulfonic acid monohydrate (TsOH) were all used as received from Aldrich. Citrate/phosphate/dextrose solution was purchased from Hospira Inc. (Lake Forest, IL). Lactate dehydrogenase (LDH) assay kits were obtained from Roche Applied Sciences (Indianapolis, IN). Oregon Green 488 (OG-488) succinimidyl ester was purchased from Molecular Probes, Inc. (Eugene, OR). DBHD/N_2O_2 was synthesized by treating *N,N'*-dibutyl-1,6-hexanediamine (DBHD, Aldrich) with NO gas (80 psi, Cryogenic Gases (Detroit, MI)) at room temperature for 24 h as previously described[11].

FTIR spectra were collected on a Perkin-Elmer BX FT-IR system (Wellesley, MA). Nitric oxide flux from polymer coatings was measured by a chemiluminescent NO analyzer (NOA™ 280, Sievers Instruments, Inc. (Boulder, CO)). A scanning electron microscope (Philips XL30 FEG, FEI Company (Hillsboro, OR)) was used to characterize the morphology of the coatings. A sputter coater system (SPI Supplies (West Chester, PA)) was used to coat a thin conductive gold layer prior to SEM analysis. Static air–water contact angles were measured by using a Cam-100 Optical Contact Angle Goniometer (KSV Instruments Ltd. (Monroe, CT)). Fluorescence spectra were recorded with a Shimadzu RF-1501 spectrofluorophotometer (Tokyo, Japan). The UV-Vis absorbance changes in the chromogenic assays were measured with a microtiter plate

reader (UV-IR-Vis Multiskan Spectrum Model 349, MTX Lab Systems, Inc. (Vienna, VA)).

2.2.2. Synthesis of Carboxylated and Aminated CarboSil

The urethane groups on CarboSil backbone were used to couple with HMDI through an allophanate reaction in the presence of a tin catalyst (DBTDL)[17]. A solution of CarboSil (10 w/v % in DMAc) was added dropwise to a ca. five-fold molar excess of HMDI solution (10 w/v % in DMAc with 0.1 v/v % DBTDL) under argon. The reaction mixture was stirred for 24 h at 40 °C, and the product was precipitated in copious anhydrous ethyl ether. The precipitate was filtered and dissolved in anhydrous DMAc and then precipitated again in anhydrous ethyl ether. After washing, the product was dried under vacuum for 2 d to remove any residual solvent. The resulting polymer with pendant isocyanate groups (CarboSil-NCO) was further used to prepare carboxylated and aminated CarboSil.

The carboxylation of CarboSil-NCO was carried out via a modified urea-forming reaction[17,18]. Equimolar of pyridine was first mixed with a glycine or triglycine suspension in anhydrous dimethylacetamide (DMAc, 10 w/v %) overnight at 60 °C. CarboSil–NCO was dissolved in DMAc to make a 10 w/v % solution and mixed with an excess of freshly prepared pyridinyl glycine/triglycine suspension. The reaction mixture was stirred under argon at 60 °C for 2 d, and then precipitated in copious ethanol/H_2O (4:1, v/v). The precipitate was filtered and washed with ethanol/H_2O (4:1, v/v) twice and then soxhlet extracted with methanol. Afterwards, it was washed again with ethyl ether and dried under vacuum for 2 d and then stored at -20 °C.

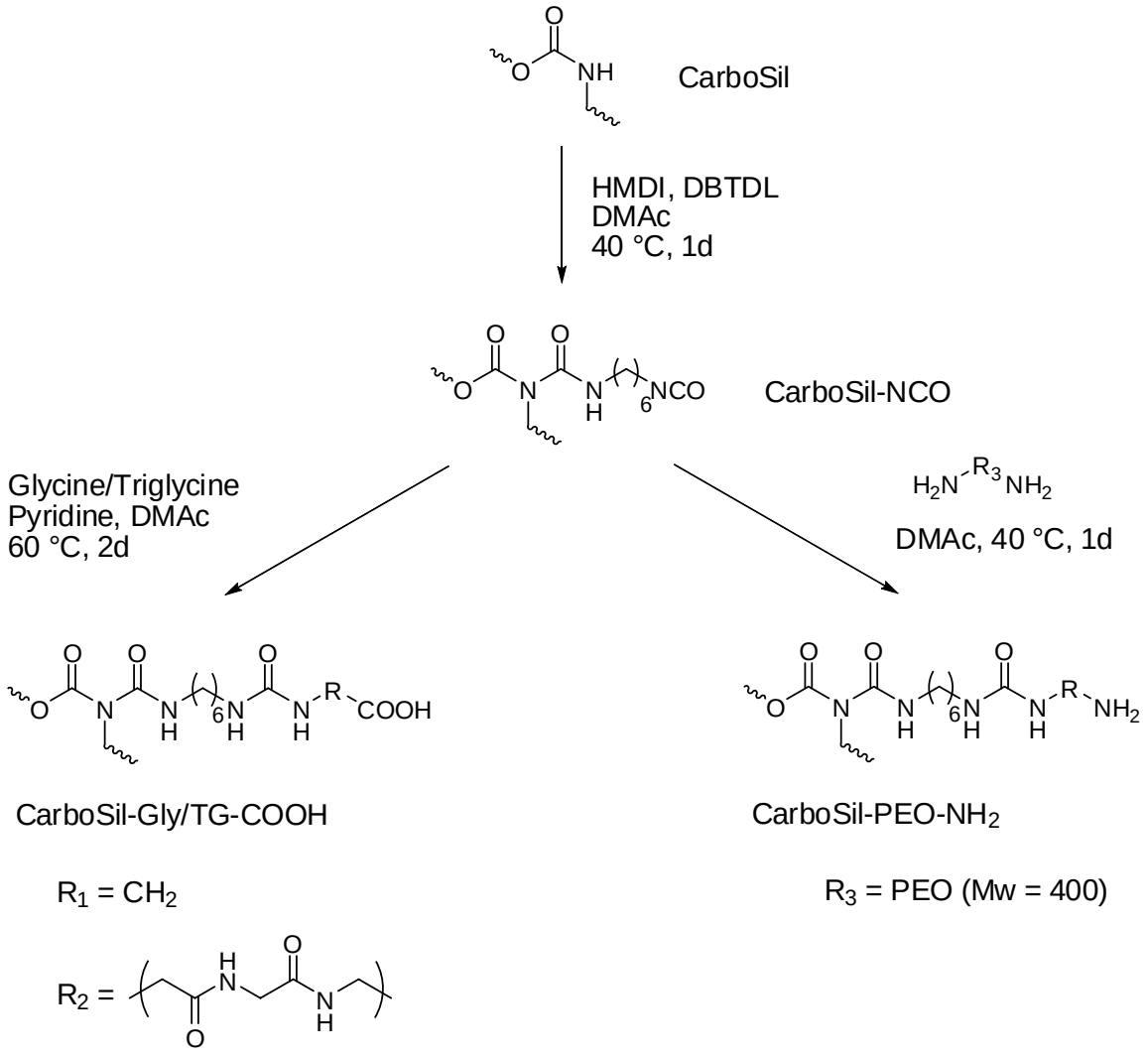

Scheme 2.2. Synthesis of carboxylated and aminated CarboSil.

The amination of CarboSil-NCO was carried out according to a previously reported method[13]. Briefly, CarboSil–NCO solution in DMAc (10 w/v %) was added dropwise to an excess of diamino–PEO (DPA-400E) solution (10 w/v % in DMAc). The reaction mixture was stirred under argon at 40 °C for 1 d, and then precipitated in copious ethyl ether. The aminated CarboSil (CarboSil–PEO–NH_2) was filtered and washed with

acetone and then ethyl ether to remove any unreacted diamine. The product was further soxhlet extracted with methanol and then washed again with ethyl ether before it was finally dried under vacuum for 2 d to remove the residual solvent and then stored at -20 °C. Scheme 2 summarizes the carboxylation and amination procedures employed to modify CarboSil.

2.2.3. Determination of Isocyanate Group Concentration on CarboSil-NCO and Amino Group Concentration on CarboSil-PEO-NH_2

The concentration of pendant isocyanate groups on CarboSil-NCO was determined via a modified titration method[19]. Approximately 20 mg CarboSil-NCO was dissolved in 20 mL DMAc under argon to form a homogeneous solution. An excess amount of DBA (50 μmol dissolved in 20 mL anhydrous toluene) was added and the mixture was shaken under argon at room temperature overnight. The remaining base was titrated with an isopropanol solution of TsOH (5 mM), and the endpoint was indicated by bromophenol blue, via a color change from purplish blue to light yellow.

A similar method was adopted for the determination of the amine content of CarboSil-PEO-NH_2. Approximately 20 mg CarboSil-PEO-NH_2 was dissolved in 20 mL DMAc. The amino groups were titrated with TsOH solution, (5 mM in isopropanol), with bromophenol blue as the indicator.

2.2.4. Preparation of Underlying NO Release Polymeric Coatings

The NO release polymeric coatings were prepared using a method similar to that previously reported by our group[13]. A cocktail containing PurSil and 1:1 (molar ratio) of

KTpClPB and DBHD/N_2O_2 was prepared by suspending KTpClPB and DBHD/N_2O_2 in PurSil solution (4 w/v % in DMAc/THF) via moderate sonication. The amount of PurSil in the cocktail was controlled so that final underlying layer of the polymeric coatings contained 8 wt % of DBHD/N_2O_2 (after a complete solvent evaporation). Silicone rubber catheter sleeves (1.5 cm in length) were sealed at one end with Dow Corning 3140 RTV SR and cured overnight under ambient conditions. Afterwards, they were dip-coated with the DBHD/N_2O_2 containing PurSil cocktail 8 times at 20-min intervals. Finally, a carboxylated or aminated CarboSil top layer was applied by dip-coating twice in a CarboSil-Gly/TG-COOH or CarboSil–PEO–NH_2 solution in DMAc/THF. The polymer concentrations ranged from 1 to 4 w/v % to achieve outer layers with different thicknesses. The catheter sleeves were allowed to dry overnight, followed by vacuum drying at room temperature for additional 2 d to remove any residual solvent. Scheme 2.1 illustrates the final bilayer polymeric coating configurations on SR catheter sleeves.

2.2.5. Heparin Immobilization on CarboSil-PEO-NH_2

Porcine heparin (unfractionated) was covalently immobilized onto the aminated CarboSil surface as previously reported[13]. Briefly, a solution of heparin (20 mg/mL) in MES buffer (pH 5.6) was reacted with EDC and NHS at room temperature for 10 min (EDC:NHS:Hep–COOH = 0.4:0.24:1.0 (molar ratio))[12]. The aminated CarboSil coatings, pre-equilibrated in PBS (pH 7.4) for 2 h at room temperature, were soaked in the activated heparin solution at room temperature for another 2 h. The resulting heparinized surface (CarboSil-PEO-Hep) was extensively washed with 4 M NaCl and then DI water.

2.2.6. TM Immobilization on Carboxylated and Heparinized CarboSil Surface

The CarboSil-Gly/TG-COOH surface was first hydrated in PBS (pH 7.4) at room temperature for 2 h. Then, the surface carboxyl groups were activated by 100 mM EDC and 50 mM NHS in PBS (pH 7.4) at room temperature. The activated carboxyl groups were then reacted with the amine groups on the lysine residues of TM (10 μg/mL in PBS, pH 7.4) at 4 °C overnight[21]. The polymeric coating was then extensively washed with PBS (pH 7.4, containing Tween 20) and then DI water to rinse off any noncovalently-linked TM. The dual-acting polymeric coating, with NO donor within the underlying PurSil layer and TM bound onto its top layer, was then further characterized (see below).

The procedure used to immobilize TM on heparinized CarboSil surface was similar to that employed for the carboxylated surface. After hydration, the CarboSil-PEO-Hep surface was reacted with 100 mM EDC and 50 mM NHS in PBS (pH 7.4) at room temperature for 30 min to activate the heparin carboxyl groups. The activated carboxyl groups on heparin were then reacted with the amine groups on the lysine residues of TM (10 μg/mL in PBS, pH 7.4) at 4 °C overnight. Any noncovalently-bonded TM was removed by extensive washing with PBS (pH 7.4, containing Tween 20) and then DI water.

2.2.7. Surface Characterization of Multifunctional Coatings

Static air–water contact angles were determined by a sessile drop method using a Cam-100 Optical Contact Angle Goniometer at ambient humidity and temperature. A 1–1.5 μL of DI water droplet was placed on the polymer surface using a microsyringe and its image was taken with a CCD camera. The contact angle was then calculated from the

image of the droplet using the software provided with the instrument. Polymer coated surfaces for contact angle measurements were prepared via spin coating a polymer solution (0.1 w/v % in THF, filtered with Whatman 0.45 μm PTFE syringe filter) onto a glass slide at 600 rpm for 40 s under nitrogen. The polymer coated glass slides were further treated to immobilize TM and/or heparin as described above. All the sample slides were first dried in nitrogen overnight and then under vacuum for another 2 d. For each polymer surface, 20 separate drops were examined on two different sample slides to obtain the average contact angle values reported.

Scanning electron microscopic characterization was performed with a Philips/FEI XL30 FEG SEM Electron Microscope. The electron beam was operated at 15 kV and the sample chamber pressure was 10^{-6} torr. Polymeric coatings were dried under vacuum for 2 d and then sputtered with gold prior to acquiring the SEM images.

2.2.8. Estimation of the Amount of Immobilized hTM

Thrombomodulin was labeled with OG-488 succinimidyl ester as follows. To a solution of 150 μL of carbonate-bicarbonate buffer (pH 9.0), 50 μL of OG-488 solution (10 mg/mL in DMSO) was added, followed by 150 μL aqueous TM solution (0.8 mg/ml). The mixture was gently vortexed at room temperature in the dark for 2 h. After the coupling reaction, the unreacted OG-488 was removed by dialysis using centrifuge devices with a cut-off molecular weight of 5K.

TM's degree of labeling (DOL) was determined by the following equation:

$$DOL = \frac{C_{OG-488}}{C_{TM}} \qquad \textbf{Eqn. 2.1.}$$

Whereas, C_{OG-488} and C_{TM} are the concentrations of OG-488 and TM, respectively, in the stock solution of OG-488 labeled TM.

The concentration of TM was measured via a Bio-Rad protein assay[20]. First three to five dilutions of HRP standards were prepared. The HRP is a protein that can be used as standard. One hundred and sixty μL of each standard and sample solution were pipetted into separate microtiter plate wells. Forty μL of dye reagent concentrate was then added to each well using a multi-channel pipet to dispense the reagent. To mix the sample and reagent in the well, the plunger on the dispenser was depressed repeatedly. The samples were then incubated at room temperature for at least 5 min and no more than 1 h. The absorbances at 590 nm of both the standards and samples were measured with a microtiter plate reader. The concentration of OG-488 was determined by measuring the fluorescence intensity of the mixture using 495 nm for excitation and 520 nm for emission.

TM-OG-488 was immobilized onto CarboSil-Gly surfaces in a similar manner as non-labelled TM. After immobilization, the surface-bound TM-OG-488 was hydrolyzed with 2 M NaOH for 1 h at 121 °C using an autoclave. After cooling the hydrolyzed mixture to room temperature, acetic acid was added, and the fluorescence intensity of the mixture was measured using 495 nm for excitation and 520 nm for emission. Blank CarboSil-Gly polymeric coatings and solutions with known TM-OG-488 concentrations were also autoclaved under the same condition to be used as controls and standards.

2.2.9. Activity of Surface-Bound Thrombomodulin

The bioactivity of surface-bound TM was analyzed by a chromogenic PC assay[16] (see Figure 1.5). In a 0.6 mL microcentrifuge tube, the 1.5 cm long polymer coated SR catheter sleeve (surface area = 0.572 cm^2) with immobilized TM was fully immersed into a solution composed of 80 μL BSA solution (7.5 w/v %), 8 μL thrombin solution (100 μg/mL), and 192 μL 20 mM Tris buffer (pH 7.4, with 3 mM $CaCl_2$, 100 mM NaCl and 0.02 % NaN_3). After incubation at 37 °C for 5 min, 40 μL of PC solution (100 μg/mL) was added and the mixture was incubated at 37 °C for 10 min. Then, 80 μL of hirudin (204.8 unit/mL) was added to bring the total volume to 400 μL and the mixture was further incubated at 37 °C for 5 min. The 400 μL mixture was then evenly divided into 4 wells of a PP 96-well microtiter plate. Ninety μL of Tris buffer (pH 7.4) and 10 μL of 2 mg/mL S-2366 substrate solution were then added and absorbance change at 405 nm was measured immediately by a Labsystems Multiskan RC 96-well microplate reader in the kinetic mode. Control experiments were also performed for surfaces without immobilized TM (carboxylated, aminated and heparinized polymeric surfaces), using the exact same assay procedure.

The stability of surface-bound TM was also tested both in PBS and sheep plasma using this APC assay. Arterial blood from pregnant ewes, weighing 70 ± 14 kg, was drawn into a 9:1 volume of blood anticoagulant (citrate/phosphate/dextrose) solution. The citrated whole blood was centrifuged at 110 g for 15 min at 22 °C and plasma was collected from the supernatant. To re-establish platelet activity, $CaCl_2$ was added to the plasma to raise $[Ca^{2+}]$ by 2 mM.

2.2.10. Activity of Surface-Bound Heparin

The bioactivity of surface immobilized heparin was determined by a chromogenic anti-FXa assay[12] (see Figure 1.3). In a 0.6 mL Fisherbrand low retention microcentrifuge tube, the 1.5 cm long SR catheter sleeve with heparinized polymer coating (surface area = 0.572 cm^2) was fully immersed in a solution composed of 80 μL BSA solution (7.5 w/v %), 80 μL AT III solution (100 μg/mL), and 232 μL PBS (pH 7.4). After incubation at 37 °C for 2 min, 8 μL of 20 μg/mL FXa was added to bring the total volume to 400 μL and the mixture was further incubated at 37 °C for 1 min. The 400 μL mixture was then evenly divided into 4 wells of a PP 96-well microtiter plate. Ninety μL of PBS (pH 7.4) and 10 μL of 2 mg/mL S-2222 solution were then added to bring the total volume in each well to 200 μL. Absorbance changes at 405 nm were measured immediately by the microplate reader in the kinetic mode. Experiments were also performed using non-heparinized surfaces (aminated polymer surface) and the heparinized surface after subsequent TM immobilization.

2.2.11. Chemiluminescence Measurements of NO Release

Nitric oxide released from the polymeric coatings was measured using a Sievers Chemiluminescence NO Analyzer. The instrument was calibrated before each experiment using an internal two-point calibration (zero gas and 45 ppm NO gas). NO was continuously swept from the headspace of the sample vessel and purged from the bathing solution with a nitrogen sweep gas and bubbler into the chemiluminescence detection chamber. The flow rate was set to 50 mL/min with a chamber pressure of 5.4 torr and an oxygen pressure of 6.0 psi.

2.2.12. In Vitro Platelet Adhesion Experiments Using Sheep Plasma

A lactate dehydrogenase assay was used to quantify platelet adhesion on polymeric coatings with an NO-release underlying layer and CarboSil-Gly top layer prepared in PP 96-well microtiter plates. Thrombomodulin was immobilized using the method described above. Microtiter plates with control polymeric coatings were also prepared. After incubation with sheep plasma, adhesion of platelets was determined by measuring LDH enzymatic activity derived from the platelets via a method reported recently by Wu *et al*[21].

Briefly, before sheep plasma incubation, the polymer coated microtiter plate wells were hydrated by incubating with 200 mL PBS for 3 h at 37 °C. Then, 100 mL of sheep plasma was added to each polymer-coated well and incubated for 1 h at 37 °C under static conditions. The plasma was then decanted and the wells were washed once with 200 mL PBS. Adhered platelets were lysed for 1 h at 37 °C using a lysing buffer (150 μL PBS with 1 w/v % Triton X-100 and 0.75 w/v % BSA per every well). Then, 100 μL of each lysate solution was pipetted into wells of a second 96-well polystyrene microtiter plate (Fisher) that contained 100 μL of reagent from an LDH assay kit. Absorbance change of each well at 490 nm was monitored by a microplate reader.

NO release properties before and after plasma incubation were investigated by NOA. SEM images for surfaces of the various polymeric films were also obtained. The polymer coatings were prepared via sequentially spin coating a DBHD/N_2O_2 containing PurSil cocktail and then a CarboSil-Gly solution in DMAc/THF onto glass slides at 600 rpm for 40 s as the underlying NO release and the top layers, respectively. All the

sample slides were first dried in nitrogen overnight and then under vacuum for 2 d. The polymer coated glass slides were then further treated to immobilize TM as described above. After plasma incubation, adhered platelets in some wells were fixed with 4 % glutaraldehyde for 1 h and then dehydrated in a series of ethanol solutions (Table 1.1) and dried overnight. The polymeric coatings with adhered platelets were sputtered with gold prior to acquiring the SEM images.

Table 2.1. Series of ethanol solutions for platelet dehydration.

Solution #	Ethanol Concentration	Immersion Time (min)
1	50 %	5 min
2	75 %	5 min
3	85 %	5 min
4	90 %	5 min
5	95 %	5 min
6	Absolute	5 min

2.3. Results and Discussion

2.3.1. Preparation and Characterization of Outer Carboxylated/Aminated CarboSil Layer

Carboxylation was carried out on CarboSil, a silicone-poly(carbonate)urethane copolymer that is used for biomedical applications[3,22]. This polymer has been suggested for longer-term *in vivo* implants, including vascular grafts, owing to its greatly improved biostability and biomcompatibility, compared to the classical polyether type polyurethanes.

The urethane groups on the polymer backbone were first coupled with a diisocyanate compound (HMDI)[23]. The coupling was confirmed using IR by the appearance of a NCO band at 2266 cm^{-1}, and another new band at 1619 cm^{-1} (corresponding to urea absorption) after reaction for 1 d (see Figures 2.1a and b). The concentration of the isocyanate groups was determined to be 401 ± 3 μmol/g (n = 3) via the modified titration method[19]. Prolonging the reaction time would increase the isocyanate concentration (data not shown) yet the polymer also became more and more difficult to dissolve due to the increasing extent of crosslinking between separate polymer chains.

The resulting polymer with pendant free isocyanate groups was further reacted with the amino groups of glycine/triglycine to form carboxylated CarboSil (CarboSil-Gly/TG-COOH). The disappearance of the 2266 cm^{-1} peak and increased intensity at 1619 cm^{-1} in the IR spectra (Figures 2.1c and d) verified the formation of the second urea bond at the expense of the isocyanate group.

The preparation of the aminated CarboSil was described previously[13]. The free isocyanate groups attached to CarboSil were further coupled to a hydrophilic diprimary amine terminated PEO chain. Surfaces coated or covalently linked with this PEO based hydrogel-like structure have been shown to suppress cell adhesion (e.g., platelet adhesion) [22,23]. The concentration of amine groups on CarboSil-PEO-NH_2 was determined to be 221 ± 4 μmol/g (n = 3) by titration. Compared to that of the isocyanate groups in CarboSil-NCO (401 ± 3 μmol/g), the decrease of functional group concentration might be attributed to the slight hydrolysis of NCO and the crosslinking of separate polymer chains by the diamine.

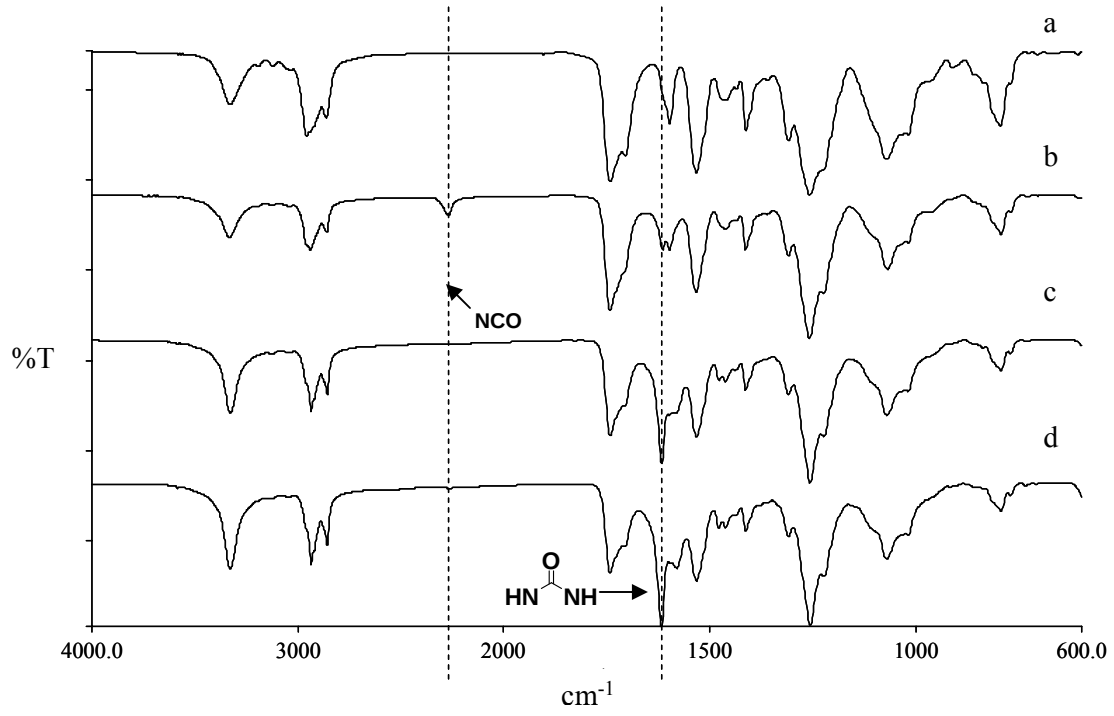

Figure 2.1. Typical IR spectra of CarboSil and its derivatives: **a)** CarboSil; **b)** CarboSil-NCO; **c)** CarboSil–Gly–COOH; **d)** CarboSil-TG-COOH.

2.3.2. Immobilization of TM on Carboxylated CarboSil as well as Heparin and TM on Aminated CarboSil

A number of methods have been adopted for the immobilization of TM using a variety of surface functional groups, including carboxylic acid[24], amine[25], and trichlorotriazine[26] to anchor TM through the formation of covalent linkages. It has also been reported that TM can be incorporated within a phospholipid membrane via *in situ* photopolymerization[27]. Here, we chose to introduce carboxylic groups (from glycine, triglycine or heparin) on the outer CarboSil polymeric surface to form stable amide bonds with the amine groups on the TM. The reaction can be carried out in very mild

conditions (pH 7.4, room temperature or 4 °C) and this helps to minimize any possible deterioration of TM's biological activity.

In one approach (see Scheme 2.1B) to link TM to the outer surface, the COOH groups on CarboSil-Gly/TG-COOH surfaces were used to react with the amino groups on lysine residues of TM to form stable amide bonds as described in the Experimental section. The unreacted TM could be collected and reused as needed.

In the second approach (see Scheme 2.1C), heparin can first be covalently immobilized on to the aminated CarboSil surfaces as described in the Experimental section. Unfractionated heparin (from porcine intestinal mucosa), as a highly negatively charged polysaccharide with a molecular weight ranging from 5 kDa to 20 kDa, has 18 COOH groups per molecule on average[12]. The EDC/NHS/Hep-COOH ratio used corresponds to a value where only one COOH group per every heparin molecule can react with the polymer surface amine groups so that maximal activity of heparin could be maintained[12], and the remaining COOH groups on immobilized heparin could be used to immobilize TM. The concentrations of EDC and NHS (100 mM and 50 mM, respectively), the activation time (30 min) and the concentration of TM (10 μg/mL) were all carefully optimized (data not shown) so that maximal activity of surface-bound TM could be obtained with the least decrease in immobilized heparin activity (see below).

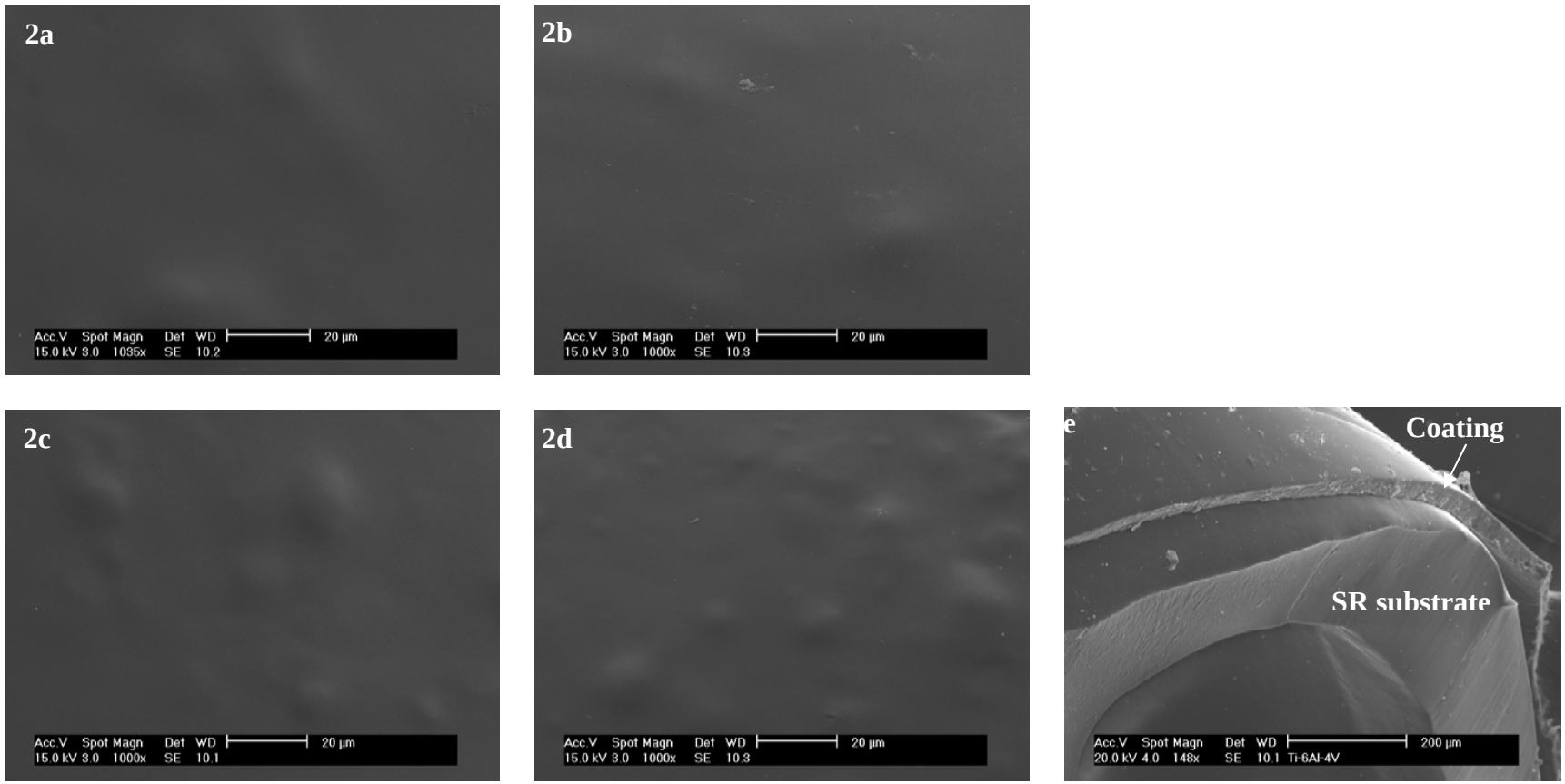

Figure 2.2. a-d): SEM pictures of polymeric surfaces with different thickness of top-coating before/after TM immobilization. The underlying layers of all coatings were doped with 8 wt % of DBHD/N_2O_2 and an equimolar amount of KTpClPB. **a)** and **b)** are surfaces before and after TM immobilization with top-coatings made by dip-coating in 2 wt % solution of CarboSil-Gly-COOH in DMAc/THF, respectively; **c)** and **d)** are surfaces before and after TM immobilization with top-coatings made by dipping the tubes in 1 wt % solution of CarboSil-Gly-COOH in DMAc/THF, respectively; **e)** Typical cross-section of the SR catheter sleeves onto which the bilayer polymeric coatingwas applied. The thickness of the bilayer coating was approx. 35-50 µm.

2.3.3. Surface Characterization

SEM images (see Figures 2.2a, b) show that the surfaces of the polymeric coatings were smooth on the micrometer scale and that no observable change in roughness was observed. Also, there was no discernible interface between the top layer and the underlying layer. The total thickness of these bilayer coatings was ca. 35-50 μm (see Figure 2.2c).

Chemically modifying the polymer surface also led to significant changes in the air–water contact angle of the material surface. As shown in Table 2.2, the contact angle of CarboSil decreased from 105 ± 3° to 91 ± 2° after glycine was attached. The contact angle of CarboSil-Gly-TM further decreased to 69 ± 3°, 22 degrees smaller than that of CarboSil-Gly-COOH, showing that the surface becomes quite hydrophilic after the immobilization of the TM protein.

Table 2.2. Contact angles of various polyurethane surfaces. (degree, $n \geq 20$)

CarboSil	CarboSil-Gly-COOH	CarboSil-Gly-TM
105 ± 3	91 ± 2	69 ± 3

2.3.4. Measurement of the Amount of Immobilized hTM

Figure 2.3 shows a typical calibration curve for HRP using the Bio-Rad protein assay. The labeled TM sample solution was diluted to fit into the linear range of the calibration curve. Figure 2.4 shows the typical emission spectrum of OG-488. The degree of labeling (DOL) of OG-488 labeled TM was determined to be 0.65 (n = 3). The

absolute amount of TM immobilized on CarboSil-Gly surfaces was estimated to be 1.77 ± 0.26 pmol/cm^2.

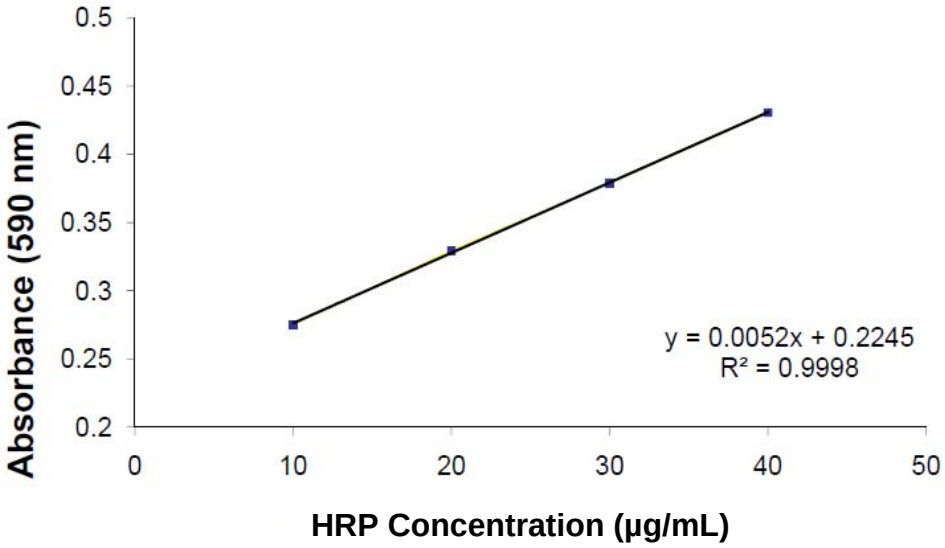

Figure 2.3. Typical calibration curve of Bio-Rad assay (via recommended microtiter procedure for microtiter plates).

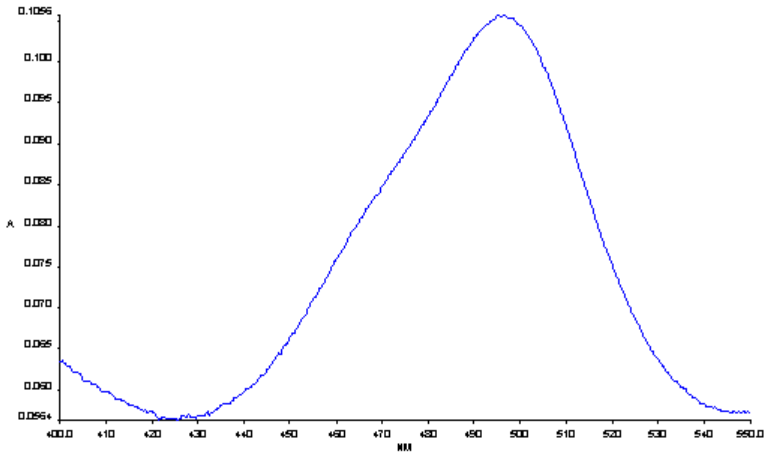

Figure 2.4. Typical emission spectrum of OG-488 labeled TM solution (using 495 nm as the emission wavelength).

2.3.5. Activity of Surface-Bound TM and Heparin

The anticoagulant activity of the immobilized TM was evaluated by a chromogenic APC assay. Activation of PC by thrombin alone is slow and has no physiological function. However, when thrombin binds to TM in the presence of Ca^{2+}, the rate by which thrombin activates PC will increase by 20,000-fold[15]. The activated PC can be quantified by measuring the cleavage rate of the chromogenic substrate S-2366 (Glu-Pro-Arg-pNA·HCl)[16]. For immobilized TM, its activity is expressed in terms of nanograms of APC generated per square centimeter per min.

The immobilized TM's activity on CarboSil-Gly-COOH was determined to be 11.7 ± 0.5 and 11.5 ± 0.5 ng APC·cm^2·min^{-1} in the presence and absence of a surface NO flux of 1.0×10^{-10} mol cm^{-1} min^{-1}, respectively. Surfaces without immobilized TM or with only physically adsorbed TM showed negligible activity (0.1 ± 0.2 and 0.3 ± 0.2 ng APC·cm^2·min^{-1}, respectively (see Figure 2.5)). This confirmed that the anticoagulant activity comes from covalently bound TM and not physically adsorbed TM; the presence of NO release does not alter the anticoagulation activity of TM.

As has been mentioned in Section 3.4, the absolute amount of TM immobilized on CarboSil-Gly surfaces was estimated to be 1.77 ± 0.26 pmol/cm^2 as determined by a fluorescence method based on labeling TM with OG-488. Such a value should correspond to a much higher PC activating capability than measured by the APC assay (see above). A possible reason for less activity is that the short spacer (i.e., glycine) between TM molecules and the polymeric surface might hinder both the mobility of TM and the accessibility of its substrates. Indeed, with longer spacers such as TG and PEO-

Hep as described below, a significant increase of TM biological activity could be detected using the same immobilization chemistry.

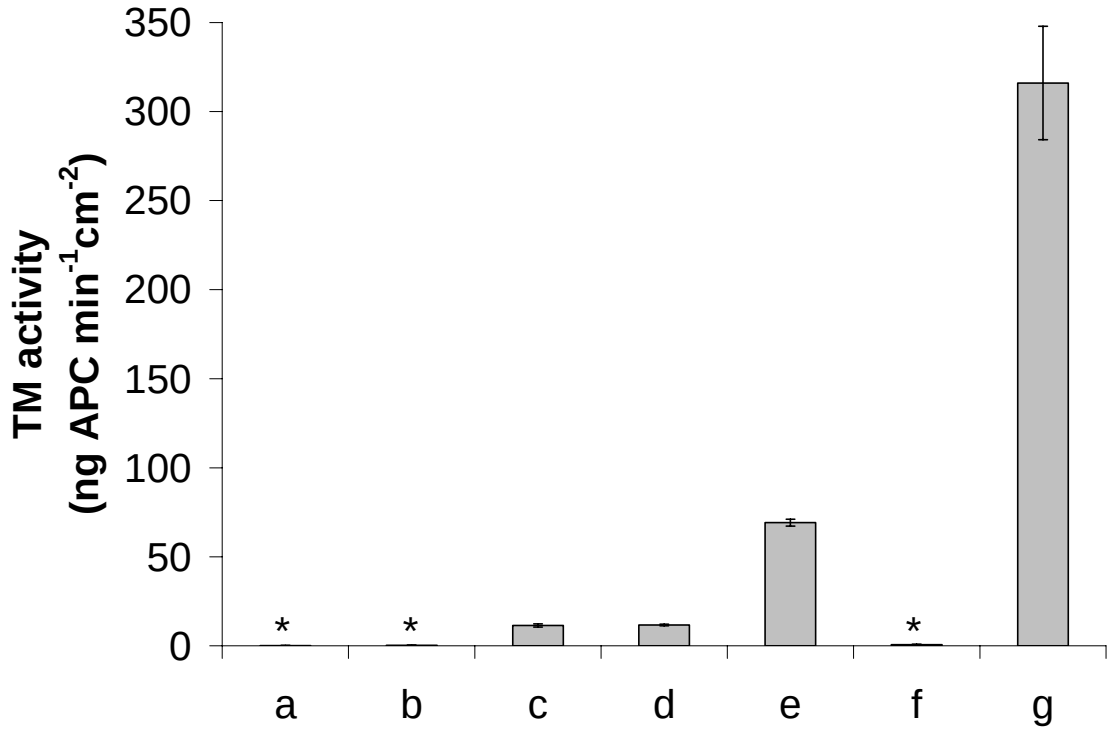

Figure 2.5. TM activity of modified polymeric surfaces (determined by APC assay): **a)** CarboSil-Gly-COOH in the absence of NO; **b)** CarboSil-Gly-COOH with physically adsorbed TM in the absence of NO; **c)** CarboSil-Gly-TM in the absence of NO; **d)** CarboSil-Gly-TM in the presence of an NO flux of ca. 1.0×10^{-10} mol·cm^{-2}·min^{-1}; **e)** CarboSil-TG-TM in the presence of an NO flux of ca. 1.0×10^{-10} mol·cm^{-2}·min^{-1}. **f)** CarboSil-PEO-Hep in the presence of an NO flux of ca. 1.0×10^{-10} mol·cm^{-2}·min^{-1}; **g)** CarboSil-PEO-Hep-TM in the presence of an NO flux of ca. 1.0×10^{-10} mol·cm^{-2}·min^{-1}. (n = 4 for each set of data) (* Activity of TM < 1.0 ng APC·cm^{-2}·min^{-1}).

In the presence of a surface NO flux of 1.0×10^{-10} mol cm^{-1} min^{-1}, the immobilized TM's activity on CarboSil-TG-COOH was determined to be 69.2 ± 1.9 ng APC cm^{2} min^{-1} (see Figure 2.5). The 6-fold increase in the activity of surface-bound TM on CarboSil-TG-COOH compared to CarboSil-Gly-COOH may be attributed to the longer chain that

links TM onto the surface and hence better accessibility of thrombin and PC to TM's active site.

Neither CarboSil-PEO-NH_2 nor CarboSil-PEO-Hep showed observable response in the PC assay. However, CarboSil-PEO-Hep-TM exhibited a significant TM activity of 316.0 ± 31.9 ng APC cm^2 min^{-1} (see Figure 2.5). This is quite reasonable given that the PEO moiety together with heparin, would form an extremely flexible spacer between TM and the polymeric surface. Hence, the immobilized TM should be quite accessible to thrombin and PC. However, it is also possible that the high local concentration of negatively-charged heparin may also contribute to the strong association of thrombin with immobilized TM for PC activation. It is conceivable that an approximation model, akin to those described for serpin-heparin-protease 'ternary complex' formation, may also contribute to the apparent activity increase[28].

TM has long been recognized for its thermostability[29]. In this study, we evaluated the stability of the surface-bound TM. An insignificant loss (< 10 %) of activity of TM immobilized on CarboSil-Gly-COOH was observed over a five-month period when CarboSil-Gly-TM coatings were stored in PBS at 4 °C (n = 4) (see Figure 2.6A). Furthermore, almost 70 % of the original activity of TM is maintained over a four-week period in PBS at 37 °C (n = 4) (see Figure 2.6B). Based on our extensive experience with the NO release coatings of the type used in this work, constant fluxes of NO for up to 2 weeks at 37°C is typically observed[11,13,21] which is quite compatible with the TM lifetime under similar conditions.

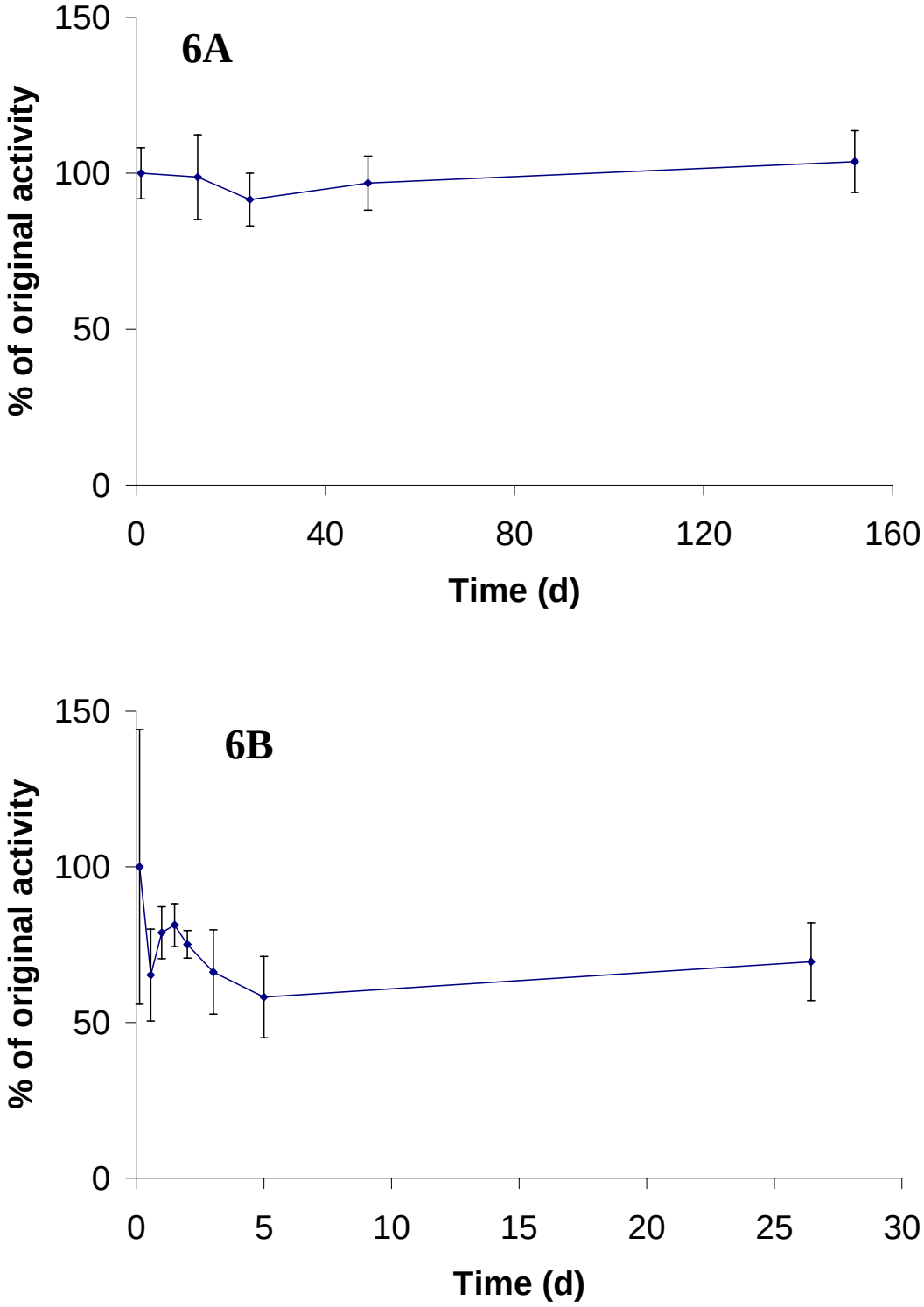

Figure 2.6. Stability of CarboSil-Gly-TM stored in PBS (pH 7.4) a) at 4 °C over a five-month period, b) under 37 °C over a four-week period. TM activity was determined by PC assay (n = 4).

The polymeric surfaces with immobilized TM were also incubated in sheep plasma for 1 h at 37 ^{o}C to assess whether plasma components can decrease TM activity. However, it was found that functional TM activity (based on APC assay) actually increased by approx. 30 % after exposure to the plasma. One possible reason is that some components in plasma might adhere onto the polymeric surfaces and cause the activation of PC and/or the cleavage of the chromogenic substrate. Further experiments are needed to verify this hypothesis.

The activity of surface-bound heparin immobilized by the same procedure used here have been evaluated in our earlier work and found to be 4.80 ± 0.08 mU/cm^2 on poly(vinyl chloride) (PVC) and 6.39 ± 0.08 mU/cm^2 on PU surfaces[13]. The activity of surface-bound heparin here was found to be 5.34 ± 0.71 mU/cm^2 (see Figure 2.7), which is comparable to the previous results. After the immobilization of TM, heparin's activity drops to 4.34 ± 0.20 mU/cm^2, a possible result of the loss of COOH groups during the TM immobilization process as well as the steric hindrance from the large TM molecule, now linked to the surface appended heparin.

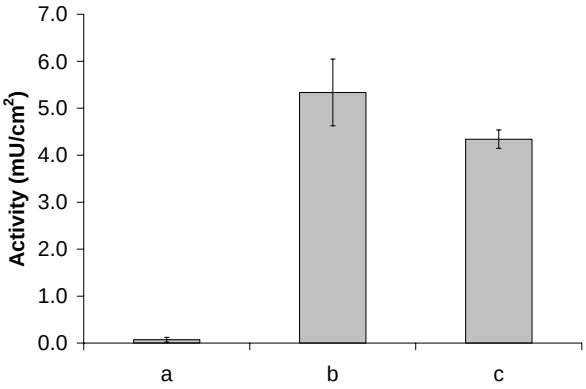

Figure 2.7. Heparin activity of modified CarboSil surfaces (all determined by anti-FXa assay in the presence of an NO flux of approx. 1.0×10^{-10} mol cm^{-2} min^{-1}): **a)** CarboSil-PEO-NH_2; **b)** CarboSil-PEO-Hep; **c)** CarboSil-PEO-Hep-TM. (n = 4 for each set of data)

2.3.6. NO Release from Polymeric Coatings with Surface-Bound TM and/or Heparin

The release of NO from the underlying polymer film containing the *N*-diazeniumdiolates (DBHD/N_2O_2) is driven by protons[11]. Therefore, exposure of this class of NO donors to physiological conditions stimulates NO release. The addition of KTpClPB, a lipophilic tetraphenylborate derivative, into the polymer coating is critical to maintain a low enough pH within the organic polymer phase to promote continued NO release[11]. In previous work, various polymer formulations and coating procedures using DBHD/N_2O_2 to fine-tune the flux and duration of NO release from hydrophobic coatings were examined[11, 13]. The flux of NO can range from 0.5 to 60 × 10^{-10} mol cm^{-2} min^{-1} (physiological level ca. 1.0 × 10^{-10} mol cm^{-2} min^{-1} [30]) and the duration can be longer than 2 weeks[13], depending on the specific polymer film composition.

In this work it was also found that by increasing the thickness of the top-layer, the NO release rate decreases. By dip-coating the SR catheter sleeves (pre-coated with NO donor containing layer) in carboxylated/aminated CarboSil solutions of different concentrations (1 to 4 w/v %), top layers with different thickness could be applied which would result in different NO fluxes (see Figure 2.8).

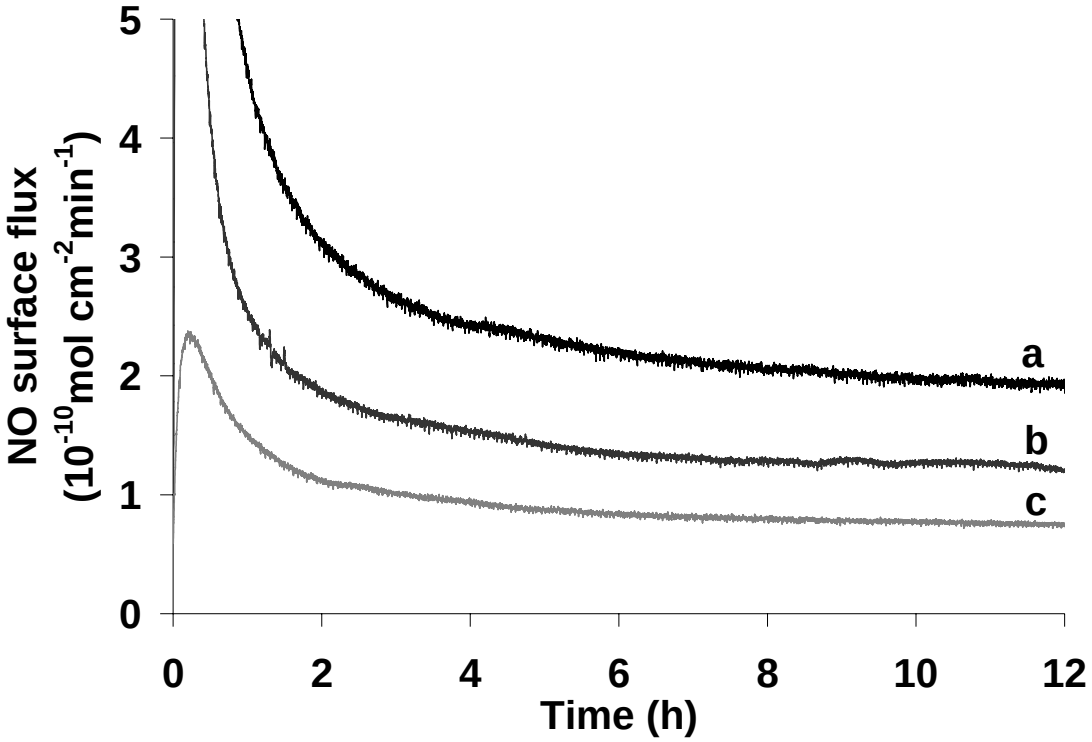

Figure 2.8. NO flux levels of DBHD/N_2O_2-loaded SR catheter sleeves before TM immobilization. The underlying layers of all three coatings were loaded with 8 wt % of DBHD/N_2O_2 and an equimolar KTpClPB, while the top-coatings were made by dip-coating the catheter sleeves into 1 w/v % **(a),** 2 w/v % **(b)** and 4 w/v % **(c)** solutions of CarboSil-Gly-COOH in DMAc/THF, respectively.

Most importantly, the immobilization procedures, which involved the contact between the coatings and water for ca. 12 h (TM immobilization on carboxylated CarboSil) to 18 h (TM and heparin immobilization on aminated CarboSil), have very limited effect on the NO flux (see Figures 2.9 and 2.10). It has been reported previously that ca. 1-2 % of NO loss was found for a PVC coating (PVC:DOS = 1:1) after ca. 8-10 h in contact with aqueous solution at room temperature[13]. Thus, it can be predicted that the NO loss during the TM and heparin immobilization process using the more hydrophobic PurSil polymer reported here (with DBHD/N_2O_2 doped PurSil as the underlying layer and

functionalized CarboSil as the top layer) should also be quite small compared to the NO reservoir in the underlying polymer film.

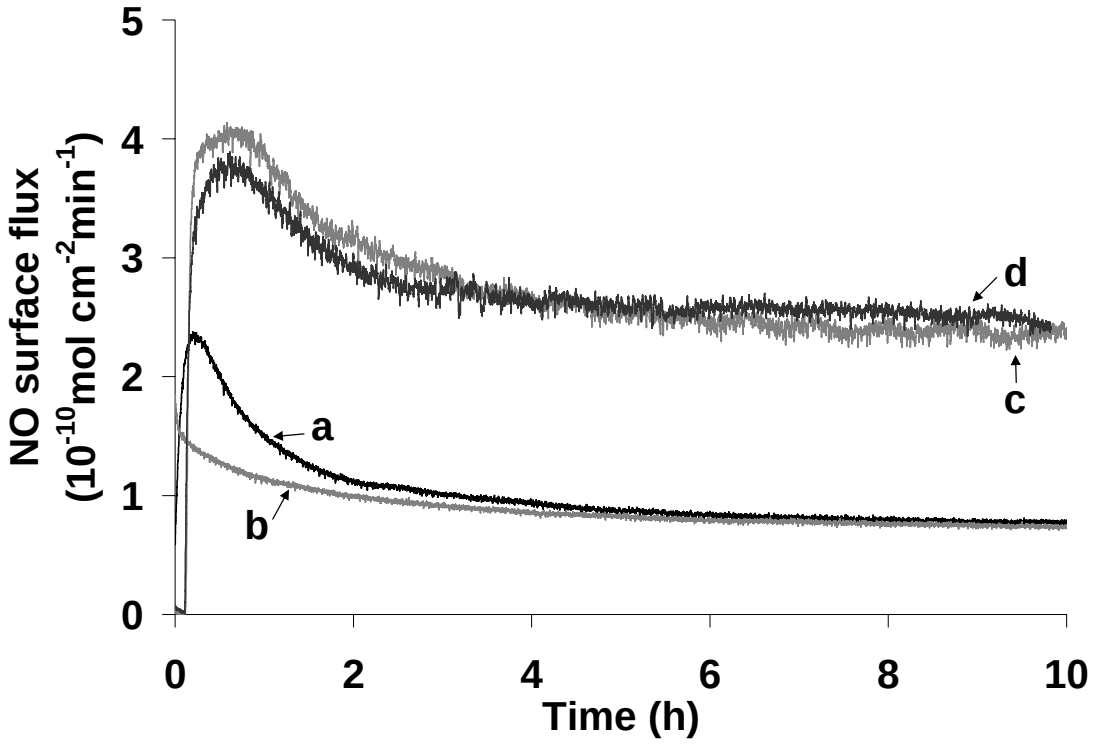

Figure 2.9. NO flux profiles of SR catheter sleeves before/after TM immobilization. The underlying layers of all four coatings were loaded with 8 wt % of DBHD/N_2O_2 and an equimolar amount of KTpClPB. The top-coatings were made by dip-coating the catheter sleeves in 4 % (w/v) solution of CarboSil-Gly-COOH (**a** and **b**) or 1 % (w/v) solution of CarboSil-TG-COOH (**c** and **d**). Coatings **b** and **d** were further immobilized with TM. **a)** CarboSil-Gly-COOH; **b)** CarboSil-Gly-TM; **c)** CarboSil-TG-COOH; **d)** CarboSil-TG-TM.

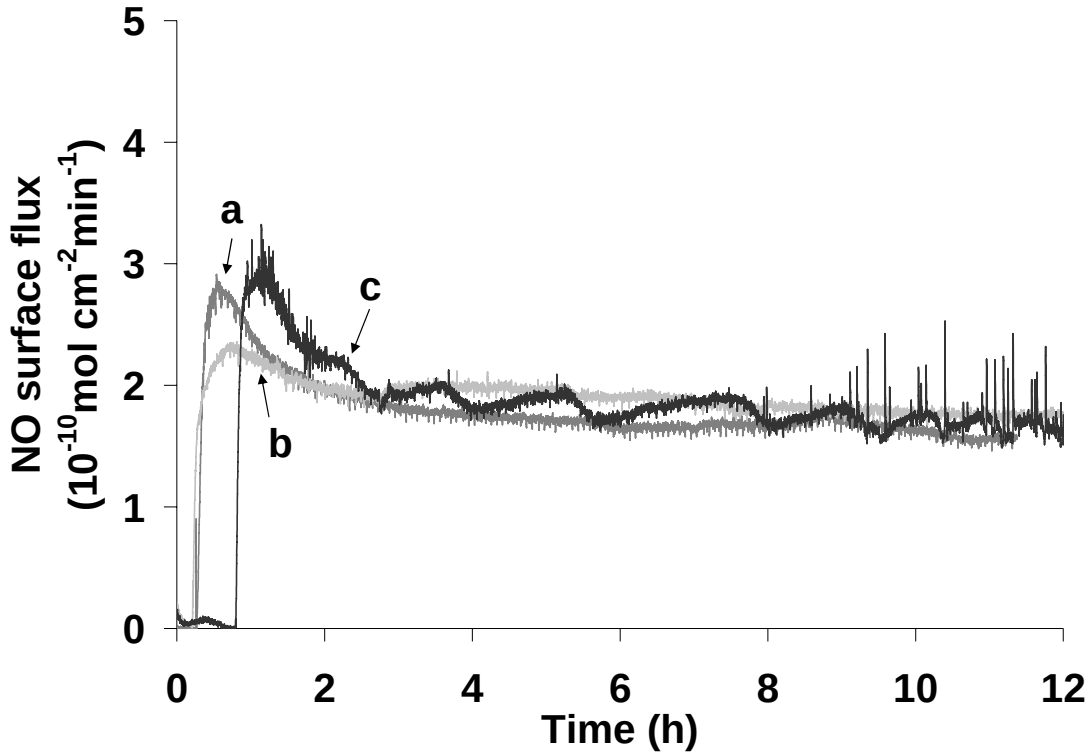

Figure 2.10. NO flux profiles of SR catheter sleeves before and after heparin/TM immobilization. The underlying layers of all three coatings were loaded with 8 wt % of DBHD/N_2O_2 and an equimolar amount of KTpClPB. The top-coatings were made by dip-coating the catheter sleeves in 1 % (w/v) DMAc/THF solution of CarboSil-PEO-NH_2. **a)** CarboSil-PEO-NH_2; **b)** CarboSil-PEO-Hep; **c)** CarboSil-PEO-Hep-TM.

NO release properties before and after plasma incubation were investigated by NOA. No significant change has been observed whether with or without surface-bound TM (see Figure 2.11).

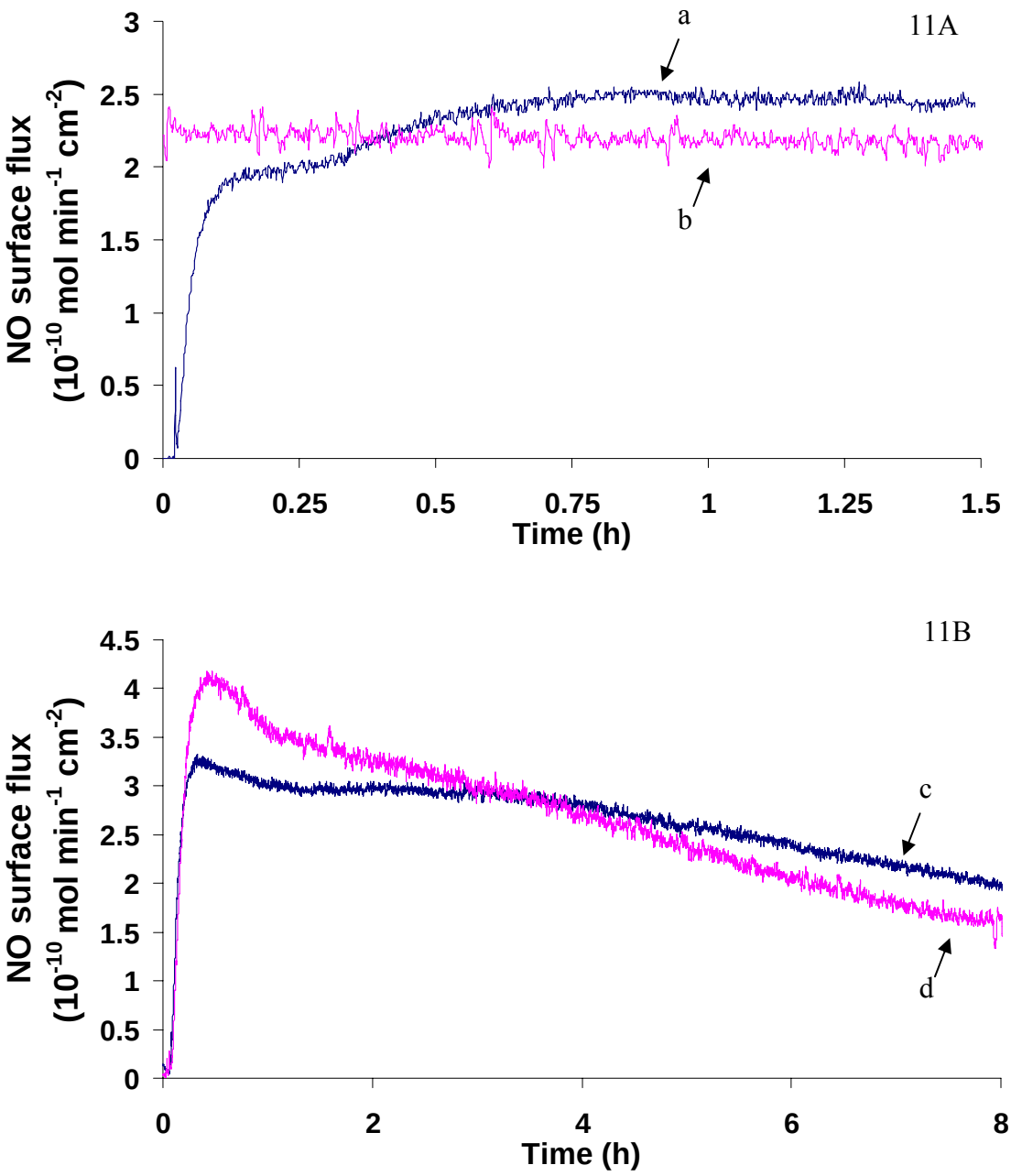

Figure 2.11. NO flux profiles of SR catheter sleeves before/after TM immobilization. The underlying layers of both coatings were loaded with 8 wt % of DBHD/N_2O_2 and an equimolar amount of KTpClPB. Both top-coatings were made by dip-coating the catheter sleeves in 4 % (w/v) solution of CarboSil-Gly-COOH. Coating **11B** was further immobilized with TM. Both coatings were incubated in sheep plasma for 1 h at 37 °C under static conditions. **a)** CarboSil-Gly-COOH before plasma incubation; **b)** CarboSil-Gly-COOH after plasma incubation; **c)** CarboSil-Gly-TM before plasma incubation; **d)** CarboSil-Gly-TM after plasma incubation.

2.3.7. Preliminary In Vitro Study of Blood Compatibility of the Bilayer Polymeric Coatings

In recent years, the lactate dehydrogenase present within platelets has been reported to provide a useful approach to study *in vitro* platelet adhesion on chemically and/or physically modified surfaces. In previous work, the LDH assay has been used to assess the platelet adhesion on NO-releasing PVC coatings[21]. In this work, a decreased amount (19.8 ± 2.7 %) of adhered platelets was detected on NO-releasing polymeric coatings compared with polymer coatings without NO release. However, the presence of surface-immobilized TM had no significant effect on platelet adhesion (see Figure 2.12 and Table 2.3). This is expected since NO, being a potent anti-platelet agent, can prohibit platelet activation and adhesion, while TM is an anticoagulant agent which asserts its antithrombotic activity in triggering the PC pathway which will down regulate the coagulation cascade. This effect of TM has already been successfully demonstrated in the previous section of the APC assays.

Table 2.3. Coating information.

Coating	Underlying Layer	Top Layer
a	N/A	CarboSil-Gly-COOH
b	Loaded with 8 wt % of DBHD/N_2O_2 and an equimolar amount of KTpClPB.	CarboSil-Gly-COOH
c	N/A	CarboSil-Gly-TM
d	Loaded with 8 wt % of DBHD/N_2O_2 and an equimolar amount of KTpClPB.	CarboSil-Gly-TM

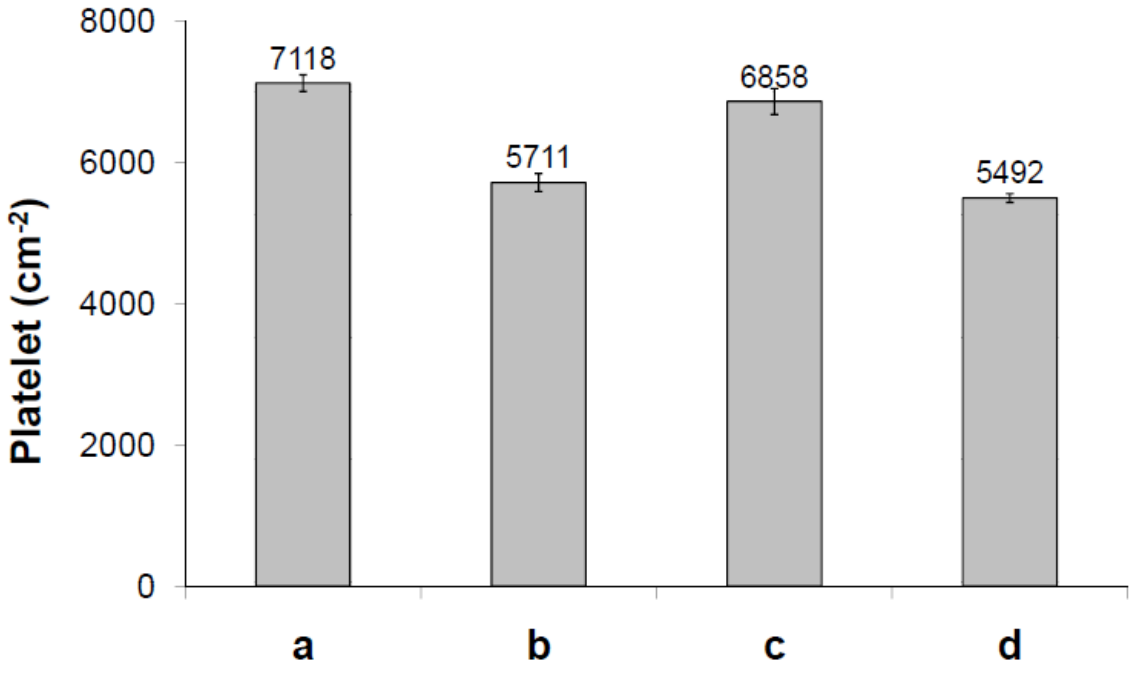

Figure 2.12. Platelet adhesion on various polymeric coatings prepared by dip coating. All coatings were incubated in sheep plasma for 1 h at 37 °C under static conditions. Adhered platelets were quantified by LDH assay. Coating information is listed in Table 2.3 above.

Similar results were also observed using SEM to image the platelet adhesion and activation on the various surfaces (see Figure 2.13). Films were prepared in the same way as listed in Table 2.3, except that glass slides were used as substrates in the place of SR tubes and spin coating was used to coat the substrate instead of dip coating. This deviation in sample preparation is required due to the nature of the static plasma incubation setting. From the SEM images, it can be seen that there was almost no activation of adhered platelets, not only on polymers with NO release and immobilized TM, but also on control polymeric coatings. This might be due to the already improved biocompatibility of the CarboSil-based top layers, compared to PVC and other less biocompatible polymeric materials.

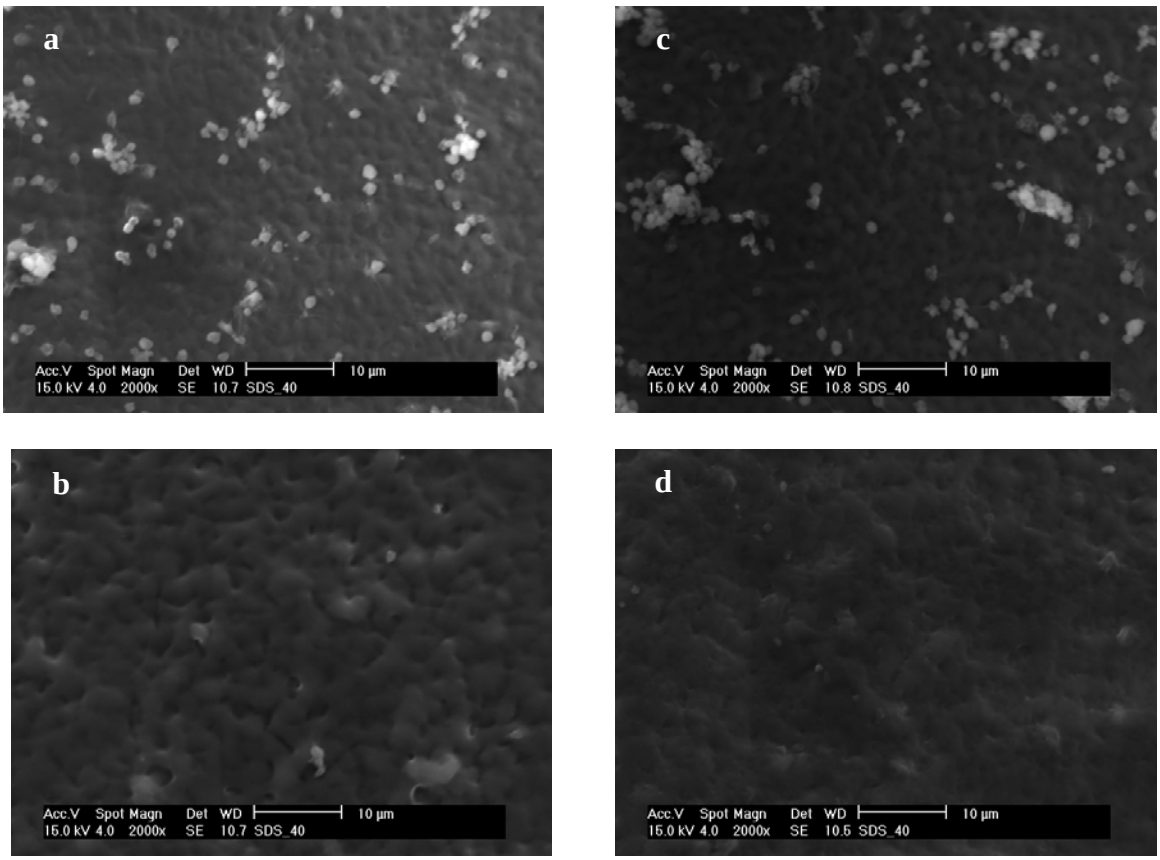

Figure 2.13. Platelet adhesion on various polymeric coatings prepared by spin coating. All coatings were incubated in sheep plasma for 1 h at 37 °C under static conditions. Polymeric urfaces and adhered platelets were characterized by SEM. Coating information is listed in Table 2.3 above.

2.4. Conclusions

Multifunctional bilayer polymeric coatings have been fabricated with both controlled NO release and surface-bound active TM or combined TM and heparin. The outer layer was made of a commercially available SR-PU copolymer (CarboSil). This outer coating material can be either carboxylated or aminated via an allophanate reaction

with a diisocyanate compound followed by a urea-forming reaction with an amino acid (glycine), an oligopeptide (triglycine) or a diprimary amine. Carboxylated CarboSil (CarboSil-Gly/TG-COOH) was used to immobilize TM through the formation of an amide bond between the surface COOH groups and the lysine residues of TM molecule. Aminated CarboSil (CarboSil-PEO-NH_2) was first heparinized, and the COOH groups on heparin could be further used to anchor TM. The anticoagulant activity of TM and heparin were evaluated by PC and anti-FXa assay, respectively. It should be noted that the length of the spacer was critical to the activity of surface-bound TM in that longer spacers likely rendered TM's active site more accessible to its substrates, and this, in turn, resulted in higher activity. Surface-bound TM showed very good stability when stored in PBS (pH 7.4) both at 4 °C and at 37 °C. Immobilized heparin maintained most of its activity after the immobilization of TM to its COOH functional groups.

The underlying layer was made with another commercial SR-PU copolymer (PurSil) mixed with a lipophilic NO donor (DBHD/N_2O_2). The NO release rate could be tuned by controlling different loadings of NO donors as well as by changing the coating procedures. In this work, we could control the NO fluxes around physiological level by applying top coatings with different thicknesses. The immobilization of TM and heparin had little influence on NO release levels, and NO release did not influence the activity of surface-bound heparin and TM.

2.5. References

1. Peppas, N.A.; Langer, R. 'New challenges in biomaterials.' *Science* **1994,** 263, 1715-1720.

2. Ratner, B.D. 'Blood compatibility - a perspective.' *J. Biomater. Sci-Polym. E* **2000,** 11, 1107-1119.

3. Xue, L.; Greisler, H.P. 'Biomaterials in the development and future of vascular grafts.' *J. Vasc. Surg.* **2003,** 37, 472-480.

4. Moncada, S.; Palmer, R.M.J.; Higgs, E.A. 'Nitric-oxide – physiology, pathophysiology, and pharmacology.' *Pharmacol. Rev.* **1991,** 43, 109-142.

5. Vane, J.R.; Botting, R.M. 'Pharmacodynamic profile of prostacyclin.' *Am. J. Cardiol.* **1995,** 75, A3-A10.

6. Woodhouse, K.A.; Weitz, J.I.; Brash, J.L. 'Lysis of surface-localized fibrin clots by adsorbed plasminogen in the presence of tissue plasminogen activator.' *Biomaterials* **1996,** 17, 75-77.

7. Hoylaerts, M.; Owen, W.G.; Collen, D. 'Involvement of heparin chain-length in the heparin-catalyzed inhibition of thrombin by antithrombin-III.' *J. Biol. Chem.* **1984**, 259, 5670-5677.

8. Whitelock, J.M.; Iozzo, R.V. 'Heparan sulfate: A complex polymer charged with biological activity.' *Chem. Rev.* **2005,** 105, 2745-2764.

9. Esmon, C.T. 'The roles of protein-C and thrombomodulin in the regulation of blood-coagulation.' *J. Biol. Chem.* **1989**, 264, 4743-4746.

10. Munoz, E.M.; Linhardt, R.J. 'Heparin-binding domains in vascular biology.' *Arterioscl. Throm. Vas.* **2004,** 24, 1549-1557.

11. Batchelor, M.M.; Reoma, S.L.; Fleser, P.S.; Nuthakki, V.K.; Callahan, R.E.; Shanley, C.J.; Politis, J.K.; Elmore, J.; Merz, S.I; Meyerhoff, M.E. 'More lipophilic dialkyldiamine-based diazeniumdiolates: Synthesis, characterization, and application in preparing thromboresistant nitric oxide release polymeric coatings.' *J. Med. Chem.* **2003,** 46, 5153-5161.

12. Wissink, M.J.B.; Beernink, R.; Pieper, J.S.; Poot, A.A.; Engbers, G.H.M.; Beugeling, T.; van Aken, W.G.; Feijen, J. 'Immobilization of heparin to EDC/NHS-crosslinked collagen. Characterization and in vitro evaluation.' *Biomaterials* **2001,** 22, 151-163.

13. Zhou, Z.R.; Meyerhoff, M.E. 'Preparation and characterization of polymeric coatings with combined nitric oxide release and immobilized active heparin.' *Biomaterials* **2005,** 26, 6506-6517.

14. Esmon, N.L.; Owen, W.G.; Esmon, C.T. 'Isolation of a membrane-bound cofactor for thrombin-catalyzed activation of protein-C.' *J. Biol. Chem.* **1982,** 257, 859-864.

15. Chromogenix 'Protein C Product Monograph**' 1995.**

16. Parkinson, J.F.; Grinnell, B.W.; Moore, R.E.; Hoskins, J.; Vlahos, C.J.; Bang, N.U. 'Stable expression of a secretable deletion mutant of recombinant human thrombomodulin in mammalian-cells.' *J. Biol. Chem.* **1990,** 265, 12602-12610.

17. Moreau, J.J.E.; Vellutini, L.; Man, M.W.C.; Bied, C.; Dieudonne, P.; Bantignies, J.L.; Souvajol, J.L. 'Lamellar bridged silsesquioxanes: Self-assembly through a combination of hydrogen bonding and hydrophobic-interactions.' *Chem-Eur. J.* **2005,** 11, 1527-1537.

18. Pittelkow, M.; Christensen, J.B.; Meijer, E.W. 'Guest-host chemistry with dendrimers: Stable polymer assemblies by rational design.' *J. Polym. Sci. A1* **2004,** 42, 3792-3799.

19. Bello. D.; Streicher, R.P.; Woskie, S.R. 'Evaluation of the NIOSH draft method 5525 for determination of the total reactive isocyanate group (TRIG) for aliphatic isocyanates in autobody repair shops.' *J. Environ. Monitor.* **2002,** 4, 351-360.

20. Bio-Rad Laboratories 'Bio-Rad Protein Assay.'

21. Wu, Y.D.; Zhou, Z.R.; Meyerhoff, M.E. 'In vitro platelet adhesion on polymeric surfaces with varying fluxes of continuous nitic oxide release.' *J. Biomed. Mater. Res. A* **2007,** 81A, 956-963.

22. Gunatillake, P.A.; Martin, D.J.; Meijs, G.F.; McCarthy, S.J.; Adhikari, R. 'Designing biostable polyurethane elastomers for biomedical implants.' *Aust. J. Chem.* **2003,** 56, 545-557.

23. Park, K.D.; Piao, A.Z.; Jacobs, H.; Okano, T.; Kim, S.W. 'Synthesis and characterization of SPUU-PEO-heparin graft-copolymers.' *J. Polym. Sci. A1* **1991,** 29, 1725-1737.

24. Sperling, C.; Salchert, K.; Streller, U.; Werner, C. 'Covalently immobilized thrombomodulin inhibits coagulation and complement activation of artificial surfaces *in vitro*.' *Biomaterials* **2004,** 25, 5101-5113.

25. Akashi, M.; Maruyama, I.; Fukudome, N.; Yashima, E. 'Immobilization of human thrombomodulin on glass-beads and its anticoagulant activity.' *Bioconjugate Chem.* **1992,** 3, 363-365.

26. Han, H.S.; Yang, S.L.; Yeh, H.Y.; Lin, J.C.; Wu, H.L.; Shi, G.Y. 'Studies of a novel human thrombomodulin immobilized substrate: surface characterization and anticoagulation activity evaluation.' *J. Biomater. Sci-Polym. E* **2001,** 12, 1075-1089.

27. Tseng, P.Y.; Jordan, S.W.; Sun, X.L.; Chaikof, E.L. 'Catalytic efficiency of a thrombomodulin-functionalized membrane-mimetic film in a flow model.' *Biomaterials* **2006**, 27, 2768-2775.

28. De Cristofaro, R.; De Candia, E.; Landolfi, R. 'Effect of high- and low-molecular-weight heparins on thrombin-thrombomodulin interaction and protein C activation.' *Circulation* **1998,** 98, 1297-1301.

29. Suzuki, K.; Kusumoto, H.; Hashimoto, S. 'Isolation and characterization of thrombomodulin from bovine lung.' *Biochim. Biophys. Acta.* **1986**, 882, 343-352.

30. Vaughn, M.W.; Kuo, L.; Liao, J.C. 'Estimation of nitric oxide production and reaction rates in tissue by use of a mathematical model.' *Am. J. Physiol.* **1998,** 274, H2163-H2176.

CHAPTER 3

Combining Nitric Oxide and Sirolimus in Polymeric Films: Potential Coatings for Stents and Other Blood-Contacting Medical Devices

3.1. Introduction

As has been mentioned in Chapter 1, thrombosis is not the only problem associated with blood-contacting medical devices. In many cases, smooth muscle cell (SMC) proliferation can be the problem as well. In the treatment of coronary artery disease, balloon angioplasty and stenting have become common procedures for the relief of arterial stenosis and to restore normal blood flow. Over time, this traditional bare-metal stent (BMS) is fully endothelialized. In roughly a third of bare-metal stenting cases, however, restenosis occurs. Tissue engulfs the stent, leading to the reduction of the blood flow, and in turn, to the subsequent coronary symptoms (see Figure 1.8). This type of restenosis is believed to be the result of an inflammatory response to injury from the initial angioplasty procedure and to the BMS itself[1].

Drug-eluting stents (DES) were developed to prevent the kind of restenosis seen with BMSs. Drug eluting stents differ from bare-metal stents mainly in that

they are coated with a polymeric coating containing a drug meant to interfere with the process of restenosis. Paclitaxel and sirolimus (rapamycin) are the most widely used drugs on DESs[13-16]. Over time, these drugs inhibit the proliferation and migration of SMCs and inflammatory cells responsible for restenosis.

Sirolimus (see Figure 1.9) is a macrolide antibiotic with potent antifungal, immunosuppressive and antimitotic properties[2]. In December 1999, the first sirolimus-eluting stents were implanted in human cornary arteries and the first published human study by Sousa *et al*. in 2001 showed a nearly complete elimination of neointimal hyperplasia[3]. However, recent findings have suggested an increased risk of late-stage thrombosis associated with DESs due to the incomplete endothelialization on the surface of the struts of the stents as sirolimus can also retard the migration and proliferation of endothelial cells (ECs)[4]. As described in Chapter 1, the drugs can prevent or delay full endothelialization of the stent allowing platelets, red blood cells, fibrin and white blood cells to adhere to the exposed struts of the stents, leading in a small fraction of patients to late-stage thrombosis[1]. The resulting thrombi can lead to narrowing or complete occlusion of the lumin which may lead to myocardioinfarction. Hence, the use of anti-restenotic drugs alone may only solve part of the issues associated with stent placement. Indeed, similar thrombosis and SMC proliferation problems exist in the case of implanted vascular grafts as well[17,18].

In addition to its antithrombotic property, some researchers have also found that nitric oxide (NO) release can enhance EC growth on surfaces. It has been reported by Dr. West's research group at Rice University that NO releasing PUs were able to promote endothelialization and suppress platelet adhesion[5,6], thus may reduce the possibility of

stent thrombosis. If this is true, NO release would help solve the fundamental problem associated with DESs, since the presence of NO would prevent thrombosis early on and then further facilitate the EC growth.

Hence, the use of a naturally occurring anti-thrombotic/anti-platelet agent such as NO, in combination with an anti-cell proliferation agent may provide the ideal solution to reduce both clotting and restenosis risk for stents as well as vascular grafts and other implanted medical devices.

Herein, we describe the first dual-functional polymeric coating that releases both sirolimus and NO[7]. The new coating can potentially suppress the migration and proliferation of SMC and at the same time, exhibit decreased thrombus formation and enhanced endothelialization.

3.2. Experimental

3.2.1. Materials and Instrumentation

Phosphate buffered saline (PBS, pH 7.4) and *N*,*N*-dimethylacetamide (DMAc) were purchased from Sigma-Aldrich (St. Louis, MO). Tetrahydrofuran (THF) was obtained from Fisher Scientific (Pittsburgh, PA) and was distilled over sodium and benzophenone prior to use. Potassium tetrakis(*p*-chlorophenyl)borate (KTpClPB), acetonitrile (both reagent and HPLC grade) and trifluoroacetic acid (TFA) were also purchased from Fisher. Sirolimus (rapamycin) was purchased from LC Laboratories (Woburn, MA). Silicone rubber RTV 3140 coating was purchased from Dow Corning Corporation (Midland, MI). PurSil-20-80A and CarboSil-20-90A were generous gifts

from The Polymer Technology Group (Berkeley, CA). Tecoflex-SG-60D was a gift from Lubrizol Advanced Materials (Cleveland, OH). DBHD/N_2O_2 was synthesized by treating *N,N'*-dibutyl-1,6-hexanediamine (DBHD, Aldrich) with NO gas (80 psi, Cryogenic Gases (Detroit, MI)) at room temperature for 24 h as previously described[8].

Nitric oxide flux from polymer coatings was measured by a chemiluminescent NO analyzer (NOA™ 280, Sievers Instruments, Inc. (Boulder, CO)). Sirolimus release rate was determined by high-performance liquid chromatography (HPLC)-based analysis (Hewlett Packard 1050 HPLC system). A scanning electron microscope (Philips XL30 FEG, FEI Company (Hillsboro, OR)) was used to characterize the morphology of the coatings.

3.2.2. Preparation of Polymer Coatings

Diazeniumdiolated *N,N'*-dibutyl-1,6-hexanediamine (DBHD/N_2O_2) was synthesized by treating *N,N'*-dibutyl-1,6-hexanediamine in CH_3CN with NO (80 psi)[8]. The NO release polymeric coatings were prepared using a method similar to that previously reported by our group[9]. A cocktail containing well-suspended DBHD/N_2O_2 in a DMAc/THF solution of 4 wt % PurSil (a commercial silicone-poly(ether)urethane copolymer) was made. Silicone rubber (SR) tubings were then dip-coated with this cocktail to form an NO release underlayer. A 1:1 molar ratio of KTpClPB (a lipophilic borate salt) was added to help reduce pH changes within polymeric coatings during the decomposition process of DBHD/N_2O_2. The concentrations of DBHD/N_2O_2 and KTpClPB in the cocktail were determined based on the calculation that DBHD/N_2O_2 constituted 16 wt% of the final underlying layer. Silicone rubber catheter sleeves (2.5

cm in length) were sealed at one end with Dow Corning 3140 RTV SR and cured overnight under ambient conditions. Afterwards, they were dip-coated with the DBHD/N_2O_2 containing cocktail 8 times at 20-min intervals and then dried overnight.

The tubings were further dip-coated twice with 20 min interval in a DMAc/THF solution of sirolimus and PurSil, CarboSil (a commercial silicone-poly(carbonate)urethane copolymer) or Tecoflex™ (a polyether polyurethane) to form a sirolimus releasing top-layer (see Scheme 3.1). The polymer concentration was 4 w/v% for PurSil and CarboSil and 2 wt % for Tecoflex. The concentrations of sirolimus in the cocktail were determined based on the calculation that sirolimus constituted 23 wt % of the final top layer. The catheter sleeves were allowed to dry overnight, followed by vacuum drying at room temperature for additional 2 d to remove any residual solvent. The final NO/SiroRel coatings were stored at -20 ºC for characterization of NO and sirolimus release and other studies.

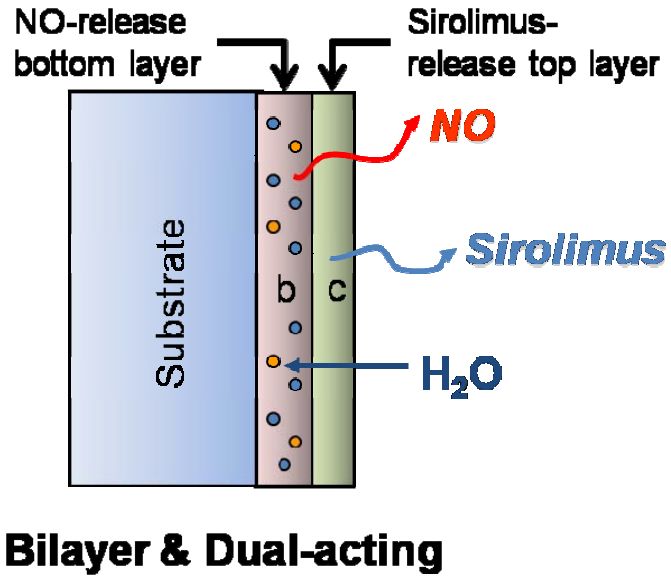

Scheme 3.1. Polymeric coating – combining NO and sirolimus release.

3.2.3. Scanning Electron Microscopy (SEM) of NOGen/SiroRel Films

Scanning electron microscopic characterization was performed with a Philips/FEI XL30 FEG SEM Electron Microscope. The electron beam was operated at 15 kV and the sample chamber pressure was 10^{-6} torr. Polymeric coatings were dried under vacuum for 2 d and then sputtered with gold prior to acquiring the SEM images.

3.2.4. Sirolimus Release Studies

To determine the pharmacological release kinetics of sirolimus, films were immersed in PBS (10 mM, pH 7.4) at 37 °C. Samples taken at distinct time points were then subjected to high-performance liquid chromatography (HPLC)-based analysis (Hewlett Packard 1050 HPLC system). Total releasable sirolimus was extracted with methanol overnight at 37 °C. The sirolimus methanol solution was injected to HPLC for quantification. Tables 3.1 and 3.2 provide detailed instrument and gradient parameters.

Table 3.1. Instrument parameters.

Item	**Parameter**
Mobile Phase – Solvent A	0.1 v/v % TFA (aq.)
Mobile Phase – Solvent A	0.1 v/v % TFA (acetonitrile)
Column	Waters, XBridge™ C_{18}, 4.6 × 150 mm, 5 μm
Injector Volume	100 μL
UV Detector Wavelength	278 nm
Auto Zero on Inject Start	enabled
Run time	9.5 min

Table 3.2. Binary solvent gradient profile parameter.

Section	Time (min)	Flow (mL/min)	% A	% B
1	0.00	1.0	90.0	10.0
2	2.00	1.0	90.0	10.0
3	22.00	1.0	70.0	30.0
4	27.00	1.0	10.0	90.0
5	32.00	1.0	10.0	90.0
6	35.00	1.0	90.0	10.0
7	40.00	1.0	90.0	10.0

3.2.5. Chemiluminescence Measurements of NO Release

Nitric oxide released from the polymeric coatings was measured using a Sievers Chemiluminescence NO Analyzer. The instrument was calibrated before each experiment using an internal two-point calibration (zero gas and 45 ppm NO gas). NO was continuously swept from the headspace of the sample vessel and purged from the bathing solution with a nitrogen sweep gas into the chemiluminescence detection chamber. The flow rate was set to 50 mL/min with a chamber pressure of 5.4 torr and an oxygen pressure of 6.0 psi.

3.3. Results and Discussion

3.3.1. Preparation of NO/Sirolimus Release Polymeric Coatings

SEM was used to characterize the morphology of the coatings on the SR tubings. For a typical coating, SEM images illustrate that the DBHD/N_2O_2 containing underlying layer has a thickness of ca. 30 μm while that of the sirolimus containing outer layer is ca. 15 μm (see Figure 3.1).

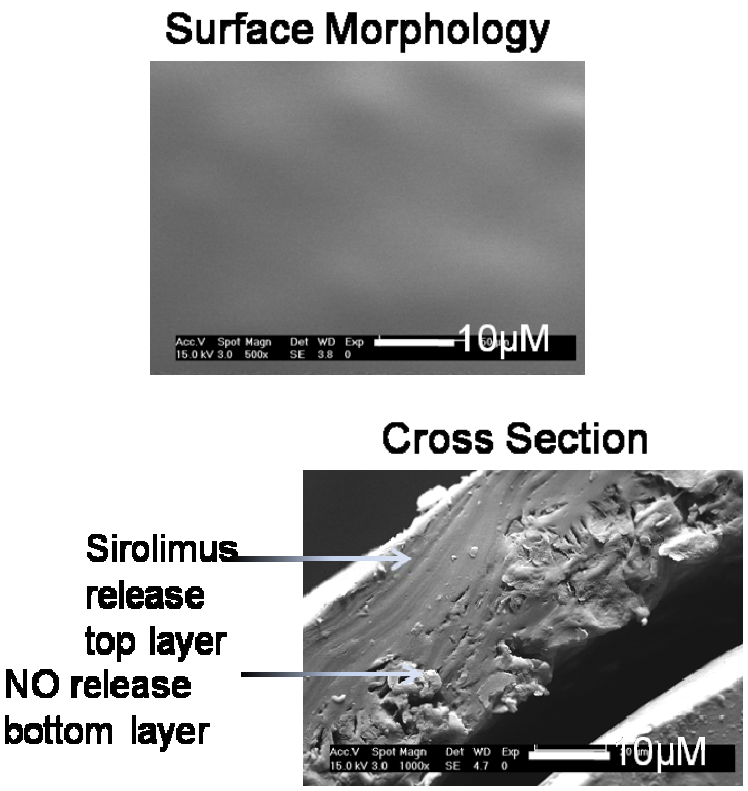

Figure 3.1. Representative SEM images of surface and cross section of NO/sirolimus release polymeric coatings.

3.3.2. Sirolimus Release Kinetics

For determination of pharmacological release kinetics, coated tubings were submersed in 300 µL PBS (pH 7.4) at 37 °C. Samples harvested at distinct time points were subjected to HPLC-based analysis. Figure 3.2 shows the typical chromatogram of sirolimus. Based on the chromatograms, the peak with a retention time of 18.6 min was the peak corresponding to sirolimus and its area could be used for quantification purposes. Figure 3.3 shows the representative calibration curve.

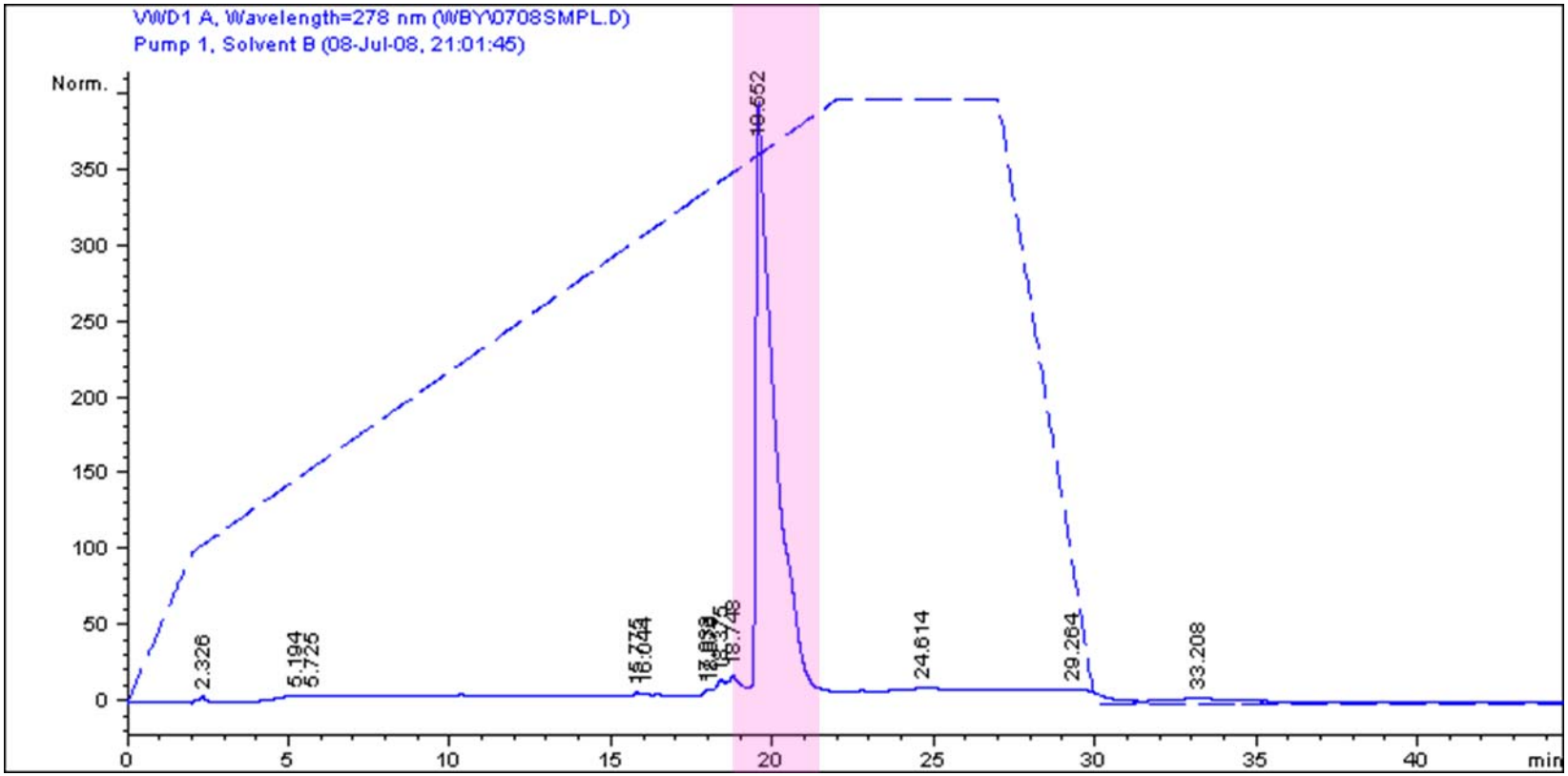

Figure 3.2. Representative chromatogram of sirolimus.

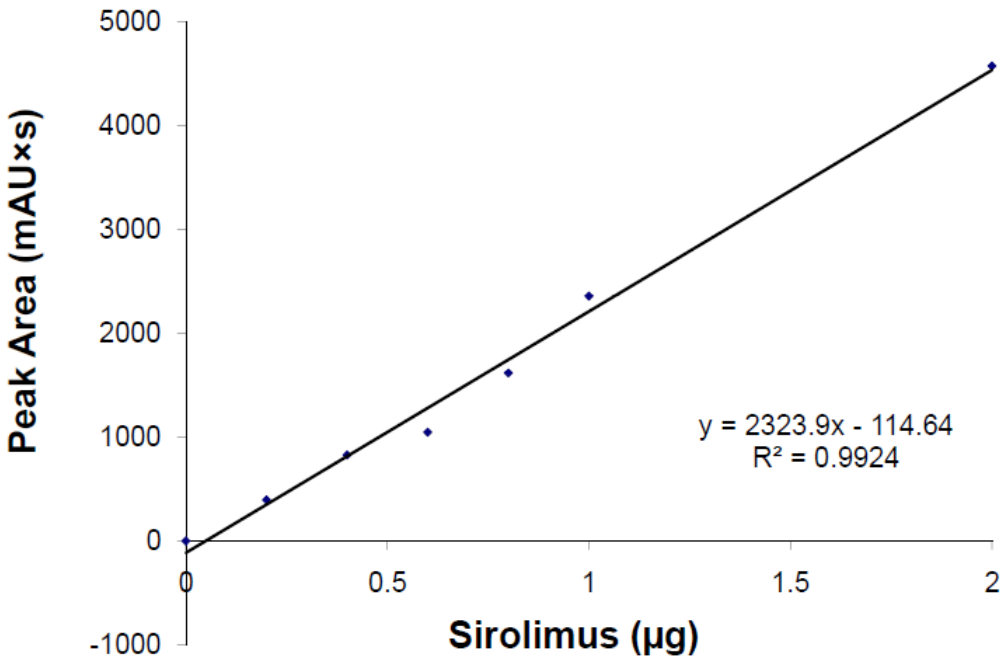

Figure 3.3. Calibration curve of sirolimus.

The sirolimus release rate was calculated according to Eqn. 3.1 below. In both cases using PurSil and CarboSil as the outer layer, sirolimus' release rate slowly decreased from ca. 3.00 to 0.10 µg cm^{-2} h^{-1} over a period of 300 h (ca. 2 weeks) (Figures 3.4 and 3.5). In the case where Tecoflex was employed as the top coating matrix, due to the reduced concentration of polymer cocktail, a lower sirolimus release rate and a shorter release window was observed (Figure 3.6).

$$SirolimusReleaseRate = \frac{SirolimusAmoutOnColumn \times \frac{ExtractionVolume}{InjectionVolume}}{ExtractionTime \times SurfaceArea} \quad \textbf{Eqn. 3.1.}$$

(In this study, the extraction volume is 300 µL, the injection volume is 100 µL, the extraction time is 1 h and the surface area is 0.572 cm^2.)

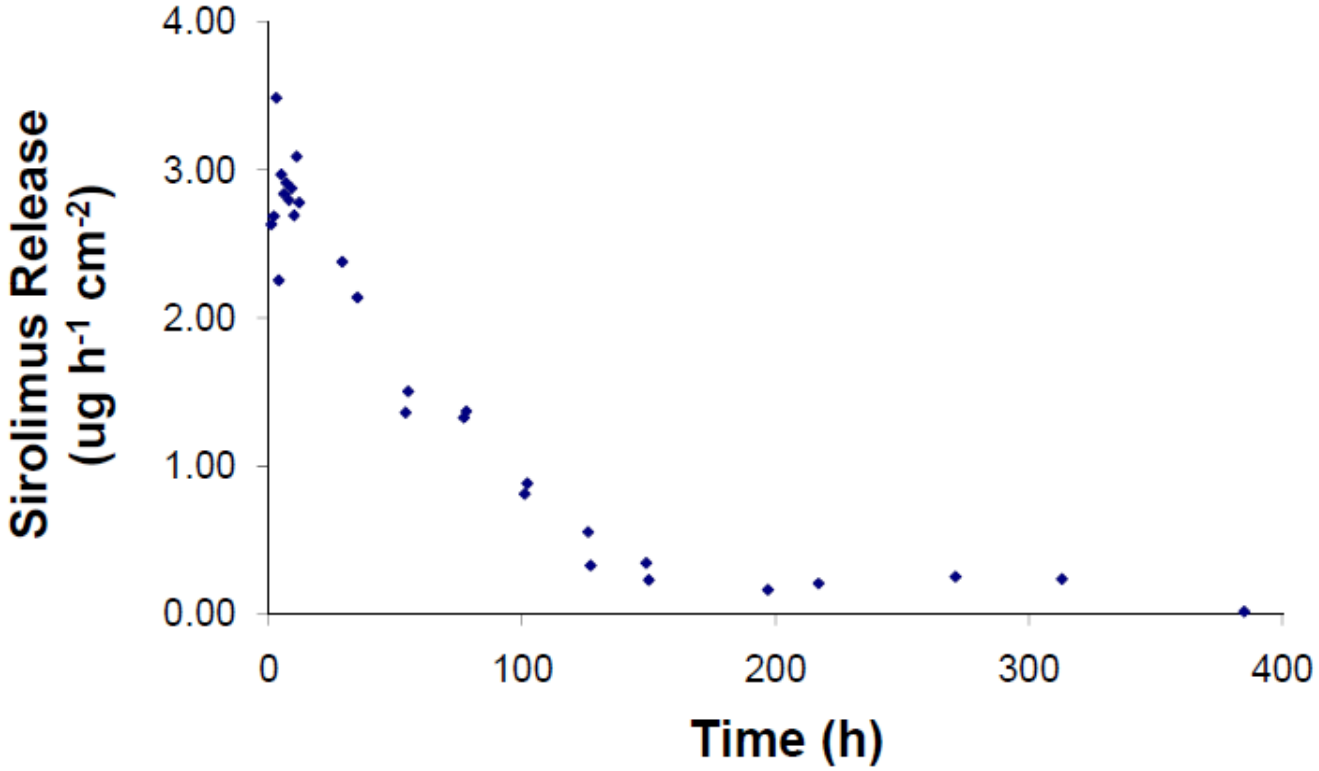

Figure 3.4. HPLC measurement of sirolimus release from a polymeric coating with NO-releasing underlying layer (16 wt % DBHD/N_2O_2 in PurSil) and PurSil top layer with 23 wt % of sirolimus. The coating was incubated in PBS (pH 7.4) under 37 °C with intermittent sampling.

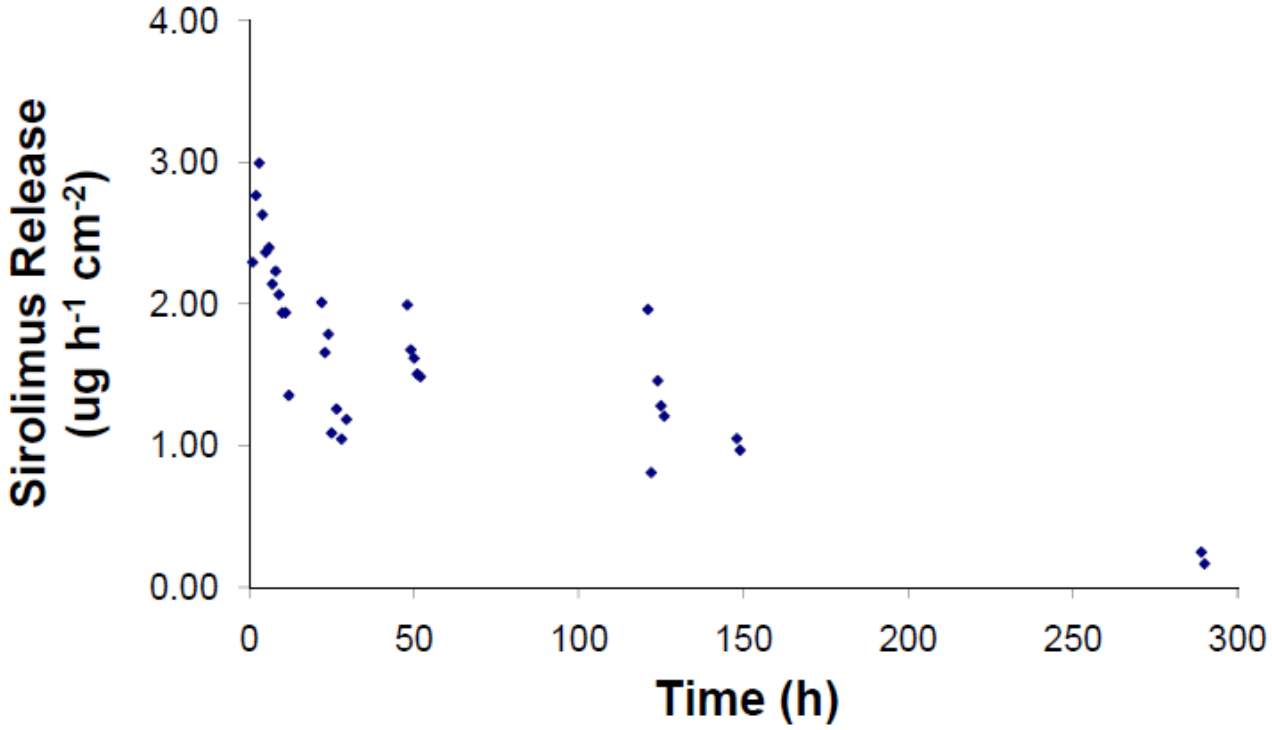

Figure 3.5. HPLC measurement of sirolimus release from a polymeric coating with NO-releasing underlying layer (16 wt % of DBHD/N_2O_2 in PurSil) and CarboSil top layer with 23 wt % of sirolimus. The coating was incubated in PBS (pH 7.4) under 37 °C with intermittent sampling.

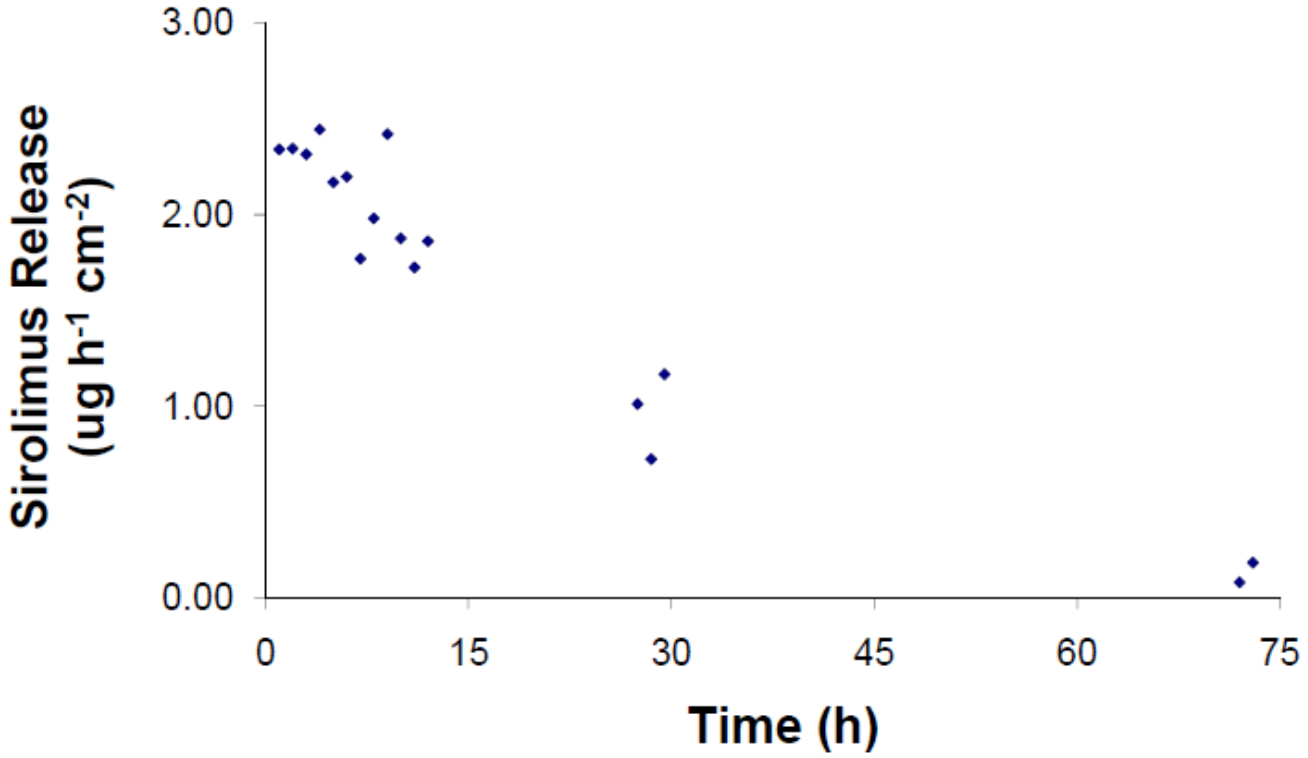

Figure 3.6. HPLC measurement of sirolimus release from a polymeric coating with NO-releasing underlying layer (16 wt % DBHD/N_2O_2 in PurSil) and Tecoflex top layer with 23 wt % of sirolimus. The coating was incubated in PBS (pH 7.4) under 37 °C with intermittent sampling. The thickness of this sirolimus-containing Tecoflex top layer is about half of those made of PurSil and CarboSil (see Figures 3.4 and 3.5).

When PurSil was used as the top layer, determination of total sirolimus dosage was performed by drug elution in 300 µL ethanol overnight at 37 °C. Sirolimus amounts were quantified by HPLC. The total releasable sirolimus from coatings with PurSil as the top layer matrix was estimated to be approximately 300 µg cm^{-2}. This is almost twice as much as the dosage of the sirolimus-coated BX Velocity stent (Cordis) (140 µg sirolimus cm^{-2})[3].

3.3.3. NO Release Studies

To prepare NO release coatings, DBHD/N_2O_2, a lipophilic NONOate, was incorporated into the underlying PurSil films to release NO. The release of NO from DBHD/N_2O_2 is proton driven[8] (see Scheme 3.2). The resulting diamines formed after the decomposition of hydrophilic diazeniumdiolates can potentially leach out of the polymer matrix and react with an oxidative intermediate of NO to form carcinogenic nitrosamines. However, DBHD/N_2O_2 is highly lipophilic and thus the corresponding diamine DBHD will stay predominately within the polymeric matrix.

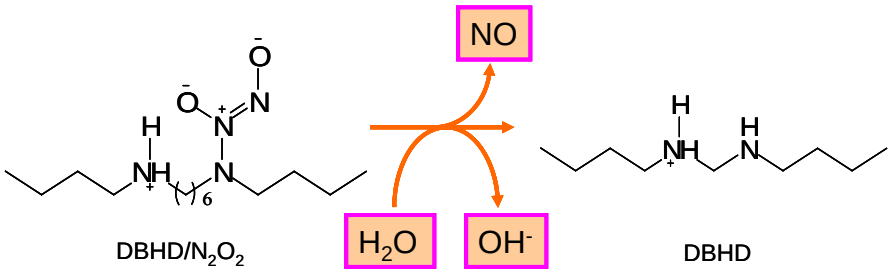

Scheme 3.2. Proton-driven decomposition of DBHD/N_2O_2.

Nitric oxide flux from polymer coatings was measured at 37 °C in PBS (pH 7.4) by a chemiluminescent NO analyzer. The NO flux released from the coatings slowly decreased from ca. 10.0×10^{-10} to 1.0×10^{-10} mol cm^{-2} min^{-1} over a two-week period after an initial burst (Figures 3.7 and 3.8). This trend is observed in both coatings with PurSil and CarboSil as their top layers. Such a level is comparable to the NO released from a healthy endothelium (ca. 1×10^{-10} mol cm^{-2} min^{-1})[10].

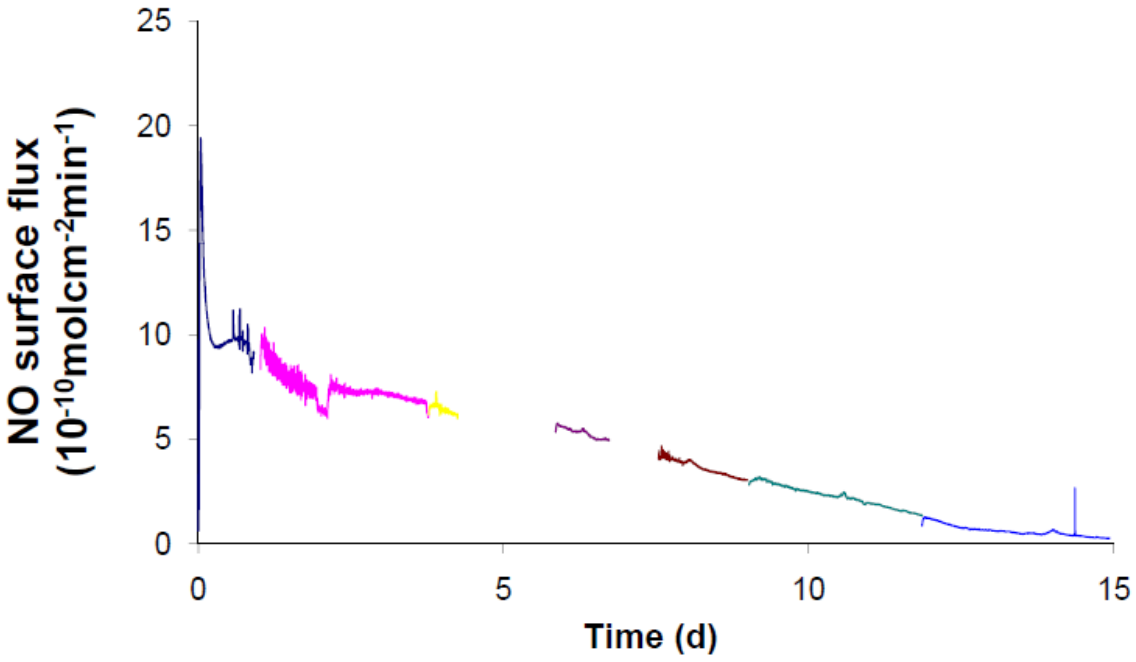

Figure 3.7. NO levels of DBHD/N_2O_2-loaded (16 wt % in PurSil underlying layer) SR tubings with PurSil sirolimus-releasing top layers (incubated in PBS (pH 7.4) under 37 °C). NO release was measured at specific time slots and the data were then integrated into the graph above. Data were not collected in the gaps.

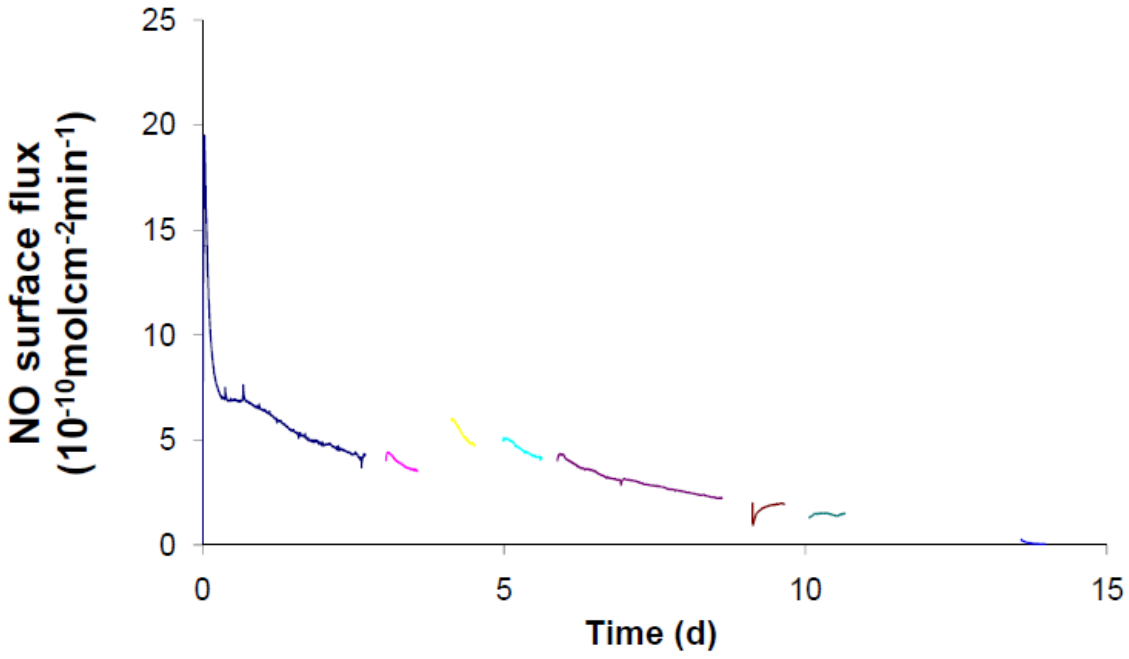

Figure 3.8. NO levels of DBHD/N_2O_2-loaded (16 wt % in PurSil underlying layer) SR tubings with CarboSil sirolimus-releasing top layers (incubated in PBS (pH 7.4) under 37 °C). NO release was measured at specific time slots and the data were then integrated into the graph above. Data were not collected in the gaps.

3.4. Conclusions

A new type of polymeric coating that can simultaneously release both NO (as an antithrombotic agent) and sirolimus (as an antiproliferative agent) was prepared and studied. Various polyurethanes (PurSil, CarboSil and Tecoflex) have been used to prepare the underlying layer and the top layer of these polymer coatings. NO and sirolimus release kinetics were studied using chemiluminescence measurements and HPLC, respectively. The NO flux released from the coatings slowly decreased from approx. 10.0×10^{-10} to 1.0×10^{-10} mol cm^{-2} min^{-1} (physiological NO flux is approx. 1.0×10^{-10} mol cm^{-2} min^{-1}) over a two-week period after an initial burst. In both cases using

PurSil and CarboSil as the outer layer, sirolimus' release rate slowly decreased from ca. 3.00 to 0.10 μg cm^{-2} h^{-1} also over a two-week period, which is comparable to the NO release duration.

Such a coating proved the concept of combining NO and sirolimus controlled release. However, while this may be useful for some biomedical devices such as small-bore vascular grafts, such coatings would be far too thick if they are to be applied to drug-eluting stents on which the coatings are usually less than 20 μm in thickness. Hence, efforts will also be made on reducing the coating thickness so that they can be used as top coatings on medical devices that require thin-layer coatings. Further, by combining sirolimus release with new NO-generating polymeric coatings (to be discussed in Chapter 5), the presence of higher surface levels of NO could be maintained for extended time periods.

3.5. References

1. http://www.nhlbi.nih.gov/health/dci/Diseases/Angioplasty/Angioplasty_Risks.html
2. Marx, S.; Marks, A. 'Bench to bedside: The development of rapamycin and its application to stent restenosis.' *Circulation* **2001**, 104, 852-855.
3. Sousa, J.; Serruys, P.; Costa, M. 'New Frontiers in Cardiology: Drug-Eluting Stents: Part I.' *Circulation* **2003**, 107, 2274-2279.
4. Shuchman, M. 'Trading restenosis for thrombosis? New questions about drug-eluting stents.' *N. Engl. J. Med.* **2006**, 355, 1949-1952.
5. Jun, H.W.; Taite, L.J.; West, J.L. 'Nitric oxide-producing polyurethanes.' *Biomacromolecules* **2005**, 838-844.

6. Taite, L.J.; Jun H.W.; Yang, P.; West J.L. 'Nitric oxide-releasing polyurethane-PEG copolymer containing the YIGSR peptide promotes endothelialization with decreased platelet adhesion.' *J. Biomed. Mater. Res. B* **2007**, 108-116.

7. Wu, B.; Studzinski, D.; Shanley, C. J.; Meyerhoff, M.E. 'Combining antiplatelet and antiproliferation – polymeric coatings that release both nitric oxide and rapamycin.' *Polymeric Materials: Science and Engineering* **2008**, 99, 78-79.

8. Batchelor, M.M.; Reoma, S.L.; Fleser, P.S.; Nuthakki, V.K.; Callahan, R.E.; Shanley, C.J. 'More lipophilic dialkyldiamine-based diazeniumdiolates: synthesis, characterization, and application in preparing thromboresistant nitric oxide release polymeric coatings.' *J. Med. Chem.* **2003**, 46, 5153–5161.

9. Zhou, Z.R.; Meyerhoff, M.E. 'Preparation and characterization of polymeric coatings with combined nitric oxide release and immobilized active heparin.' *Biomaterials* **2005**, 26, 6506–6517.

10. Vaughn, M.W.; Kuo, L.; Liao, J.C. 'Estimation of nitric oxide production and reaction rates in tissue by use of a mathematical model.' *Am. J. Physiol.* **1998,** 274, H2163-H2176.

11. Cha, W.; Meyerhoff, M.E. '*S*-Nitrosothiol detection via Amperometric nitric oxide sensor with surface modified hydrogel layer containing immobilized oganoselenium catalyst.' *Langmuir* **2006**, 22, 10830-10836.

12. Cha, W.; Meyerhoff M.E. 'Catalytic generation of nitric oxide from *S*-nitrosothiols using immobilized oganoselenium species.' *Biomaterials* **2007,** 28, 19-27.

13. http://www.cypherstent.com/cypher-stent/specifications/pages/index.aspx.

14. http://www.stent.com/DisplayPage.bsci/id/3/1a1/m/IC/heart-stent-products/landing.html/page.bsc

15. Boston Scientific 'Express^2 Monorail Coronay Stent Delivery System and Over-the-Wire Stent Delivery System – Instructions for Use.'

16. Boston Scientific 'Liberte Monorail Over-the-Wire Coronary Stent System – Instructions for Use.'

17. O'Brien, J.E. ; Ormont, M.L.; Shi, Y.; Wang, D.; Zalewski, A.; Mannion, J.D. 'Early injury to the media after saphenous vein grafting.' *Ann. Thorac. Surg.* **1998,** 65, 1273-1278.

18. Hanson, S.R.; Kotze, H.F.; Savage, B.; Harker, L.A. 'Platelet interactions with Dacron vascular grafts – A model of acute thrombosis in baboons.' *Arteriosclerosis* **1985**, 5, 595-603.

CHAPTER 4

Potassium Tetrakis[3,5-bis(trifluoromethyl)phenyl]borate and Sulfonated Polyurethanes for Sustained Nitric Oxide Release from Diazeniumdiolate Doped Polymer Films: Solution to Borate Cytotoxicity Problem

4.1. Introduction

In Chapter 3 it was proposed that the use of a naturally occurring anti-thrombotic/anti-platelet agent, such as nitric oxide (NO)[1], in combination with an anti-cell proliferation agent may provide the ideal solution to reduce both clotting and restenosis risk for stents as well as vascular grafts and other implanted medical devices. Indeed, the first dual-functional polymeric coating that releases both sirolimus (rapamycin[2]) and NO was described in that chapter.

It should be noted that in order to achieve long-term release of NO from polymeric materials using diazeniumdiolate type NO donors, anionic site additives are required within the polymeric films[3]. These additives actually serve as 'buffers' to ensure that the pH of the organic phase remains low enough to promote exhaustive reaction of the diazeniumdiolate species (Scheme 4.1). Without the anionic site additives,

generation of excess secondary amines in the polymer after initial release of NO will cause the pH within the organic films to increase, decreasing NO production from the remaining diazeniumdiolates (Figure 4.1). In studies to date, potassium tetrakis(*p*-chlorophenyl)borate (KTpClPB) (Figure 4.2) has generally been employed as the polymer additive, typically at 100 mol % of the diazeniumdiolate concentration in the polymer film.

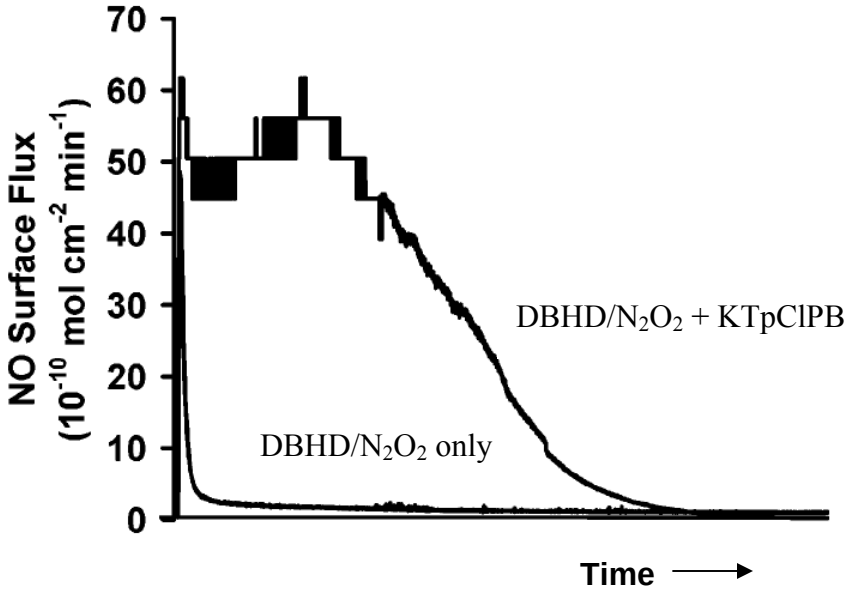

Figure 4.1. NO surface flux for diazeniumdiolated *N,N'*-dibutyl-1,6-hexanediamine (DBHD/N_2O_2) dispersed in a 1:2 PVC/DOS matrix (circular disks with a diameter of 8 mm and a thickness of 150 μm) with and without potassium tetrakis(*p*-chlorophenyl)borate (KTpClPB) (1:1 mol ratio KTpClPB:DBHD/N_2O_2) soaked in PBS buffer (pH 7.4) at 37 °C. NO was measured directly by chemiluminescence. Figure adapted from Batchelor M.M. *et al, J. Med. Chem.* **2003**[3]. The stepwise signal at higher NO level is because NO flux reached the low sensitivity range of NOA (> 700 ppb) when the NOA response changes every 100 ppb. NO signals were converted from NOA output (ppb) to surface flux (10^{-10} mol cm^{-2} min^{-1}) per coating surface area.

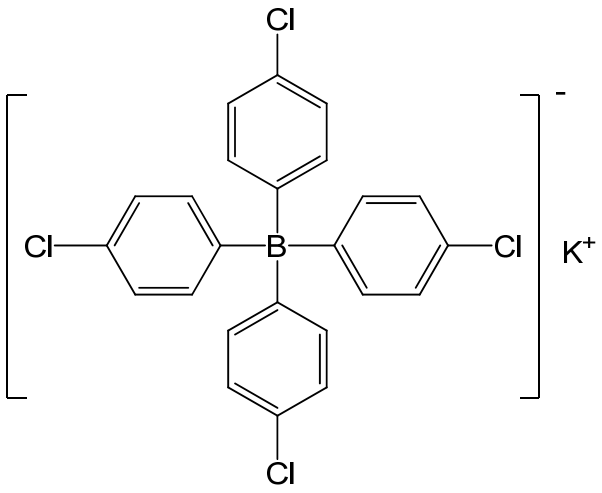

Figure 4.2. Structure of KTpClPB.

In order to assess whether the new coating described in Chapter 3 really suppresses the migration and proliferation of smooth muscle cells (SMCs), and at the same time, exhibits decreased thrombus formation and enhanced endothelialization, we collaborated with Dr. Charles Shanley at Beaumont Hospital (Royal Oak, MI). The compatibility with respect to the growth of endothelial cells (ECs) and SMCs directly on the surface of such films has been examined. Interestingly, during the course of these studies, it was found that both EC and SMC growth was inhibited on one of the control polymeric films which contained only the borate additive, KTpClPB. Such inhibition of cell proliferation was not observed on plain biomedical grade PurSil polymers that do not contain the borate species.

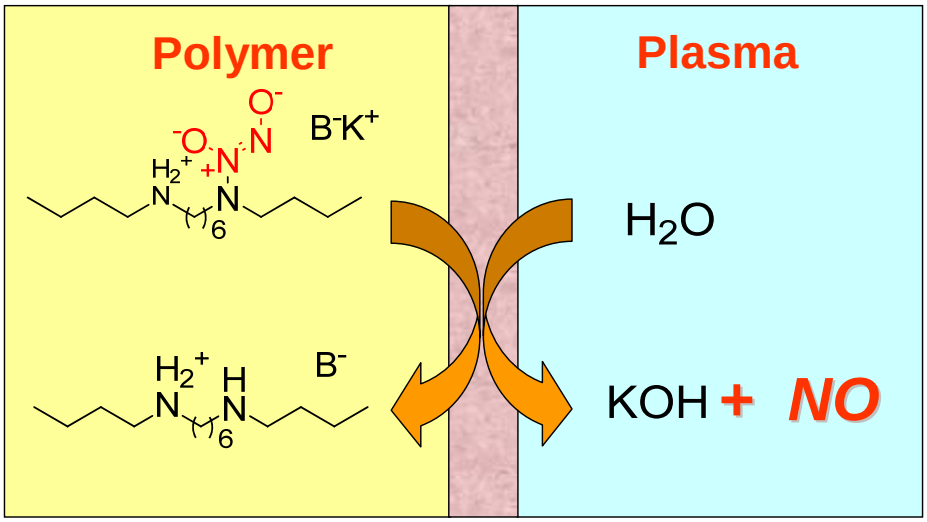

Scheme 4.1. Proton-driven decomposition of diamine diazeniumdiolates and buffering effect of borate additives in the polymer matrix.

The cytotoxicity towards ECs and SMCs suggested that there were some toxicity issues with respect to the use of this borate additive as a polymeric-phase pH stabilizer. KTpClPB is very lipophilic and does not leach appreciably from the films[4]. However, it is possible that potentially toxic radical species can be generated due to the cleavage of the carbon-boron bond in the proton-induced or oxidative degradation of the KTpClPB species[5]. Furthermore, the resulting triphenylboronates could also leach out of the polymeric phase and be toxic to cells.

Several studies have been published comparing the stability of various tetraphenylborate derivatives[6] since they have been commonly used as the anionic additives in ion-selective polymeric membrane electrodes[4]. While KTpClPB has been found to be more stable than simple sodium tetraphenylborate (NaTPB, Figure 4.3a), potassium tetrakis[3,5-bis(trifluoromethyl)phenyl]borate (KTFPB, Figure 4.3b) has been

found to be even more lipophilic, and substantially more stable and less susceptible to acid-catalyzed degradation than KTpClPB[6]. The electron withdrawing properties of the fluorine atoms significantly decrease the electron density of the boron anionic site, which in turn, significantly increases the stability of the tetraphenylborate species.

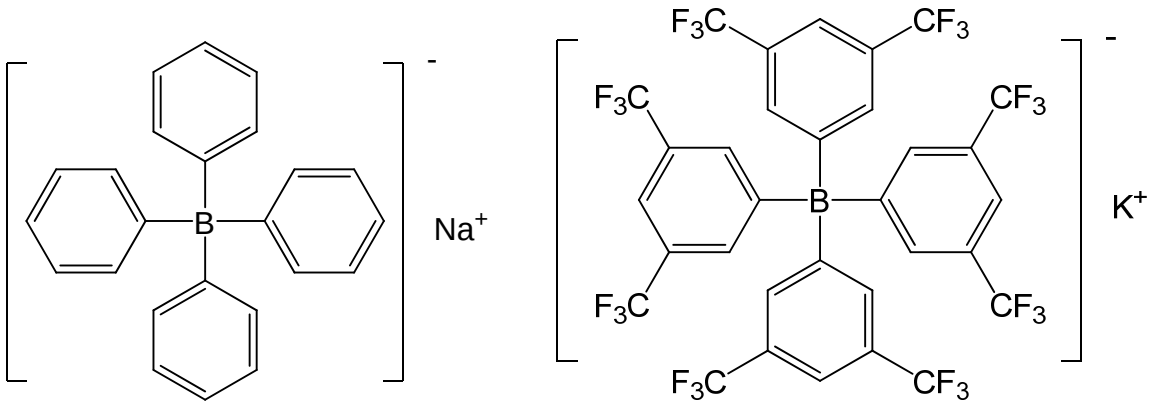

Figure 4.3. a (Left) – Structure of NaTPB; **b (Right)** – Structure of KTFPB.

Therefore, to overcome the lack of stability and apparent cytotoxicity of KTpClPB, the use of KTFPB was investigated to prepare polymer coatings that can release NO on nearly constant fluxes for extended time periods.

In addition to using the small molecule additives as the pH buffering agents in the polymeric films, the potential of a new sulfonated derivative of biomedical grade polyurethanes (PUs) is also examined in this chapter (Scheme 4.2). Since the sulfonate anionic groups are chemically tethered to the polymer backbones[7], the possibility of the leaching of low molecular weight species would be eliminated.

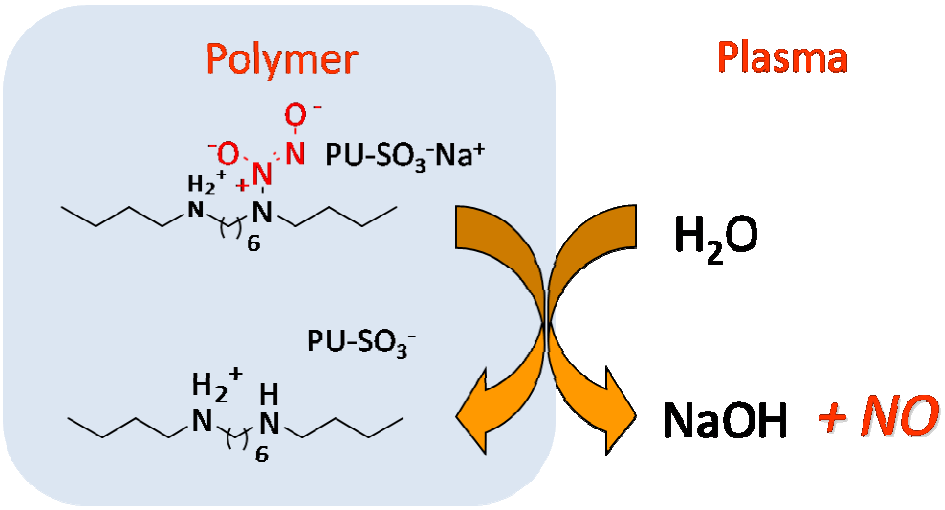

Scheme 4.2. Proton-driven decomposition of diamine diazeniumdiolates and buffering effect of sulfonate groups in the polymer matrix.

Herein, the new polymeric coatings with more lipophilic and stable borate and polymer-tethered sulfonate groups are examined as the pH stabilizer in the NO releasing polymeric coatings. Such non-toxic endothelium-mimicking polymeric coatings can potentially be used in various blood-contacting medical devices including vascular grafts, heart valves, extracorporeal circuits and stents.

4.2. Experimental

4.2.1. Materials and Instrumentation

Phosphate buffered saline (PBS, pH 7.4), sulfuric acid, hydrochloric acid, sodium hydride (60 w/w % suspension in mineral oil), propane sultone, anhydrous diethyl ether, ethanol and *N*,*N*-dimethylacetamide (DMAc) were purchased from Sigma-Aldrich (St. Louis, MO). Tetrahydrofuran (THF) was from Fisher Scientific (Pittsburgh, PA) and was

distilled over sodium and benzophenone prior to use. KTpClPB, KTFPB, methanol, acetonitrile (both reagent and HPLC grade) and trifluoroacetic acid (TFA) were also purchased from Fisher. Sirolimus (rapamycin) was obtained from LC Laboratories (Woburn, MA). PurSil-20-80A was a gift from The Polymer Technology Group (Berkeley, CA). Tecoflex-SG-80A and Tecophilic-93A-100 were gifts from Lubrizol Advanced Materials (Cleveland, OH). DBHD/N_2O_2 was synthesized by treating *N,N'*-dibutyl-1,6-hexanediamine (DBHD, Aldrich) with NO gas (80 psi, Cryogenic Gases (Detroit, MI)) at room temperature for 24 h as previously described in Chapter 2.

Reagents for the *in vitro* studies were as follows: Human umblicial artery smooth muscle cells (SMC), human umbilical vein endothelial cells (EC), SMGM®-2 smooth muscle growth medium Bullet Kit and EGM®-2 endothelial cell growth medium Bullet Kit were purchased from Lonza Group Ltd. (Switzerland). Costar 24 well culture plates, glasscover slips (12 mm), neutral buffered formalin, aqueous mounting medium and glass slides were all products of Thermo Fisher Scientific (Hanover Park, IL). Dulbecco's phosphate buffered saline (D-PBS) and Hoechst 33342 nuclear dye were purchased from Invitrogen (Carlsbad, CA). Hematoxylin QS was from Vector Labs (Burlingame, CA),

Nitric oxide flux from polymer coatings was measured by a chemiluminescent NO analyzer (NOA™ 280, Sievers Instruments, Inc. (Boulder, CO)). Cells were imaged on a Nikon TE 2000 fluorescent microscope. Elemental (carbon, hydrogen, nitrogen, sulfur and oxygen) combustion analysis was performed by Carol Carter with a Perkin-Elmer 2400 Series II CHNS/O Analyzer (PerkinElmer Life And Analytical Sciences, Inc, Waltham, MA) in the Chemistry Department of University of Michigan (Ann Arbor, MI). Thermal profiles of polymers were characterized by a TA Q2000 differential scanning

calorimeter (DSC) (TA Instrument, New Castle, DE). UV-Vis spectra were recorded with a Shimadzu UV-1601 UV-VIS spectrometer (Shimadzu Scientific Instruments, Columbia, MD).

4.2.2. Preparation of NO-Release Polymer Coatings and Control Coatings on Glass Coverslips with Borate Additives

DBHD/N_2O_2 was synthesized by treating *N,N'*-dibutyl-1,6-hexanediamine in acetonitrile with NO (80 psi)[3]. The NO release polymeric coatings for cell culture experiments were prepared on clear glass coverslips with a diameter of 12 mm (surface area = 1.19 mm^2). A cocktail containing well-suspended DBHD/N_2O_2 in a DMAc/THF (2:3, v/v) solution of 4 wt % PurSil was made. A 1:1 molar ratio of borate, either KTpClPB or KTFPB, was added to help reduce pH changes within polymeric coatings during the decomposition process of DBHD/N_2O_2. The concentrations of DBHD/N_2O_2 and borates in the cocktail were determined based on the calculation that DBHD/N_2O_2 constituted 16 wt % of the final underlying layer. Fifty μL of this cocktail was added on each pre-cleaned glass coverslip and dried in gentle nitrogen flow to form an NO release under-layer.

One hundred μL 2 wt % PurSil solution in DMAc/THF (1:4, v/v) was added on top of each NO release under-layer to form the PurSil top layer on the glass coverslips. The bilayer NO releasing coatings were allowed to dry in gentle nitrogen flow overnight, followed by vacuum drying for additional 2 d to remove the residual solvent. The final NO release coatings were stored at -20 ºC. They were incubated in PBS (10

mM, pH 10) at room temperature with gentle agitation for 6 h (PBS changed every 3 h) to completely remove any residual organic solvents prior to cell culture experiments.

Borate containing control coatings were prepared with a similar procedure and the only difference is that the underlying layer did not contain any NO donor. PurSil control coatings were prepared by directly adding 100 μL 2 wt % PurSil solution on each pre-cleaned glass coverslip followed by the drying and solvent extraction steps. Both control and blank coatings were stored at -20 ºC and extracted with PBS at room temperature to completely remove any residual organic solvents prior to cell culture experiments.

4.2.3. UV-Vis Studies of Borate Leaching

KTpClPB was dissolved in methanol to make a 1 mg/mL stock solution and 30 μL of this solution was further diluted in 2.97 mL PBS (10 mM, pH 7.4) to reach a final borate concentration of 10 μg/mL. A blank solution was prepared by dissolving 30 μL methanol in 2.97 mL PBS. The UV spectra of KTpClPB and blank solutions were recorded with a Shimadzu UV-1601 UV-VIS spectrometer.

Borate control coatings were prepared according to the process described in Section 2.2 and were used here for the leaching studies. Borate control coatings without a top layer were also prepared and the process is identical except that a top coating wasn't applied after the KTpClPB-containing underlying layer was coated. Both borate control coatings (with and without top layer) together with PurSil blank coatings were incubated in PBS (10 mM, pH 7.4) for 3 h at 37 ºC with a surface-area-to-solution ratio of approx. 1 cm^2 vs. 1 mL, i.e., 1 coverslip (1.19 cm^2) per 1 mL PBS. For each kind of coating,

extraction solutions from 5 coverslips were combined and UV spectra were recorded in the wavelength range from 200 to 300 nm.

4.2.4. Sulfonation of Polyurethanes (PUs)

Sulfonation of the PUs was described in a paper published by Cooper's group in 1989[7]. Tecoflex and Tecophilic were dissolved in anhydrous THF to make 10 w/v % solutions. Urethane nitrogen atom was first deprotonated through the reaction of a 10 w/v % polymer solution in THF with a 60 w/w % suspension of sodium hydride in mineral oil. The nitrogen content in the polymer was measured by elemental analysis performed in Chemistry Department, University of Michigan (Ann Arbor, MI). Sodium hydride was added in 3 to 5 portions over a period of 10 min. This procedure was performed at -5 to 0 ºC to prevent polymer chain scission. After 15 min, a slight excess of propane sultone was added to react with the nitrogen anion to produce the derivatized urethane linkage. The mixture was allowed to warm to room temperature and then heated to approximately 50 ºC for 1 h (see Scheme 4.3).

The reaction mixture was cooled to room temperature and diluted sulfuric acid or hydrochloric acid (1 N) was added to neutralize the unreacted sodium hydride. Inorganic salts could precipitate out of the mixture as a result of NaH's neutralization by H_2SO_4 or HCl. The suspension was filtered and the solution was precipitated with a copious amount of diethyl ether. The polymer was collected and washed successively with diethyl ether, ethanol and DI water to remove both the organic and inorganic residues. The polymer was further washed with ethanol and diethyl ether to make the solvent phase easier to remove. The purified polymer was dried in vacuum for 2 d and stored at -20 ºC.

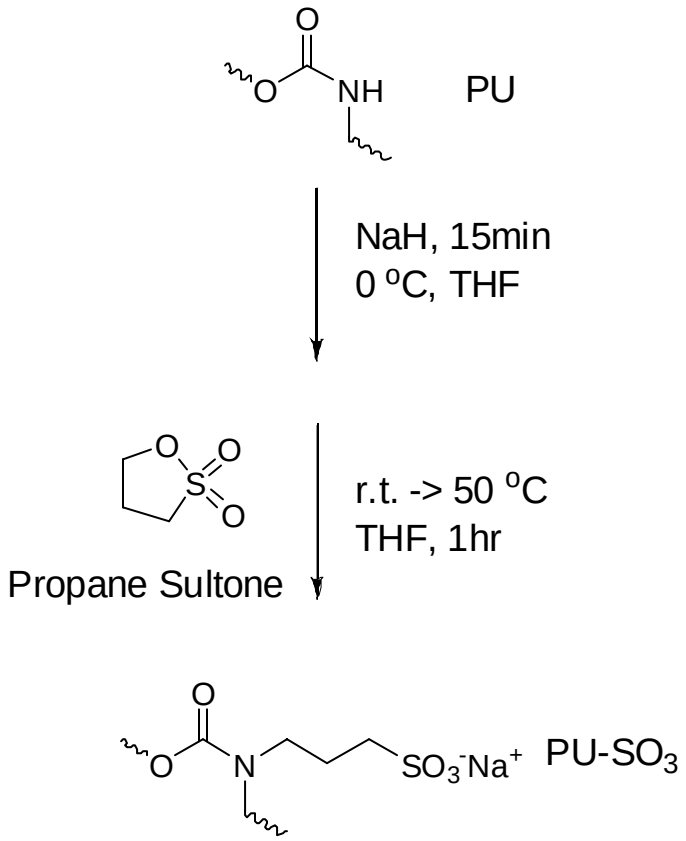

Scheme 4.3. Synthesis of PU-SO_3.

4.2.5. Characterization of Sulfonated Polyurethanes (PU-SO_3)

Elemental (CHNS/O) combustion analysis was performed by Carol Carter with a Perkin-Elmer 2400 Series II CHNS/O Analyzer in the Chemistry Department at the University of Michigan to determine the sulfur concentration and the degree of sulfonation. The water absorption of the PU-SO_3 was measured according to the following procedure: a piece of polymer (ca. 20-30 mg) was weighed and its exact mass was recorded as W_1. After 24 h of immersion in DI water, the piece of polymer was taken out and its surface moisture was blotted off by KimWipes and its weight quickly

measured again by an analytical balance and recorded as W_2. The percent water absorption was calculated according to the following formula:

$$WaterAbsorption\% = \frac{W_2 - W_1}{W_1} \times 100\% \qquad \textbf{Eqn. 4.1.}$$

A differential scanning calorimeter was used to characterize the thermal profile of the polymers. Approx. 5 mg of either PU-SO_3 or control polymer samples was placed in Tzero aluminum pan and placed in TA Q2000 DSC. An empty pan was used as the reference. The samples were equilibrated at -20.00 °C and then the temperature was ramped to 280.00 °C at a rate of 20.00 °C/min. Heat flow was recorded and the onset transition temperatures were measured.

4.2.6. Preparation of NO-Release Polymeric Coatings and Control Coatings on Glass Coverslips with PU-SO_3

The NO release polymeric coatings for cell culture experiments were prepared on clear glass coverslips with a diameter of 12 mm (surface area = 1.19 mm^2). A cocktail containing well-suspended DBHD/N_2O_2 in a THF solution of Tecoflex and sulfonated Tecoflex (Tecoflex-SO_3) mixture was made. The ratios of Tecoflex vs. Tecoflex-SO_3 varied with a fixed total polymer concentration of 4 w/v %. The concentration of DBHD/N_2O_2 in the cocktail was determined based on the calculation that DBHD/N_2O_2 constituted 16 wt % of the final underlying layer. Fifty μL of this cocktail was added on each pre-cleaned glass coverslip and dried in gentle nitrogen flow to form an NO release under-layer.

One hundred μL 2 wt % PurSil solution in DMAc/THF (1:4, v/v) was added on top of each NO release under-layer to form the PurSil top layer on the glass coverslips. The bilayer NO releasing coatings were allowed to dry in gentle nitrogen flow overnight, followed by vacuum drying for additional 2 d to remove the residual solvent. The final NO release coatings were stored at -20 ºC. They were incubated in PBS (10 mM, pH 10) at room temperature with gentle agitation for 6 h (PBS changed every 3 h) to completely remove any residual organic solvents prior to cell culture experiments.

Tecoflex-SO_3 control coatings were prepared using a similar procedure with the only difference being that the underlying layer didn't contain any NO donor.

4.2.7. Chemiluminescence Measurements of NO Release

Nitric oxide released from various polymeric coatings was measured using a Sievers Chemiluminescence NO Analyzer. The instrument was calibrated before each experiment using an internal two-point calibration (zero gas and 45 ppm NO gas). NO was continuously swept from the headspace of the sample vessel and purged from the bathing solution (PBS, 10 mM, pH 7.4) with a nitrogen sweep gas and bubbler into the chemiluminescence detection chamber. The flow rate was set to 50 mL/min with a chamber pressure of 5.4 torr and an oxygen pressure of 6.0 psi.

4.2.8. In Vitro Smooth Muscle Cell (SMC) and Endothelial Cell (EC) Proliferation and Differentiation Studies on Polymeric Coatings

In vitro studies were done in collaboration with Ms Diane Studzinski in Dr. Shanley's Surgical Research Lab at Beaumont Hospital (Royal Oak, MI). Glass

coverslips were coated with NO release or control coatings, and placed in 24 well tissue culture plates. Human umbilical artery smooth muscle cells (HASMC) and human umbilical vein endothelial cells (HUVEC) were plated to evaluate the effects of the different polymer matrices and the release of NO on cell viability, proliferation and differentiation.

Cells were grown in cell-specific medium in 24 well culture plates. At specific time points (24 h, 48 h, 5 d), cells were rinsed in PBS, fixed with 10 % neutral buffered formalin for 10 min, and rinsed again with PBS. Each polymer coating and time point was done on triplicate samples in a total of 4 experiments. For cell viability and proliferation studies, cells were stained with Hoechst 33342 nuclear dye (10 μg/mL aqueous solution) and then rinsed in DI water. For cell differentiation studies, cells were stained with Hematoxylin QS for 45 seconds and then rinsed with tap water. All coverslips were mounted on glass slides and imaged with a Nikon TE 2000 microscope with fluorescence filters (Hoechst) or brightfield imaging (Hematoxylin) under a 10x objective. Images were captured and stored using the Metamorph imaging program. Quantitative analysis of cell proliferation was determined by counting viable cell nuclei in three random fields per coverslip. Numbers were totaled for the three fields per coverslip and averaged over the three coverslips per condition. Numbers of cell nuclei on test coverslips were compared to those on controls.

4.3. Results and Discussion

4.3.1. In Vitro SMC and EC Studies of KTpClPB-Containing Polymeric Coatings

In order to assess whether the new NO/Sirolimus releasing coatings (Chapter 3) can really suppress the migration and proliferation of SMCs, and at the same time exhibit enhanced endothelialization, the compatibility with respect to the growth of ECs and SMCs directly on the surface of such films was tested. Interestingly, during the course of these studies, it was found that growth of both EC and SMC were inhibited on one of the control polymeric films that contained the borate additive, KTpClPB (Figures 4.4b and 4.4d). Such an inhibition of cell proliferation was not observed on plain biomedical grade PurSil polymers without the borate (Figures 4.4a and 4.4c).

4.3.2. The Leaching of KTpClPB and Its Degradation Products

The inhibition of cell proliferation suggested that there was some cytotoxicity with respect to the use of the KTpClPB additive as a polymeric-phase pH stabilizer. A borate leaching study was performed using UV-Vis as the detector. The KTpClPB spectrum it showed an absorption peak at 235 nm (see Figure 4.5). Phosphate buffered saline (10 mM, pH 7.4) was used to extract the leachable borate species out of the control coatings. However, minimal amount of borate could be detected in the solution phase (Figure 4.6c), confirming that KTpClPB is very lipophilic and does not leach appreciably from the films[4].

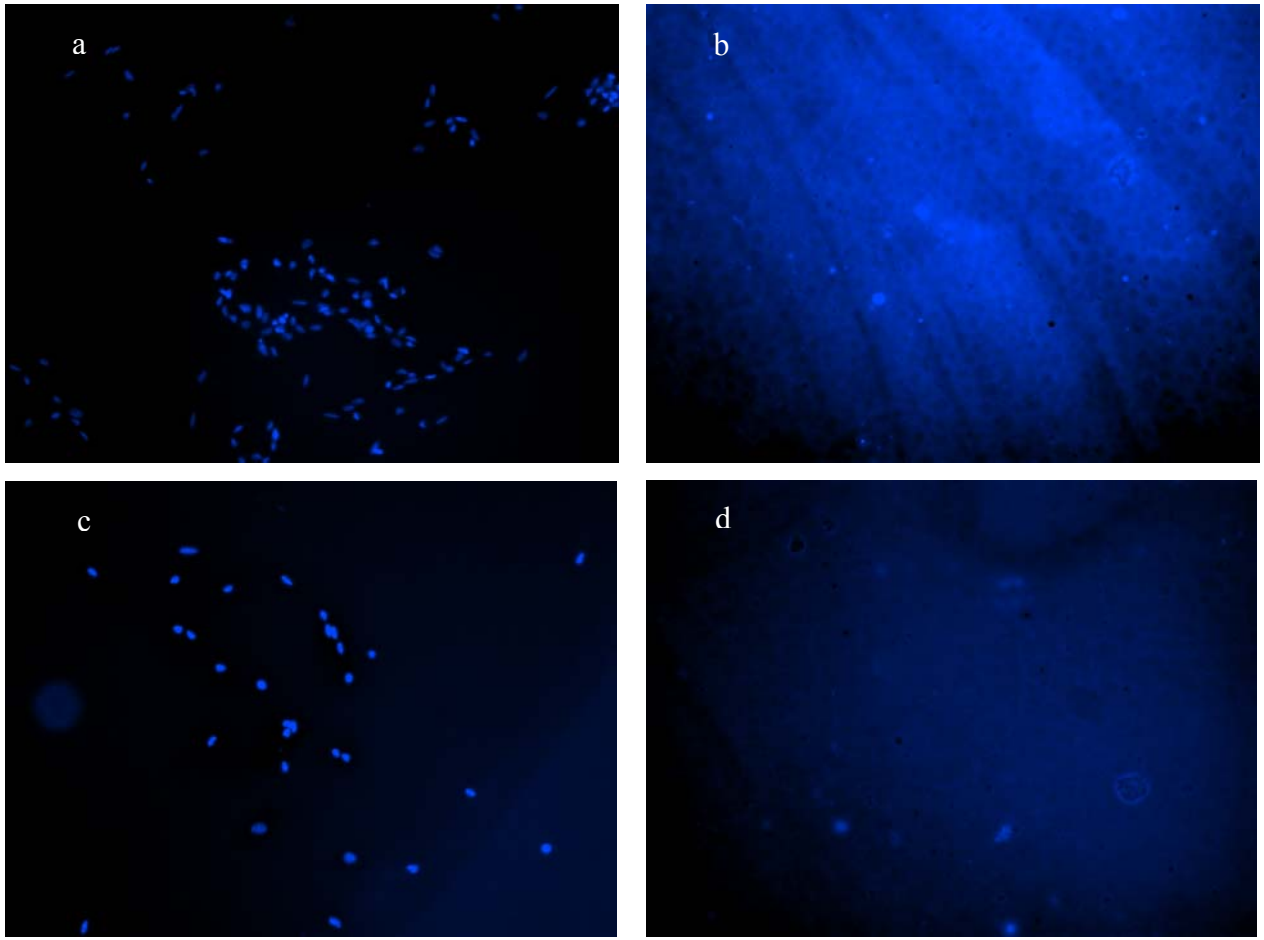

Figure 4.4. HUVECs were plated and grown in EC culture medium on KTpClPB-containing and PurSil blank polymeric films for 24 h and 48 h. Cells were fixed, and their nuclei were stained with Hoechst 33342 dye. The images were taken with a Nikon TE 2000 fluorescent microscope using a 10x objective. **a** – PurSil blank, 24 h; **b** – KTpClPB-containing PurSil underlying layer and PurSil top layer, 24 h; **c** – PurSil blank, 48 h; **d** – KTpClPB-containing PurSil underlying layer and PurSil top layer, 48 h. The strong blue fluorescence background came from the added KTpClPB.

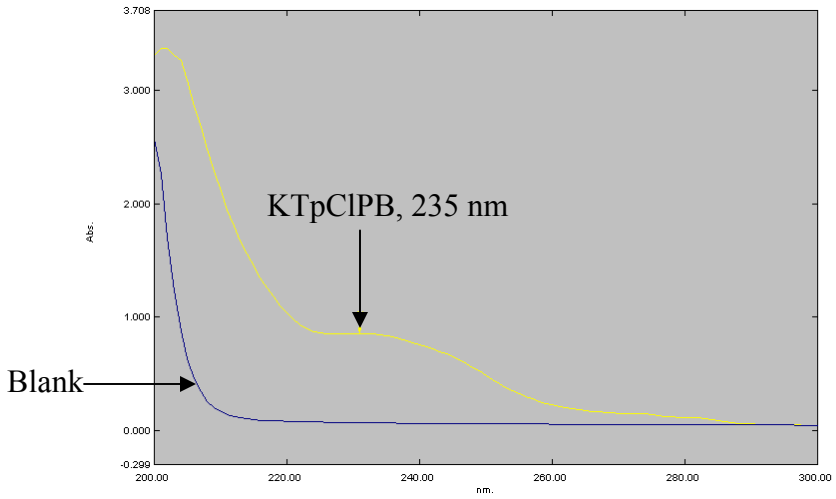

Figure 4.5. UV spectra of KTpClPB and blank PBS solution. KTpClPB was dissolved in methanol to make a 1 mg/mL stock solution and 30 µL of this solution was further diluted in 2.97 mL PBS (10 mM, pH 7.4) to reach a final borate concentration of 10 µg/mL. A blank solution was prepared by dissolving 10 µL methanol in PBS. The UV spectra were recorded with a Shimadzu UV-1601 UV-VIS spectrometer.

However, it is possible that potentially toxic radical species can be generated due to the cleavage of the carbon-boron bond in the proton-induced or oxidative degradation of the KTpClPB species[5]. Furthermore, the resulting triphenylboronates could also leach out of the polymeric phase. These borate species, even though very small in amount, can still be toxic to cells. To test this hypothesis, a KTpClPB-containing control coating was prepared without a top layer and the borate extracted under the same condition but with much enhanced signal due to the removal of the diffusion barrier. This time, a significant increase of the UV absorbance in the lower 200 nm range could be observed (see Figure 4.6), indicating the possible existence of borate degradation products.

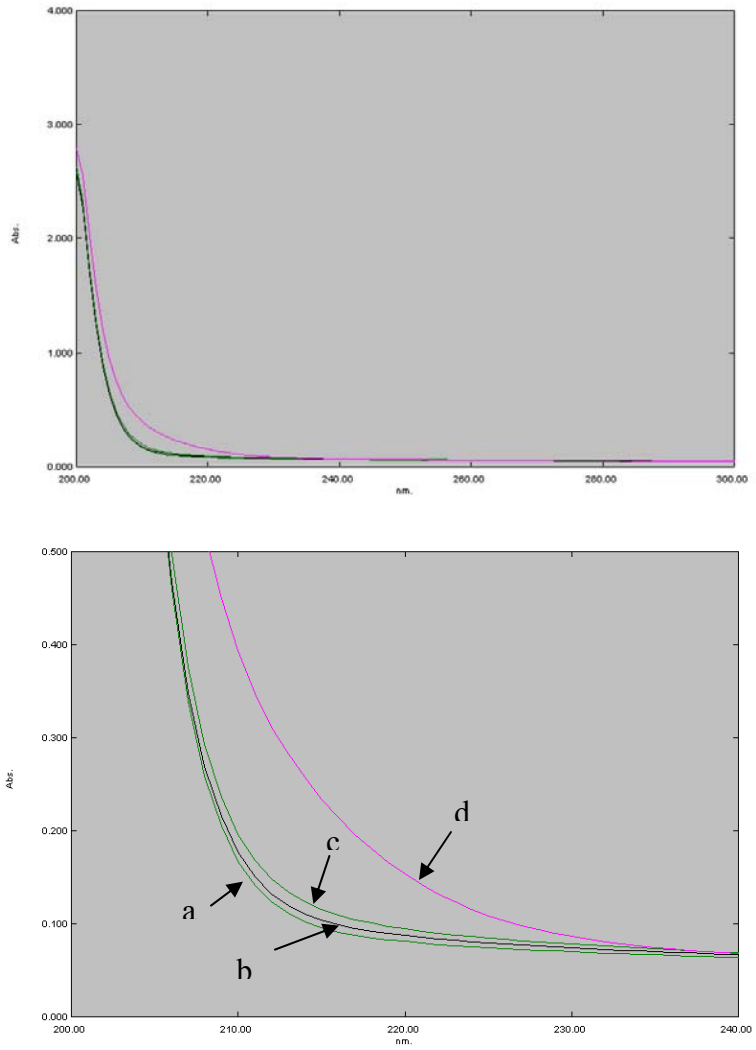

Figure 4.6. UV spectra of extraction solutions from borate-containing films, PurSil control films and PBS blank. Both borate control coatings (with and without top layer) together with PurSil blank coatings were incubated in PBS (10 mM, pH 7.4) for 3 h at 37 ºC with a surface area to solution ratio of approx. 1 cm^2 vs 1 mL. The extraction solutions were used for UV scan from 200 to 300 nm. **a** – PBS (10 mM, pH 7.4); **b** – PBS extraction solution from PurSil blank films; **c** – PBS extraction solution from KTpClPB-containing films with PurSil top layer; **d** – PBS extraction solution from KTpClPB-containing flims without top layer. The UV spectra were recorded with a Shimadzu UV-1601 UV-VIS spectrometer.

4.3.3. In Vitro Cell Viability Studies on KTFPB-Containing Control Coatings

In ion-selective polymeric membrane electrodes, tetraphenylborate derivatives have been commonly used as the anionic additives[4]. Several studies have been published comparing their stability. It has been found that the less electro-negative the central boron atom is, the less susceptible it is to acid-catalyzed degradation. While KTpClPB has been found to be more stable than simple TPB, the derivative TFPB has been found to be even more lipophilic, and substantially more stable than KTpClPB[6].

Thus control films were prepared with KTFPB in the place of KTpClPB as the borate additive in the underlying layer. It was exciting to find that the viability of both ECs and SMCs improved significantly (Figure 4.7) compared to that of the KTpClPB-containing coatings (Figure 4.4), indicating a much reduced degradation and/or leaching of KTFPB as a more stable and lipophilic borate additive. More importantly, over a longer period of time (5 d), both cell types were able to differentiate properly (Figure 4.8).

4.3.4. NO Release from Polymeric Coatings with KTFPB as the pH-Buffering Agent

Nitric oxide flux from polymeric coatings with KTFPB as the borate additive in the underlying layer was measured at 37 ºC in PBS (10 mM, pH 7.4) by a chemiluminescent NO analyzer. The NO flux from these coatings was compared with that from polymeric coatings with KTpClPB as the pH-buffering agent. From Figure 4.9 it is clear that these two types of films exhibited similar NO release rates.

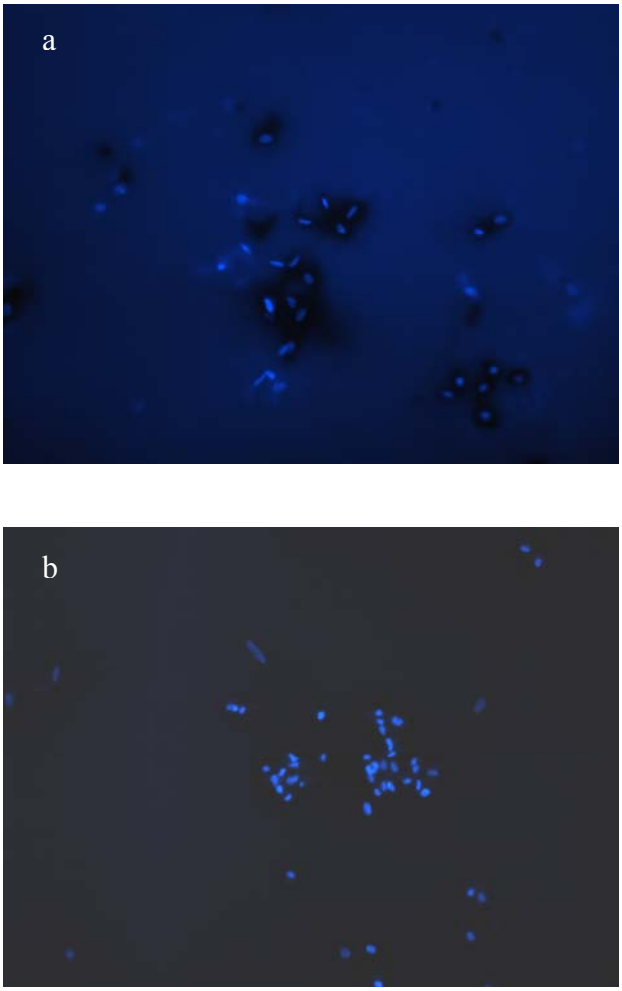

Figure 4.7. HUVECs and HASMCs were plated and grown in cell specific culture medium on KTFPB-containing control polymeric films for 24 h (underlying layer – KTFPB-containing PurSil; top layer – PurSil). Cells were fixed, and their nuclei were stained with Hoechst 33342 dye. The images were taken with a Nikon TE 2000 fluorescent microscope using a 10x objective. **a** – HUVEC; **b** – HASMC. The slight blue fluorescence background is due to the added KTFPB.

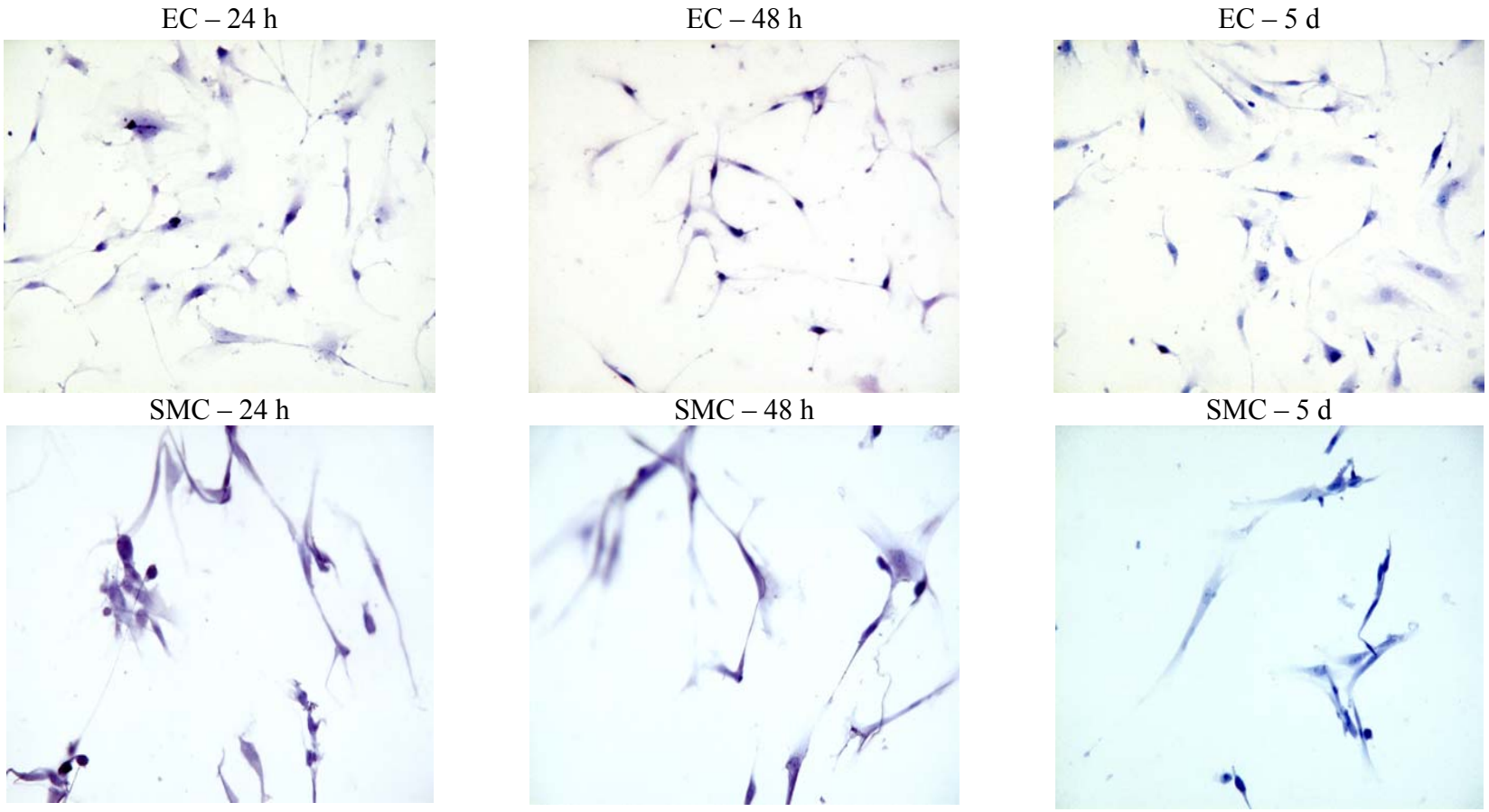

Figure 4.8. ECs and SMCs were plated and grown in cell specific culture medium on KTFPB-containing control polymeric films for 24 h, 48 h and 5 d (underlying layer – KTFPB-containing PurSil; top layer – PurSil). Cells were fixed and stained with hematoxylin. Images were taken with a Nikon TE 2000 fluorescent microscope in bright field mode using a 10x objective.

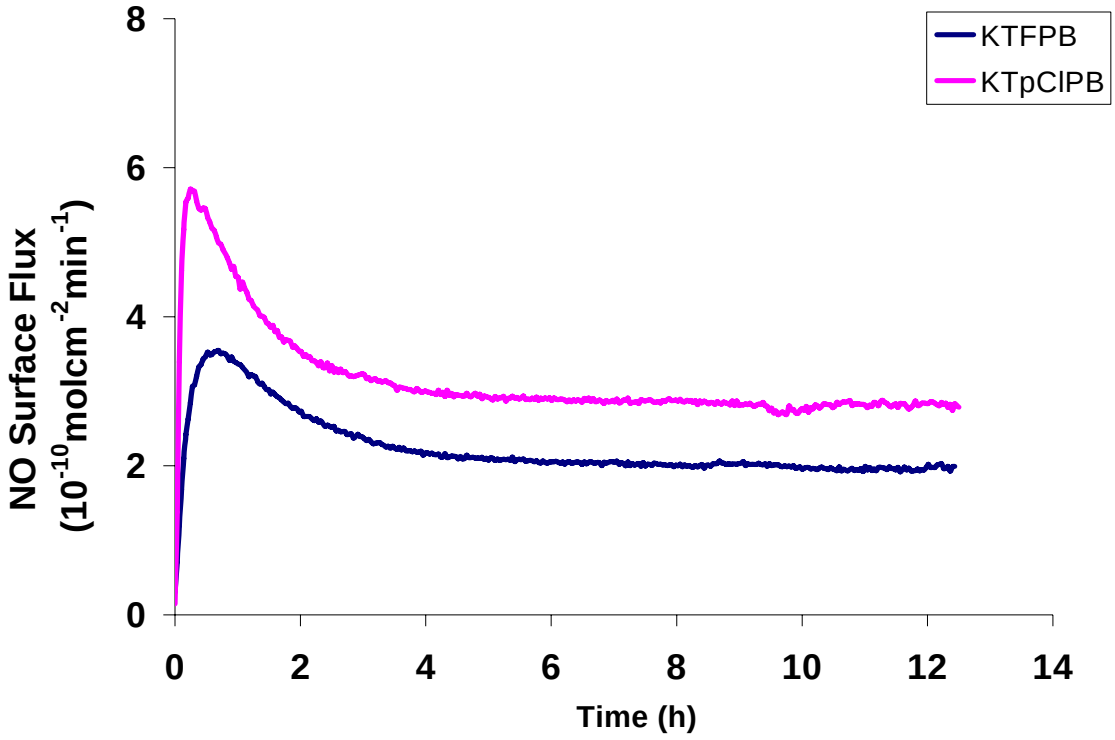

Figure 4.9. Typical NO level of DBHD/N_2O_2-loaded (16 wt % in KTFPB- or KTpClPB-contaning underlying layer) bilayer polymeric films (top layer – PurSil). The coatings (on glass coverslip) were incubated in PBS (10 mM, pH 7.4) under 37 °C and their NO flux measured by NOA.

4.3.5. Sulfonation of Tecophilic and Tecoflex

By using KTFPB, an extremely lipophilic and stable borate additive, as the pH buffering agent, non-cytotoxic polymeric films with sustained NO release could be prepared. However, since KTFPB is a small molecule, there is still some possibility for a fraction of this additive to diffuse out of the polymer coating to elicit potential adverse effects *in vivo* or *in vitro*. To eliminate such possibility, we chemically immobilized

anionic sites to the polymer backbones by derivatizing two biomedical grade PUs (Tecoflex and Tecophilic) with sulfonate groups.

For Tecophilic-93A-100, the elemental analysis (duplicates) showed a nitrogen concentration of 3.3 wt %, indicating there existed 2.4 mmol urethane groups per every gram of polymer. After sulfonation, the sulfur concentration was detected to be 1.2 wt %, indicating that the sulfate group concentration is 0.38 mmol/g. The water uptake was measured to be 96 %. Actually, due to the extremely high water uptake, Tecophilic-SO_3 swelled too much and would easily peel off from the glass coverslip matrix. Thus it was proved unsuitable for this study. In this case, all the following cell studies and NO release studies were done using Tecoflex-SO_3.

4.3.6. Thermal Properties of Tecoflex-SO_3 PUs

A differential scanning calorimeter was used to characterize the thermal profile of the polymers. In Figure 4.10, the heat flow curve of Tecoflex showed an endothermic peak with an onset temperature (T_o) at 68.14 ºC, a peak temperature (T_p) at 86.27 ºC and an enthalpy change (ΔH) at 11.35 J/g. The heat flow curve of Tecoflex-SO_3 was more complicated with two overlapping endothermic transitions. The T_o and T_p of the first transition were 56.40 ºC and 79.49 ºC, respectively, both were approx. 7-8 degrees lower than those of Tecoflex. This was probably due to the derivatization of the urethane nitrogen atom which might disrupt the hydrogen bonding in the ordered structure of the thermoplastic polyurethane elastomer's hard segments. The second transition had a T_o at the 110.35 ºC and a T_p and 125.38 ºC, respectively. This was probably due to the introduction of sulfonate groups to the polymer backbones which generated a new

phase/hard segment with strong ionic forces and thus needed a higher temperature and more energy to 'melt'. Indeed, the summed ΔH of these two transitions is 14.78 J/g which was a little higher than that of the ΔH of Tecoflex control. No thermal transitions above 280 ºC were measured as Tecophilic started to decompose and gasify.

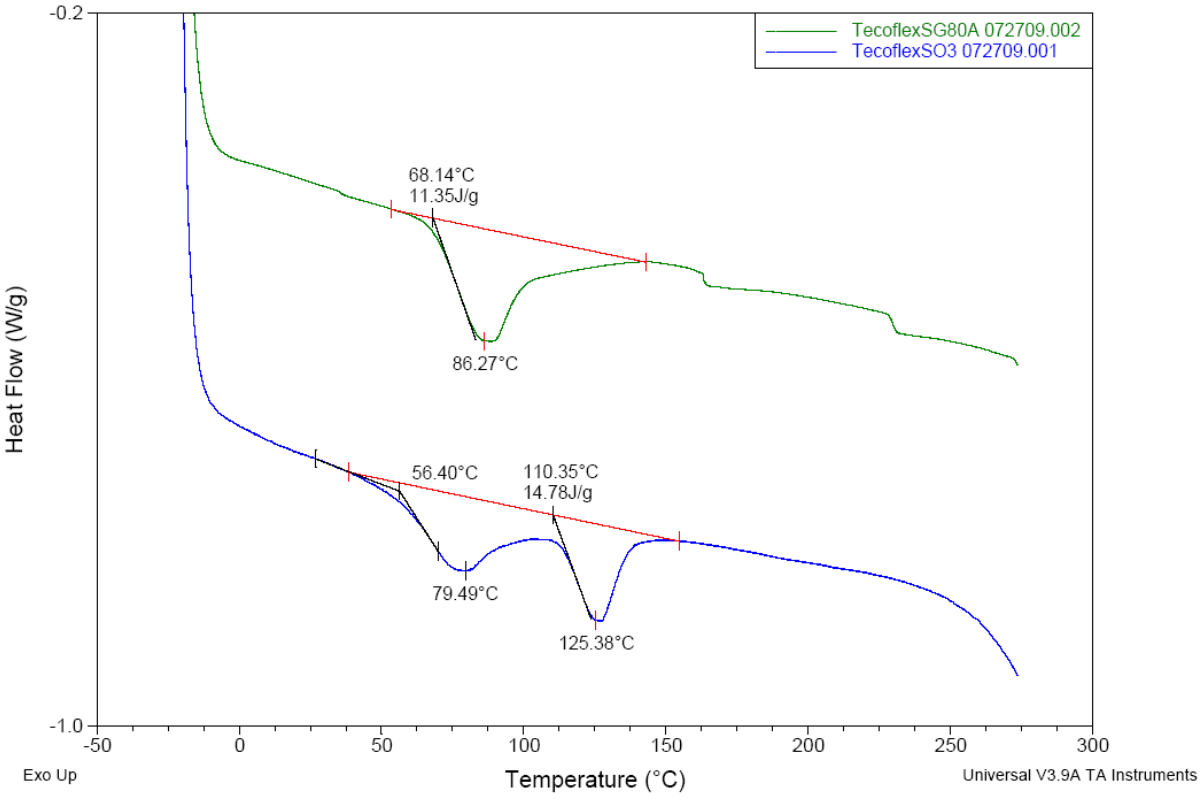

Figure 4.10. Heat flow curves of Tecoflex and Tecoflex-SO_3. Approx. 7-9 mg polymer samples was placed in Tzero aluminum pan and placed in TA Q2000 DSC. The samples were equilibrated at -20.00 °C and then the temperature would ramp to 280.00 °C at a rate of 20.00 °C/min.

4.3.7. In Vitro Cell Viability Studies on Tecoflex-SO_3 Control Coatings

Control films with Tecoflex-SO_3 as the underlying layer were prepared and were tested. No suppression of ECs and SMCs proliferation (Figure 4.11) was observed.

More importantly, over a longer period of time (5 d), both cell types were able to differentiate properly (Figure 4.12).

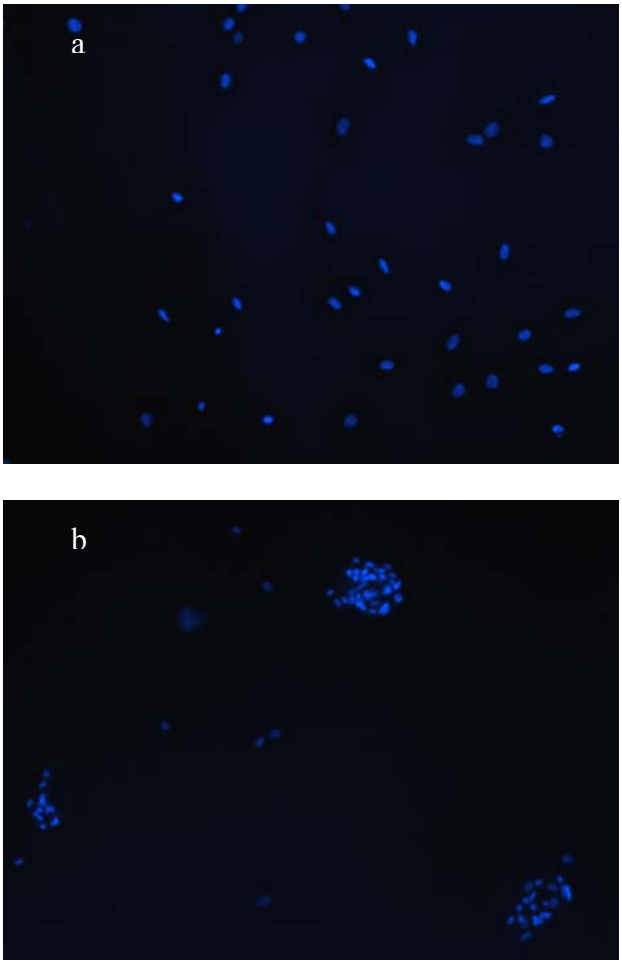

Figure 4.11. ECs and SMCs were plated and grown in cell specific culture medium on control polymeric films with Tecoflex-SO_3 as the underlying layer for 24 h (top layer – PurSil). Cells were fixed, and their nuclei were stained with Hoechst 33342 dye. The images were taken with a Nikon TE 2000 fluorescent microscope using a 10x objective. **a** – EC; **b** – SMC.

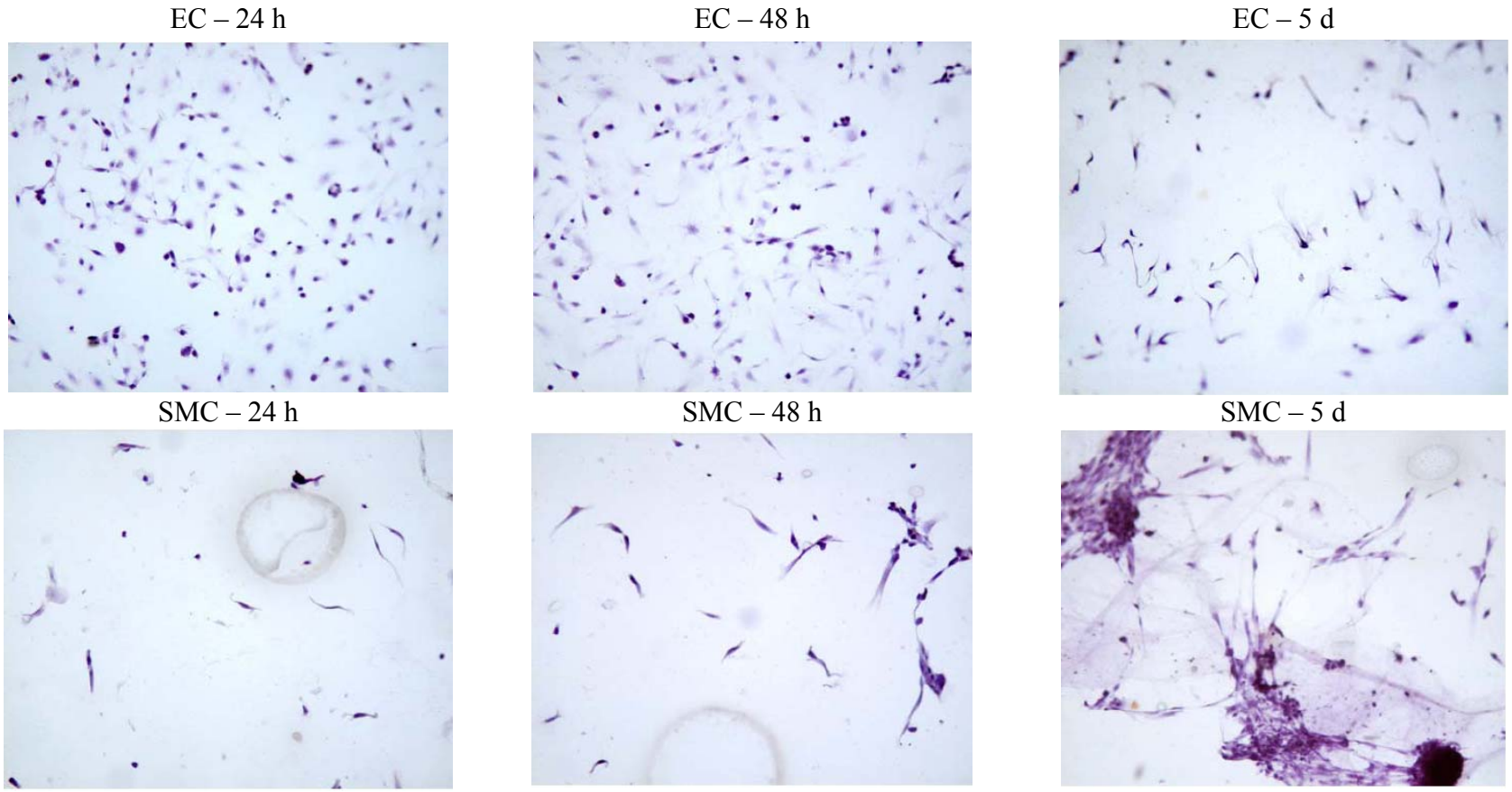

Figure 4.12. ECs and SMCs were plated and grown in cell specific culture medium for 24 h, 48 h and 5 d on control polymeric films with Tecoflex-SO_3 as the underlying layer and PurSil as the top layer. Cells were fixed and stained with hematoxylin. Images were taken with a Nikon TE 2000 fluorescent microscope in bright field mode using a 10x objective.

4.3.8. NO Release from Tecoflex-SO_3 films

Nitric oxide flux from polymeric coatings with Tecoflex-SO_3 as the underlying layer was measured at 37 ºC in PBS (10 mM, pH 7.4) by a chemiluminescent NO analyzer. NO was able to be released almost stoichiometrically for at least 23 d through the decomposition of the diazeniumdiolate NO donor DBHD/N_2O_2 (Figure 4.13). However whether the sulfonate groups on the polymer backbones were indeed able to buffer the pH change in the polymer matrix needs to be further verified.

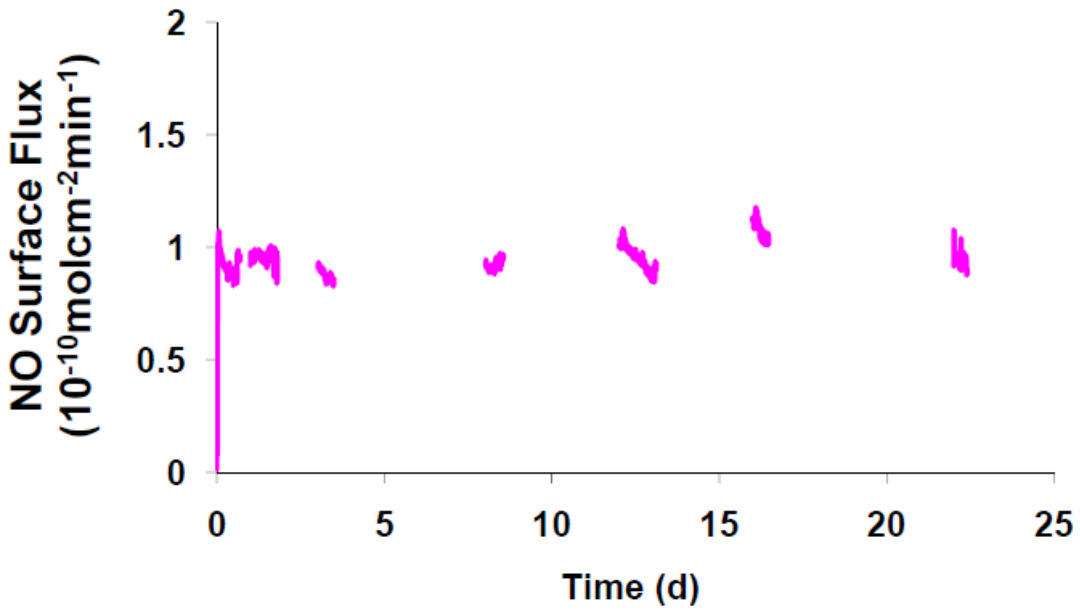

Figure 4.13. Typical NO level of DBHD/N_2O_2-loaded bilayer polymeric films (underlying layer – 16 wt % DBHD/N_2O_2 in Tecoflex-SO_3; top layer – PurSil). The coating (on glass coverslip) was incubated in PBS (10 mM, pH 7.4) under 37 °C. The loaded DBHD/N_2O_2 was 2.5 µmol (calculated based on polymer film weight and the wt percentage of the doped NO donor). The total released NO amount was detected to be 3.66 µmol, which was approx. 73 % of the total releasable NO (5.0 µmol). NO release was measured at specific time slots and the data were then integrated into the graph above. Data were not collected in the gaps.

In addition, different blends of Tecoflex vs. Tecoflex-SO_3 with DBHD/N_2O_2 added at a constant level have been tested for their NO release rates. It has been found that with increased Tecoflex-SO_3 content, NO flux would increase proportionally, both with and without the existence of a top coating as the diffusion barrier (Figures 4.14 and 4.15). This is an evidence that sufonate anionic groups serve as extremely lipophilic anionic sites that stabilize the pH value in the polymeric phase.

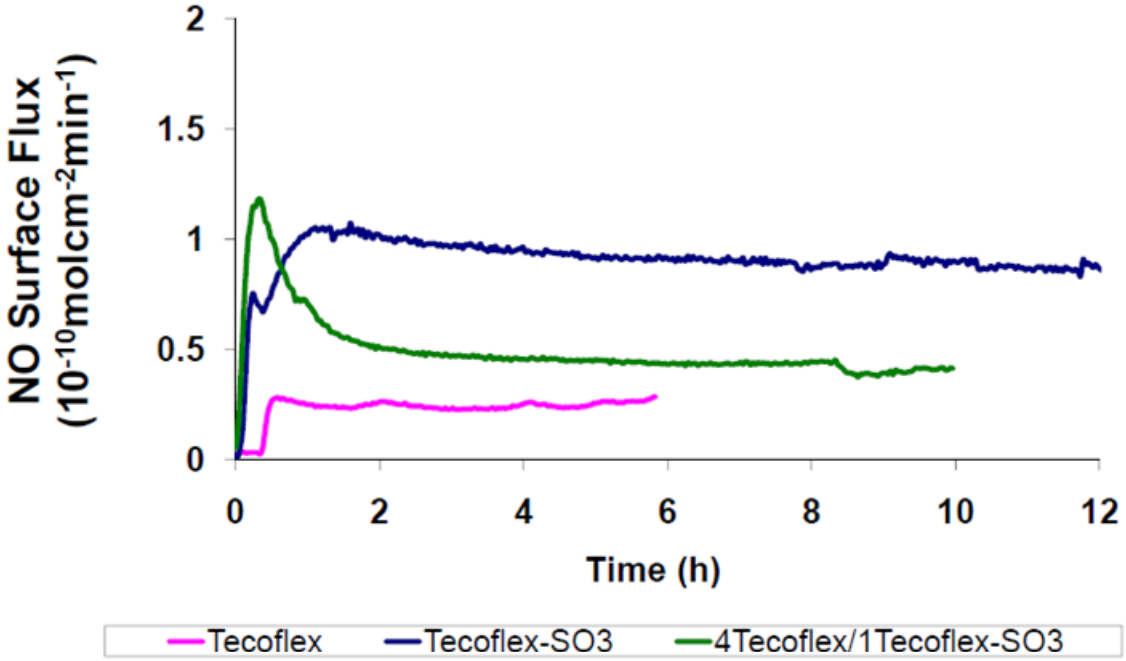

Figure 4.14. NO levels of DBHD/N_2O_2-loaded polymeric films with PurSil as the top layer. The Tecoflex/Tecoflex-SO_3 ratios of the underlying NO release layers (containing 16 wt % DBHD/N_2O_2) varied. All coatings were incubated in PBS (10 mM, pH 7.4) under 37 ºC and their NO fluxes were measured by NOA.

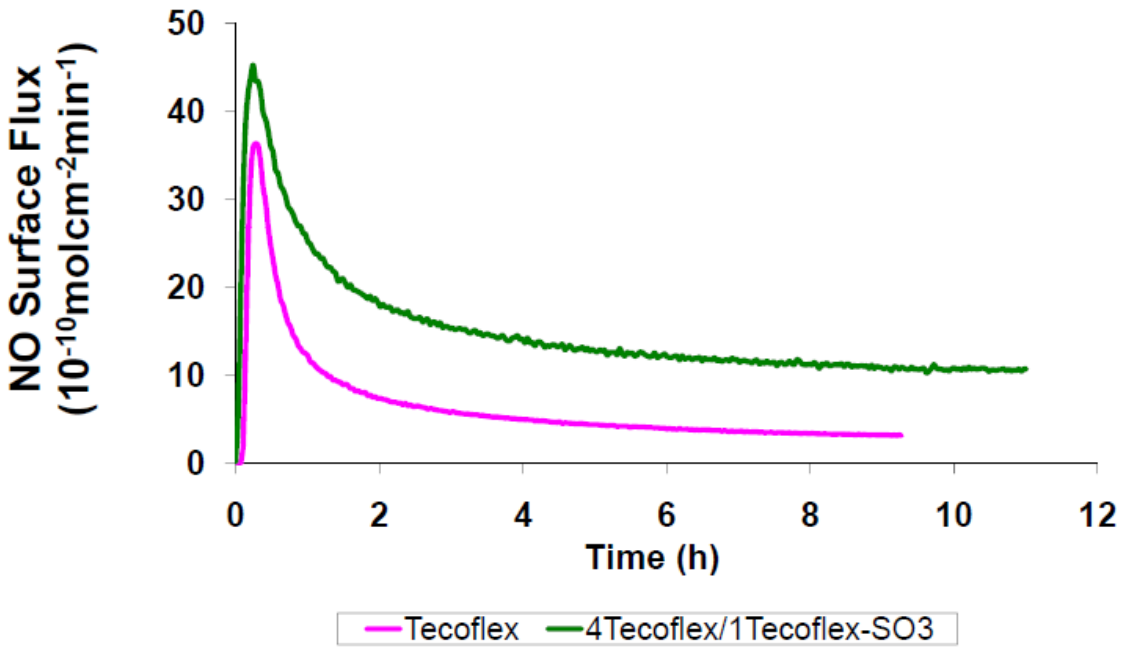

Figure 4.15. NO levels of DBHD/N_2O_2-loaded polymeric films without top layer. The Tecoflex/Tecoflex-SO_3 ratios of the NO-release layers (containing 16 wt % DBHD- N_2O_2) varied. Both coatings were incubated in PBS (10 mM, pH 7.4) under 37 ºC and their NO fluxes were measured by NOA.

4.3.9. In Vitro SMC Proliferation Studies on NO Release Polymeric Coatings

Glass coverslips were coated with NO-release (either with KTFPB or Tecoflex-SO_3) or control coatings. SMCs were plated to evaluate the effects of the release of NO on cell proliferation. Based on Hoechst 33342 nuclear staining of triplicate coverslips/condition, suppression of SMC proliferation has been observed on the NO-release coatings (Figure 4.16).

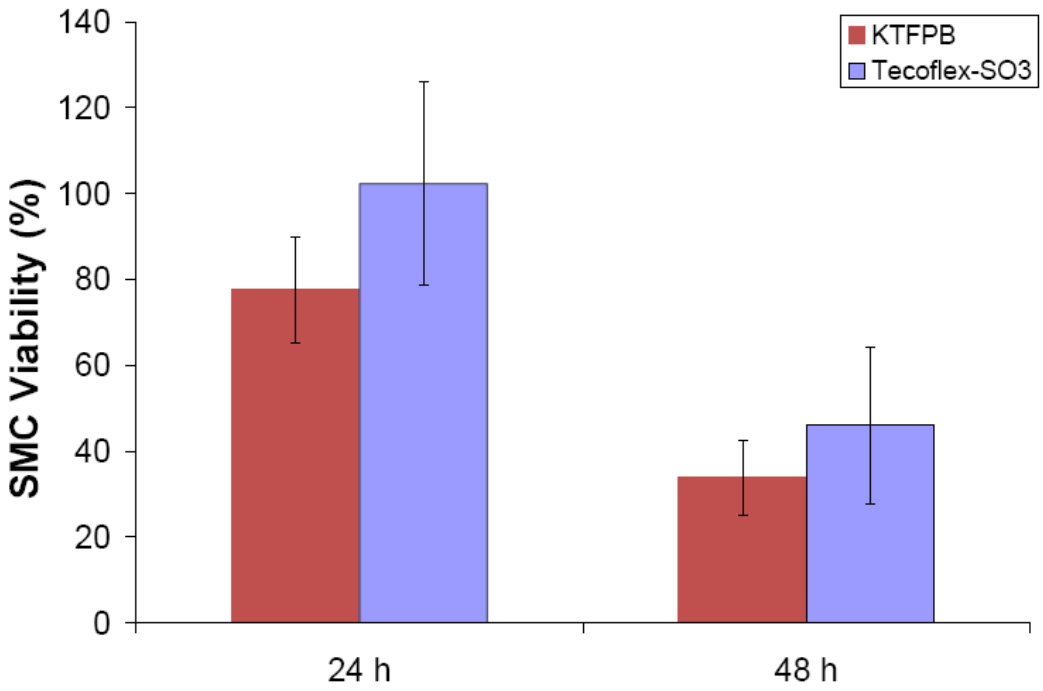

Figure 4.16. SMC viability on NO-release polymeric coatings with either KTFPB as the pH-stabilizing additive or Tecoflex-SO_3 as the matrix of the underlying layer (top layer – PurSil). Cells were stained with Hoechst 33342 nuclear dye and then imaged with a Nikon TE 2000 fluorescent microscope using a 10x objective. SMCs were counted in three random fields per coverslip and their total numbers were calculated per coverslip. Each polymer coating and time point was done on triplicate samples in a total of four experiments. Percent viability data were normalized to control coatings with KTFPB-containing PurSil or Tecoflex-SO_3 as the underlying layer.

4.4. Conclusions

To potentially overcome the lack of stability and apparent cytotoxicity of KTpClPB, we investigated the use of KTFPB, a much more stable borate additive, to prepare polymer coatings that had much reduced cytotoxicity towards ECs and SMCs. In addition to using the small molecule additives as the pH buffering agents in the polymeric

films, a sulfonate derivative of biomedical grade PUs has been synthesized to eliminate the possibilities of the leaching of low molecular weight species.

As has been shown in the cell proliferation data, the new polymeric coatings with non-toxic borate and polymer-tethered sulfonate groups have minimal cytotoxicity to both ECs and SMCs. Indeed, the preliminary *in vitro* studies have shown that these NO-release novel bilayer polymeric coatings are suppressive to human vascular SMCs. Such non-toxic NO-release polymeric coatings have the potential to be used in various blood-contacting medical devices such as vascular grafts, heart valves, extracorporeal circuits and stents.

4.5. References

1. Moncada, S.; Palmer, R.M.J.; Higgs, E.A. 'Nitric-oxide – physiology, pathophysiology, and pharmacology.' *Pharmacol. Rev.* **1991,** 43, 109-142.

2. Marx, S.; Marks, A. 'Bench to bedside: The development of rapamycin and its application to stent restenosis.' *Circulation* **2001**, 104, 852-855.

3. Batchelor, M.M.; Reoma, S.L.; Fleser, P.S.; Nuthakki, V.K.; Callahan, R.E.; Shanley, C.J. 'More lipophilic dialkyldiamine-based diazeniumdiolates: synthesis, characterization, and application in preparing thromboresistant nitric oxide release polymeric coatings.' *J. Med. Chem.* **2003**, 46, 5153–5161.

4. Ammann, D.; Pretsch, E.; Simon, W.; Lindner, E.; Bezech, A.; Pungor, E. 'Lipophilic salts as membrane additives and their influence on the properties of macro- and micro-electrodes based on neutral carriers.' *Analytica Chimico Acta,* **1985**, 171, 119-129.

5. Nishida, H.; Takada, N.; Yoshimura, M.; Sonoda, T.; Kobayashi, H. 'Tetrakis[3,5-bis(trifluoromethyl)phenyl]borate. Highly lipophilic stable anionic agent for solvent extraction of cations.' *Bull. Chem. Soc. Jpn.* **1984**, 57, 2600-2604.

6. Fujiki, K.; Ichikawa, J.; Kobayashi, H.; Sonoda, A.; Sonoda, T. ‘Synthesis of lipophilic tetraakylborate ions substituted with many perfluoroakyl groups and their stability under acid conditions.’ *J. Fluorine Chem.* **2000,** 102, 293-300.

7. Grasel, T.G.; Cooper, S.L. ’Properties and biological interactions polyurethane anionomers: Effect of sulfonate incorporation.’ *J. Biomed. Mater. Res*. **1989**, 23, 311-338.

CHAPTER 5

Combining Nitric Oxide Generation and Sirolimus Release in Polymeric Films: Potential Coatings for Stents and Other Blood-Contacting Medical Devices

5.1. Introduction

Placement of stents by balloon angioplasty represents a major advance in the treatment of obstructive coronary artery diseases. The number of percutaneous coronary interventions performed has been expanding considerably each year. Unfortunately, many patients develop in-stent restenosis which is an exaggerated vascular neointimal proliferation after stenting. Many drug-eluting stents (including sirolimus-eluting stents) have emerged as a potential solution for this restenosis problem[1].

Sirolimus is a macrolide antibiotic with potent antifungal, immunosuppressive and antimitotic properties[2]. In December 1999, the first sirolimus-eluting stents were implanted in human cornary arteries and the first published human study by Sousa *et al.* in 2001 showed a nearly complete elimination of neointimal hyperplasia[1]. However, as indicated in Chapter 1, recent findings have suggested an increased risk of late thrombosis associated with drug-eluting stents due to the incomplete endothelialization

on the surface of the struts of the stents since sirolimus can also retard the migration and proliferation of endothelial cells (ECs)[3,4]. It is becoming clearer that using anti-restenotic drug alone may only solve part of the issues associated with stent placement. Indeed, similar thrombosis and smooth muscle cell (SMC) proliferation problems exist in the case of implanted vascular grafts as well. Hence, the use of a naturally occurring anti-thrombotic/anti-platelet agent, such as nitric oxide (NO), in combination with an anti-cell proliferation agent may provide the ideal solution to reduce both clotting and restenosis risk for stents as well as vascular grafts and other implanted medical devices.

Nitric oxide, an endogenous small molecule that continuously diffuses from healthy endothelium to adjacent blood stream, is able to inhibit both platelet adhesion to endothelial wall as well as platelet activation[5]. In addition, NO has also been found to facilitate EC migration and proliferation[6]. Recent research carried out in this laboratory[18,19] and elsewhere[7,8] has demonstrated the efficacy of NO producing polymers in preventing platelet adhesion and activation. The materials are doped with NO donors and are capable of releasing low but controllable levels of NO at the polymer/blood interface, which are comparable to that generated by the healthy EC layer under the physiological conditions[17] (ca. 1×10^{-10} mol·cm^{-2}·min^{-1}).

Although these NO releasing materials can be employed in a wide range of medical applications, the finite NO donor reservoirs may limit their potential applications in some medical devices that require an ultra-thin coating for long-term implantation (i.e., vascular stents). The limited amount of loaded NO donor may influence the level and duration of the NO release which may, in turn, affect the effective prevention of platelet adhesion and activation on such device surfaces.

To overcome this shortcoming, recent research has suggested a completely new approach to produce NO from polymers. The new polymers contain a organoselenium (RSe) moiety[7,8] that can catalytically generate NO from a variety of *S*-nitrosothiol species that are known to exist in blood. Physiological *S*-nitrosothiols (RSNOs) such as *S*-nitrosoglutathione (GSNO), *S*-nitrosocysteine (CySNO), and *S*-nitrosoalbumin (AlbSNO) are known to serve as storage and transfer agents of NO[20]. The RSe moiety is indeed mimicking the active center of a selenium-containing enzyme, glutathione peroxidase (GPx), which is able to catalytically decompose RSNOs into NO and the corresponding free thiols[15,16]. RSe-derivatized polymers, such as RSe-cellulose and RSe-polyethyleneimine, have recently been synthesized and have demonstrated the ability to generate NO catalytically from endogenous RSNO species[7,8].

Herein, we report the first dual-functional polymeric coating that can both generate NO from endogeneous RSNO species and simultaneously release sirolimus at a controlled rate. Such coatings are made from a sirolimus-doped RSe-derivatized biomedical-grade polyurethane (Tecophilic®) and are able to utilize the theoretically infinite RSNO reservoir in blood to generate a continuous flux of NO while also releasing sirolimus into the blood stream (Scheme 1). The new coatings can potentially suppress SMC proliferation and thrombosis, as well as facilitate endothelialization at a given implant site.

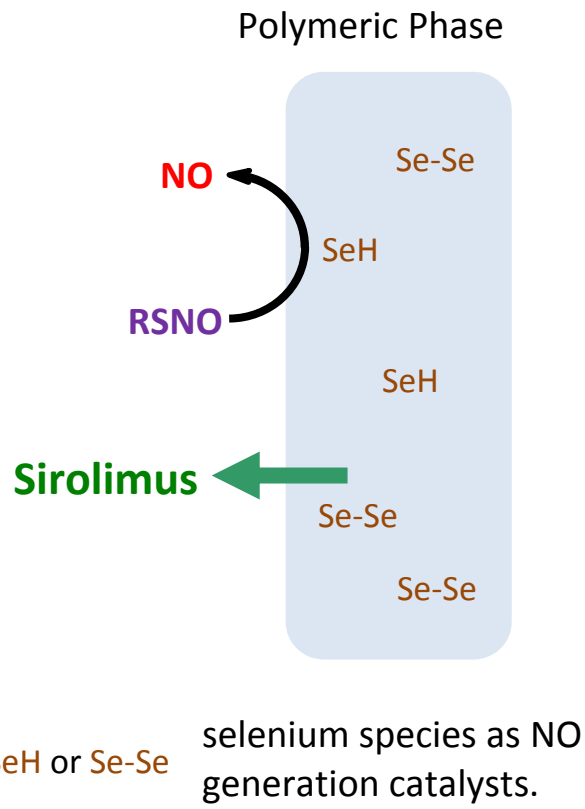

Scheme 5.1. PU coatings that generate NO and release sirolimus.

5.2. Experimental

5.2.1. Materials and Instrumentation

Hexamethylene diisocyanate (HMDI) from Sigma-Aldrich (St. Louis, MO) was distilled at reduced pressure right before use. Triethylamine, anhydrous ether, dibutyltin dilaurate (DBTDL), sodium borohydride ($NaBH_4$), sodium cyanoborohydride ($NaCNBH_3$), Ethylenedinitrilotetraacetic acid disodium salt (EDTA), reduced glutathione (GSH), phosphate buffered saline (PBS, pH 7.4) were all used as received from Sigma-Aldrich. Selenium cystamine (SeCA) is a small diselenide compound synthesized in our

group[7,8]. Anhydrous methyl sulfoxide (DMSO), methanol were from Fisher Scientific (Pittsburgh, PA) and used as received. Tetrahydrofuran (THF) was also from Fisher Scientific and was distilled over sodium and benzophenone prior to use. Sirolimus (rapamycin) was purchased from LC Laboratories (Woburn, MA). Tecophilic® HP-93A-100 was a product of Lubrizol Advanced Materials (Wilmington, MA). Vegetable oil was obtained from Kroger (Ann Arbor, MI). Balb/c mice were purchased from Harlan Laboratories.

FTIR spectra were collected on a Perkin-Elmer BX FT-IR system (Wellesley, MA). Nitric oxide flux from polymer coatings was measured by a chemiluminescent NO analyzer (NOA™ 280, Sievers Instruments, Inc. (Boulder, CO)). The selenium concentrations in the polymers were quantified by a Finnigan Element (inductively coupled plasma) ICP-mass spectrometer. Thermal profiles of polymers were characterized by a TA Q2000 differential scanning calorimeter (DSC) (TA Instrument, New Castle, DE). Sirolimus release rate was determined by high-performance liquid chromatography (HPLC)-based analysis (Hewlett Packard 1050 HPLC system).

5.2.2. Synthesis of PU-NCO

The urethane groups on CarboSil backbone were used to couple with HMDI through an allophanate reaction in the presence of a tin catalyst (DBTDL)[9] (see Scheme 5.2). A solution of Tecophilic (10 w/v % in anhydrous THF) was added dropwise to a ca. 5-fold molar excess of HMDI solution (10 w/v % in anhydrous THF with 0.1 v/v % DBTDL) under argon. The reaction mixture was stirred for 24 h at 40 °C, and the product was precipitated in copious anhydrous ethyl ether. The suspension was

centrifuged and the solid was collected and washed 3 times with anhydrous ethyl ether. After washing, the product was dried under vacuum for 1 d to remove any residual solvent. The resulting polymer with pendant isocyanate groups (PU-NCO) was further used to prepare organoselenium-derivatized polyurethanes (RSe-PUs).

5.2.3. Synthesis of Tecophilic-SeCA

Further derivatization of PU was carried out via a modified urea-forming reaction (see Scheme 5.2)[10, 11]. Five mL triethylamine (excess) was first mixed with 250 mg SeCA (0.78 mmol) in 25 mL anhydrous DMSO overnight at room temperature under argon. Tecophilic–NCO was dissolved in anhydrous DMSO under argon to make a 10 % w/v solution and added dropwise to the freshly prepared triethylamine/SeCA solution. The yellow reaction mixture was stirred under argon at room temperature and then heated to 40 °C for 24 h. The reaction mixture was cannulated to copious ethyl ether to precipitate the SeCA-derivatized Tecophilic (Tecophilic-SeCA). The suspension was centrifuged and the pale yellow Tecophilic-SeCA polymer was collected and washed 3 times with copious amount of ethylether. Afterwards, it was dried under vacuum for 2 d to remove the residual solvent and then stored at -20 °C until further experiments.

5.2.4. Reduction of Tecophilic-SeCA to Tecophilic-SeH

The resulting Tecophilic-SeCA was reduced with $NaBH_4$, $NaCNBH_3$ or GSH to remove the uncoupled halves of the SeCA molecules to generate Tecophilic-SeH (see Scheme 5.2).

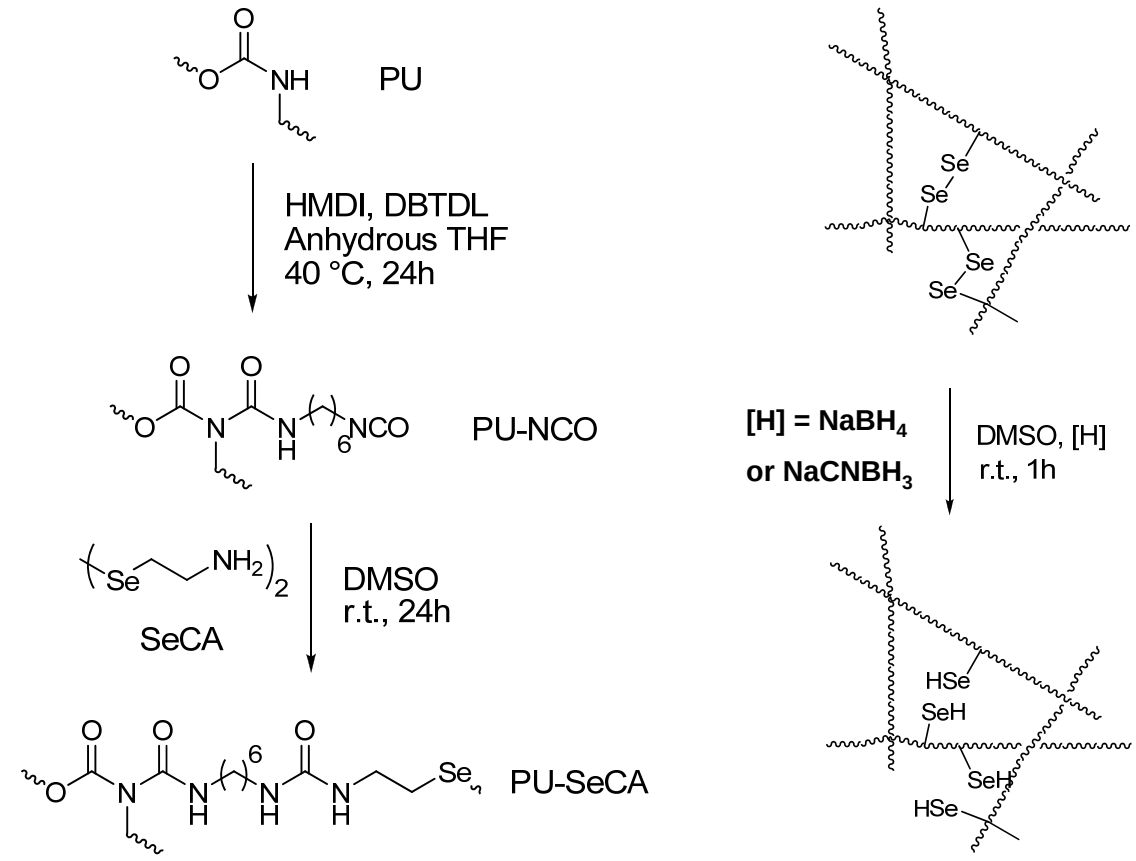

Scheme 5.2. Synthesis of PU-SeH.

To reduce Tecophilic-SeCA in GSH, a piece Tecophilic-SeCA polymer (approx. 10 mg) was placed in 5 mL deoxygenated PBS (100 mM, pH 7.4) with 200 μM GSH and 200 μM GSNO for 2 h with gentle shaking at room temperature. After reduction, the polymer piece turned from pale yellow to white due to the reduction of the diselenide bond to form Tecophilic-SeH. The resulting polymer was rinsed with copious amount of deoxygenated DI water and then with anhydrous ethylether to remove the water. Finally, the Tecophilic-SeH was dried in vacuum to remove the residual solvent and stored at -20 °C until further experiments.

The reduction using $NaBH_4$ or $NaCNBH_3$ was done following the synthesis of Tecophilic-SeCA as a one-pot reaction. Before precipitation, the reaction mixture was cooled from 40 °C to room temperature. Then, 60 mg of $NaBH_4$ or 100 mg of $NaCNBH_3$ (1.57 mmol) was added to the vigorously stirred Tecophilic-SeCA reaction mixture in 3 portions over 15 min. The reduction was performed under room temperature for 1 h and the color of the mixture turned from yellow to pale yellow. Several drops of 2 M HCl were added to the suspension to neutralize the polymer under vigorous stirring. The product, Tecophilic-SeH, was precipitated in copious anhydrous ethyl ether and the suspension was centrifuged and the solid was collected. Crude Tecophilic-SeH polymer was washed 3 times with ethyl ether, 3 times with deoxygenated DI water and then 3 times with ethyl ether. After washing, the product was dried under vacuum for 1 d to remove any residual solvent and stored at -20 °C until further experiments.

5.2.5. Characterization of RSe-PU

The selenium content in the polymers was quantified by ICP-MS. RSe-PU samples as well as blank polymer samples (accurately weighed, 15-25 mg for each sample) were dissolved in 0.5 mL fuming HNO_3 at room temperature. DI water was added to bring the volume to exactly 2 mL. Selenium concentrations in the solutions were analyzed by Ted Huston in the Department of Geological Sciences in University of Michigan (Ann Arbr, MI) and then converted to the concentrations in corresponding polymers.

A differential scanning calorimeter was used to characterize the thermal profile of the polymers. Approx. 5 mg of either RSe-PU or control polymer samples was placed in

Tzero aluminum pan and placed in TA Q2000 DSC. An empty pan was used as the reference. The samples were equilibrated at -20.00 °C and then the temperature would ramp to 280.00 °C at a rate of 20.00 °C/min. Heat flow was recorded and the onset transition temperatures were measured.

5.2.6. Systemic Toxicity Studies of Tecophilic-SeH

The potential acute toxic adverse effects of the PU-SeH coatings within organs and tissues that are remote from the site of contact were tested in collaboration with Yang Wang in Dr. Roy-Chaudhury's internal medicine research lab in the University of Cincinnati according to ISO standard 10993-11[12] and 10993-12[14]. Balb/c mice (9 weeks old, 25-30 g) were used in this study. Fluid extracts of the polymer coatings were prepared in saline and vegetable oil at 37 °C for 24 h with a 30 cm^2 surface area to 10 mL fluid volume ratio. Single doses (0.10 mL/mouse for saline extracts through intravenous (IV) injection and 0.15 mL/mouse for oil extracts through intraperitoneal (IP) injection) were administered to groups of five mice. Control mice were injected accordingly with extraction fluids alone. After injection, the mice were observed for adverse signs, such as convulsions or prostration, and were weighed daily.

5.2.7. Preparation of NOGen/SiroRel Films

To prepare combined NO generation/sirolimus releasing polymer films, 300 mg of Tecophilic-SeH was dissolved in 30 mL THF and then 7.5 mg sirolimus was added to make a cocktail. A film was made by using this cocktail in a Teflon mold (25 mm × 75 mm) and drying under a nitrogen stream for 24 h. The film was then further dried in

vacuum for 2 d to remove any residual solvent. The final NOGen/SiroRel films were stored at -20 ºC and cut to smaller sizes for characterization of NO and sirolimus release and other studies.

5.2.8. Preparation of RSNOs and NO detection

GSH stock solutions (5 mM) were made by dissolving 15.35 mg GSH in 10 mL DI water with 25 μM EDTA. The GSNO stock solution (5 mM) was prepared as described earlier[7, 8]. Briefly, equal volumes of fresh 10 mM reduced glutathione in 60 mM H_2SO_4 and 10 mM of $NaNO_2$ (with 25 μM EDTA) were mixed at room temperature. GSNO stock solution should sit for at least 5 min before use and solutions should be stored between 0 to 4 °C and should be discarded 6 h after preparation.

GSNO and GSH were directly injected into a working buffer solution (PBS, pH 7.4 solution containing 25 μM EDTA) to obtain the desired concentrations of RSNOs and RSHs. Typically, the NO generated during the catalytic RSNO decomposition was purged from the test solution with nitrogen and detected by using the NOA. The amount of NO evolved from the test solution can be calculated based on the calibration curves of the NOA.

5.2.9. Sirolimus Release Studies

To determine the pharmacological release kinetics of sirolimus, films were immersed in PBS (10 mM, pH 7.4) at 37 °C. Samples taken at distinct time points were then subjected to HPLC-based analysis. Total releasable sirolimus was extracted with

methanol overnight at 37 °C. Sirolimus methanol solution was injected to HPLC for quantification.

5.3. Results and Discussion

5.3.1. Synthesis and Characterization of RSe-Derivatized Polyurethanes

Derivatization was carried out on Tecophilic, a commercially available polyether polyurethane that has been developed specifically for biomedical applications[13]. The urethane groups on the Tecophilic backbones were used to couple with HMDI through an allophanate reaction in the presence of a tin catalyst[8]. The reaction was carried out at a mild temperature (40 °C) with slow addition of Tecophilic solution into a great excess of HMDI to reduce the possibility of HMDI cross-linking separate polymer chains. The coupling was confirmed using IR by the appearance of a NCO absorption band at 2266 cm^{-1}, and another new band at 1619 cm^{-1} (corresponding to urea absorption) after reaction for 1 d (see Figure 5.1). The resulting isocyanated Tecophilic (Tecophilic-NCO) was worked-up in an anhydrous environment and stored in argon at -20 °C to prevent hydrolysis.

The resulting polymer with pendant free isocyanate groups was then reacted with amine groups of SeCA, a small diselenide compound[7,8]. The resulting Tecophilic-SeCA was then reduced with $NaBH_4$, $NaCNBH_3$ or GSH to remove the uncoupled halves of the SeCA molecules to generate Tecophilic-SeH (see Scheme 5.2).

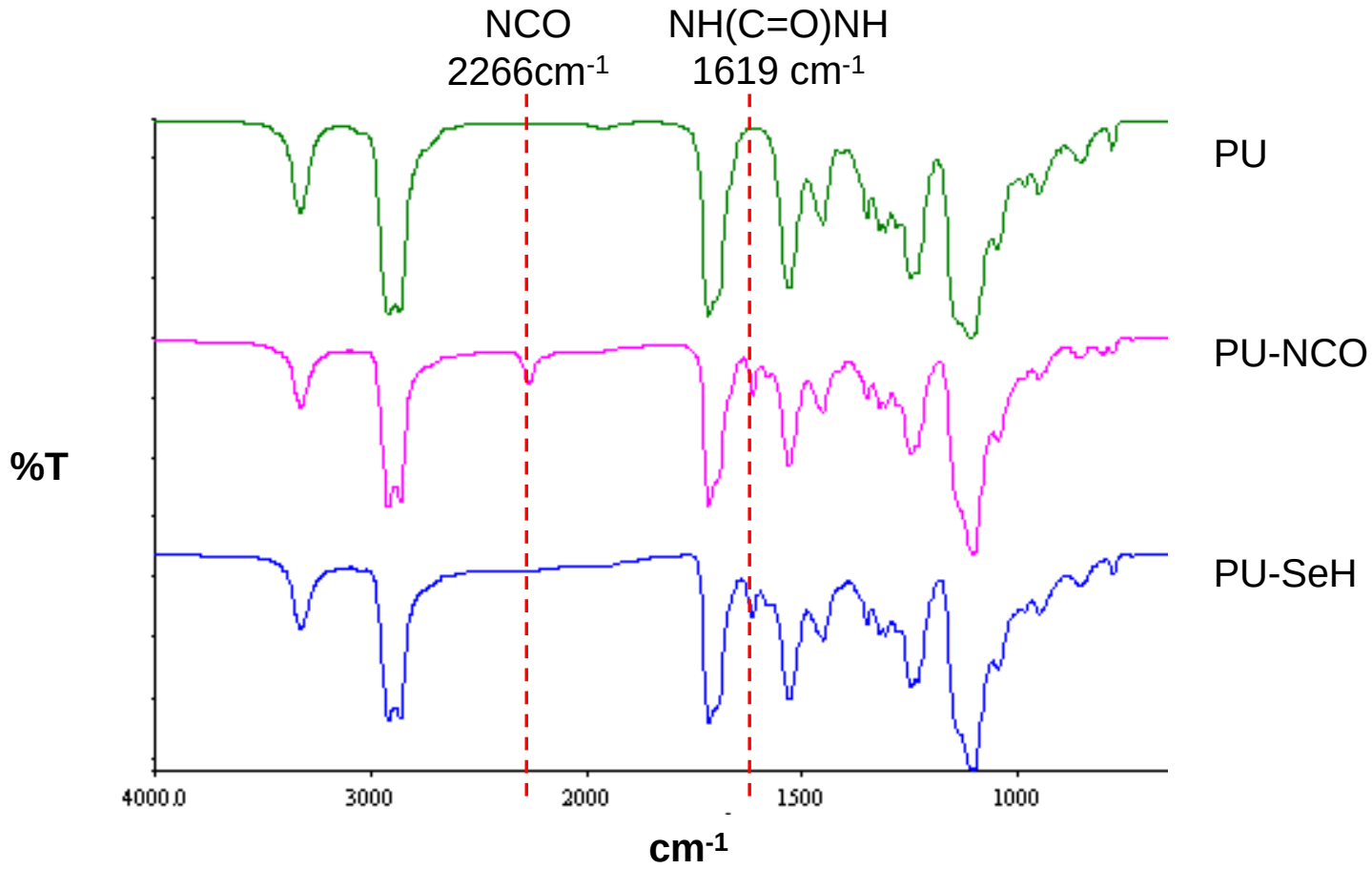

Figure 5.1. IR spectra of various PUs.

RSe-derivatized polyurethanes were dissolved in fuming HNO_3 and the selenium concentrations in the polymers were quantified by ICP-MS. Elemental analyses (see Figure 5.2) showed that the concentrations of selenium in the unreduced RSe-derivatized Tecophilic material was 247 ± 12 μmol/g. In the chemically reduced RSe-derivatized PUs, the amount of selenium dropped to approx. 100-150 μmol/g, depending on which reducing agent had been employed (hence different reducing efficiency). More specifically, for Tecophilic-SeH reduced with GSH, the selenium concentration was 114 ± 6 μmol/g. For Tecophilic-SeH reduced with $NaBH_4$, the selenium concentration was 105 ± 5 μmol/g. For Tecophilic-SeH reduced with $NaCNBH_3$, the selenium concentration was 157 ± 8 μmol/g. This decrease was due to the removal of unbound small organoselenium molecules (SOSM) and the removal of pendent halves of the diselenides. The reduction step was very critical in that it greatly decreased the leaching of selenium species in subsequent solution phase testing of the new polymer. It also greatly improved the processing of the polymer since it broke the diselenide bonds and thus reduced the degree of crosslinking of polymer backbones, which, in turn, increased the solubility of the newly prepared RSe-PUs.

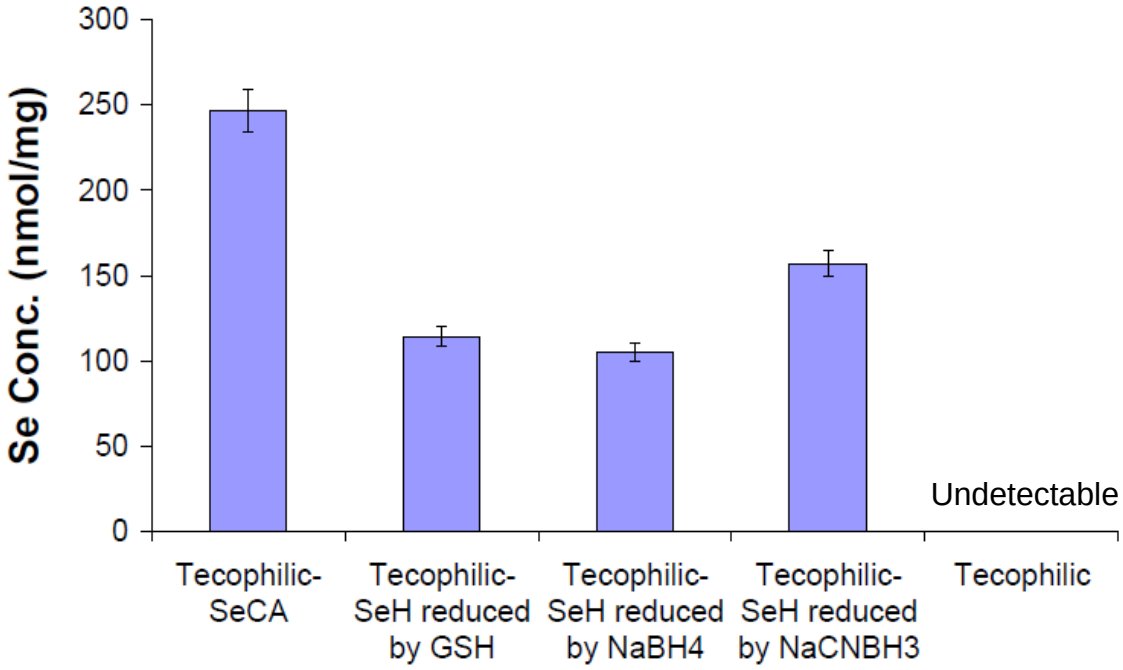

Figure 5.2. Selenium content in RSe derivative of Tecophilic treated with varying reducing agents.

5.3.2. Thermal Properties of Tecophilic-SeH

A differential scanning calorimeter was used to characterize the thermal profile of the polymers. The heat flow curves (Figure 5.3) showed that both Tecophilic and Tecophilc-SeH have broad melting peaks while the latter's onset T_m is approx. 15 ºC lower. This is probably due to the derivatization of the urethane nitrogen atom with a half selenium cystamine moiety which disrupts, to some extent, the hydrogen bonds in the ordered structure of the thermoplastic polyurethane elastomer's hard segments. No thermal transitions above 280 ºC were measured as Tecophilic started to decompose and gasify.

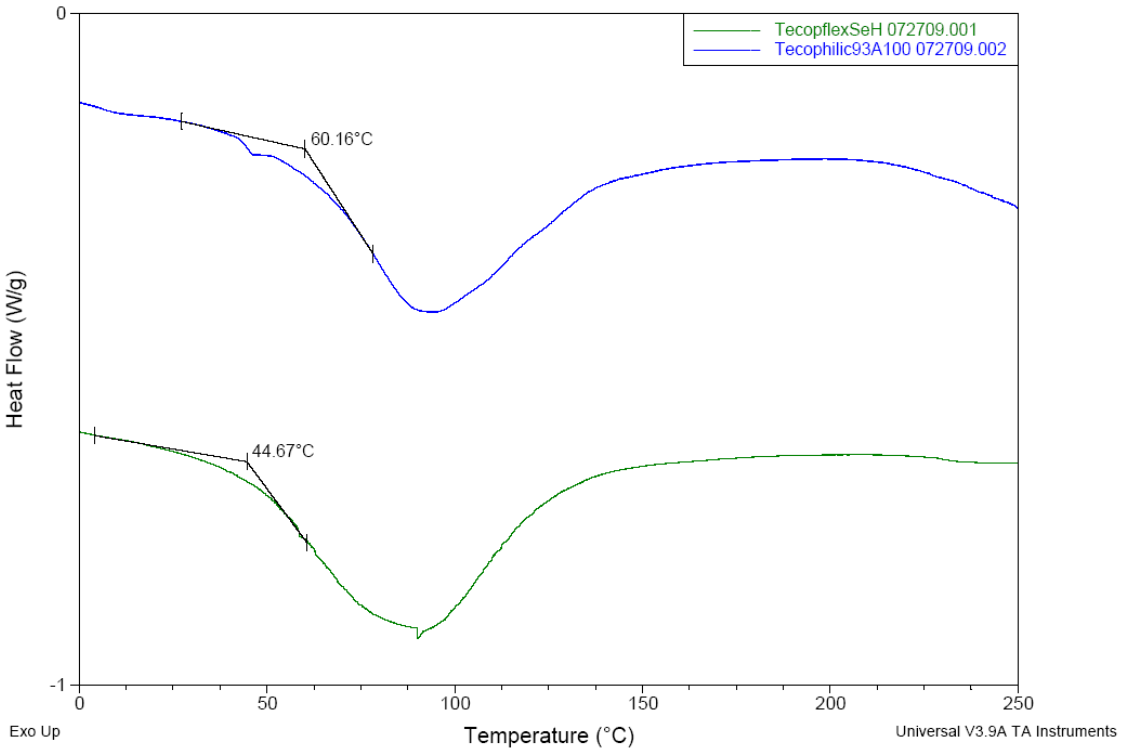

Figure 5.3. Heat flow curves of Tecophilic and Tecophilic-SeH. Approx. 5 mg polymer samples was placed in Tzero aluminum pan and placed in TA Q2000 DSC. The samples were equilibrated at -20.00 °C and then the temperature would ramp to 280.00 °C at a rate of 20.00 °C/min.

5.3.3. Systemic Toxicity Studies of Tecophilic-SeH

The potential acute systemic toxicity of Tecophilic-SeH was tested according to ISO 10993-11[12] and 10993-12[14]. No weight loss of Balb/c mice was observed after injection of either aqueous or organic extract solutions (see Figure 5.4). In addition, no adverse signs (prostration, convulsion, etc.) were observed. The lack of systemic toxicity indicates that Tecophilic-SeH is a good candidate for implantable biomedical devices.

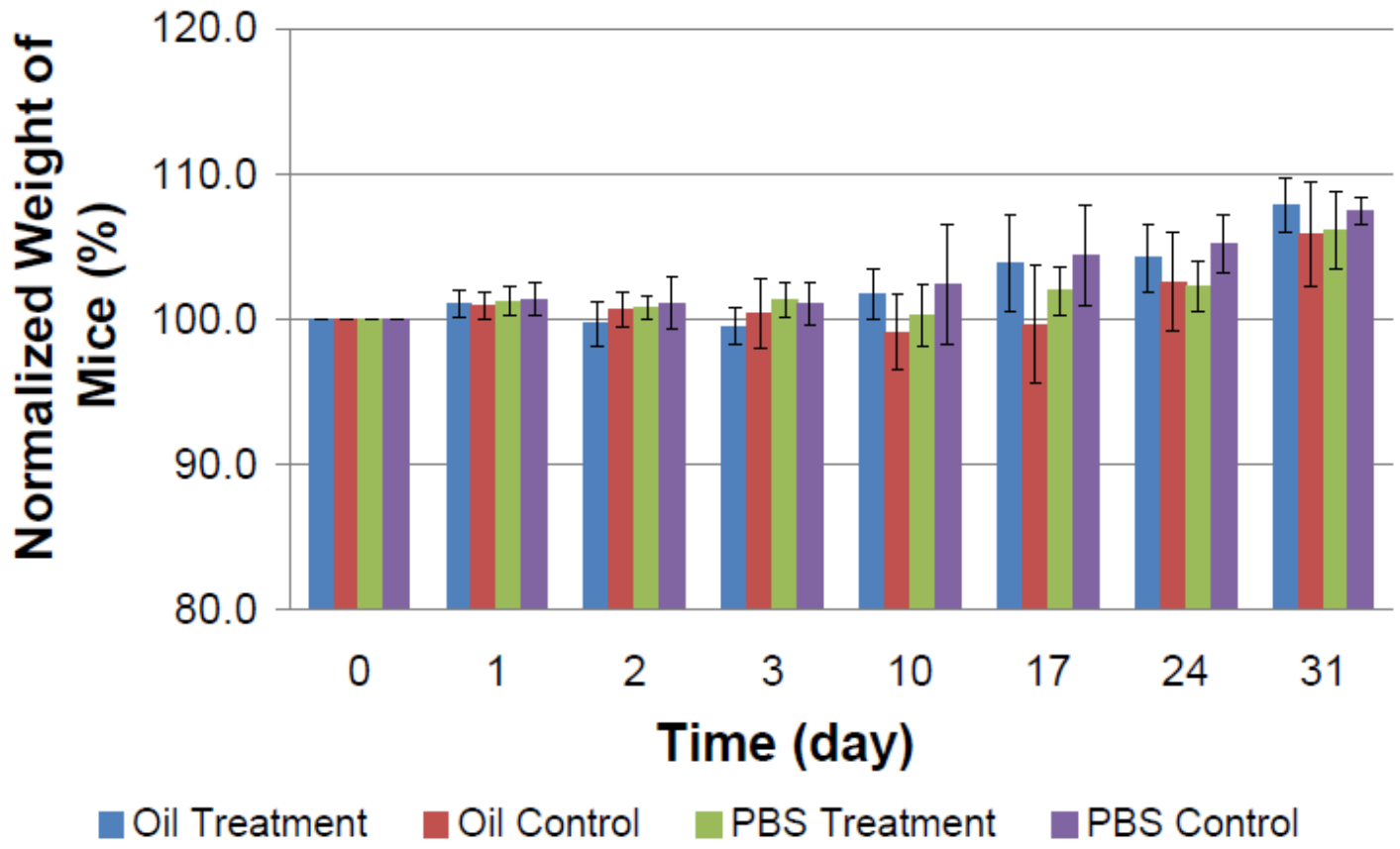

Figure 5.4. Weights of Balb/c mice after IP injection of oil extracts/control or IV injection of saline extracts/control over a 31-day period (n = 5).

5.3.4. NO Generation Studies

Organoselenium compounds have been studied previously as mimics of glutathione peroxidase (GPx, EC 1.11.1.9), a selenoenzyme that catalyzes the reduction of a variety of hydroperoxides using GSH as the reducing substrate[15]. It has also been shown that RSe compounds, including the SeCA as well as naturally occurring GPx, can generate NO from RSNOs via a catalytic reaction[16]. This type of catalyst is highly selective for reduction of *S*-nitrosothiol and exhibits no catalytic activity for nitrite or nitrate reduction[7,8]. A mechanism has been proposed which comprises a fast denitrosation of RSNO by diselenide (Scheme 5.3, eq 4), and a slower catalytic cycle involving a selenolate intermediate which is regenerated by the reducing agent (Scheme 5.3, eqs 1-3).

The catalytic activity of Tecophilic-SeH was investigated by measuring NO generation via chemiluminescence measurement (see Figure 5.5). Nitric oxide production was initiated upon introducing the RSe-derivatized polymer into solutions containing GSNO as the NO donor and GSH as the reducing agent. NO fluxes plateaued to a steady level and then ceased almost entirely upon the removal of the film, indicating GSNO catalytically broke down at the polymer solution interface. Repeated immersion and removal of the slide replicate the up-and-down NO generation pattern. The NO flux decreased slightly over time which is likely attributed to the consumption of the GSNO in the bulk test solution. The marginal baseline increase after film removal suggested a small leaching of selenium catalyst from the polymer film into the test solution during the measurements. The leached selenium small molecules could initiate a homogeneous GSNO decomposition which is much faster than the heterogeneous surface reaction

mediated by the polymer-bound selenium species. The mechanism of leaching is still under more detailed investigation.

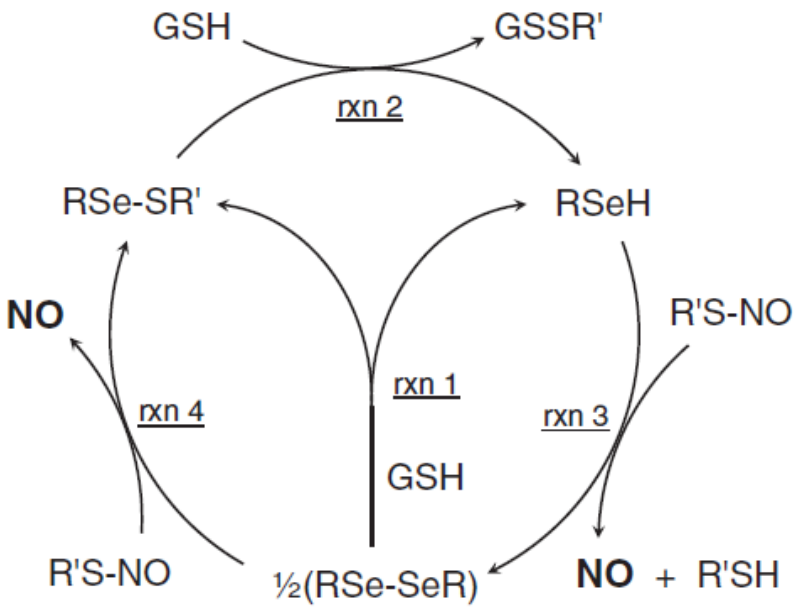

$$\text{RSe-SeR} + \text{GSH} \rightleftarrows \text{RSe-SG} + \text{RSe}^- + \text{H}^+ \quad (1)$$

$$\text{RSe-SG} + \text{GSH} \rightleftarrows \text{RSe}^- + \text{H}^+ + \text{GS-SG} \quad (2)$$

$$\text{RSe}^- + \text{H}^+ + \text{R'S-NO} \rightleftarrows \tfrac{1}{2}\text{RSe-SeR} + \text{R'SH} + \text{NO} \quad (3)$$

$$\text{RSe-SeR} + 2\text{R'S-NO} \rightleftarrows 2\text{RSe-SR'} + 2\text{NO} \quad (4)$$

Scheme 5.3. Proposed reaction mechanism of RSNO decomposition catalyzed by organoselenium species in the presence of glutathione as a reducing agent. Each species represents: diselenide (RSe-SeR), thiol (R'SH and GSH (glutathione)), selenosulfide (RSe-SR' and RSe-SG (a glutathione adduct)), selenolate (RSe^-, a conjugate base of selenol), and *S*-nitrosothiol (R'SNO). (Adapted from Cha, W.; Meyerhoff, M.E. *Biomaterials* **2007,** 28, 19-27[8].)

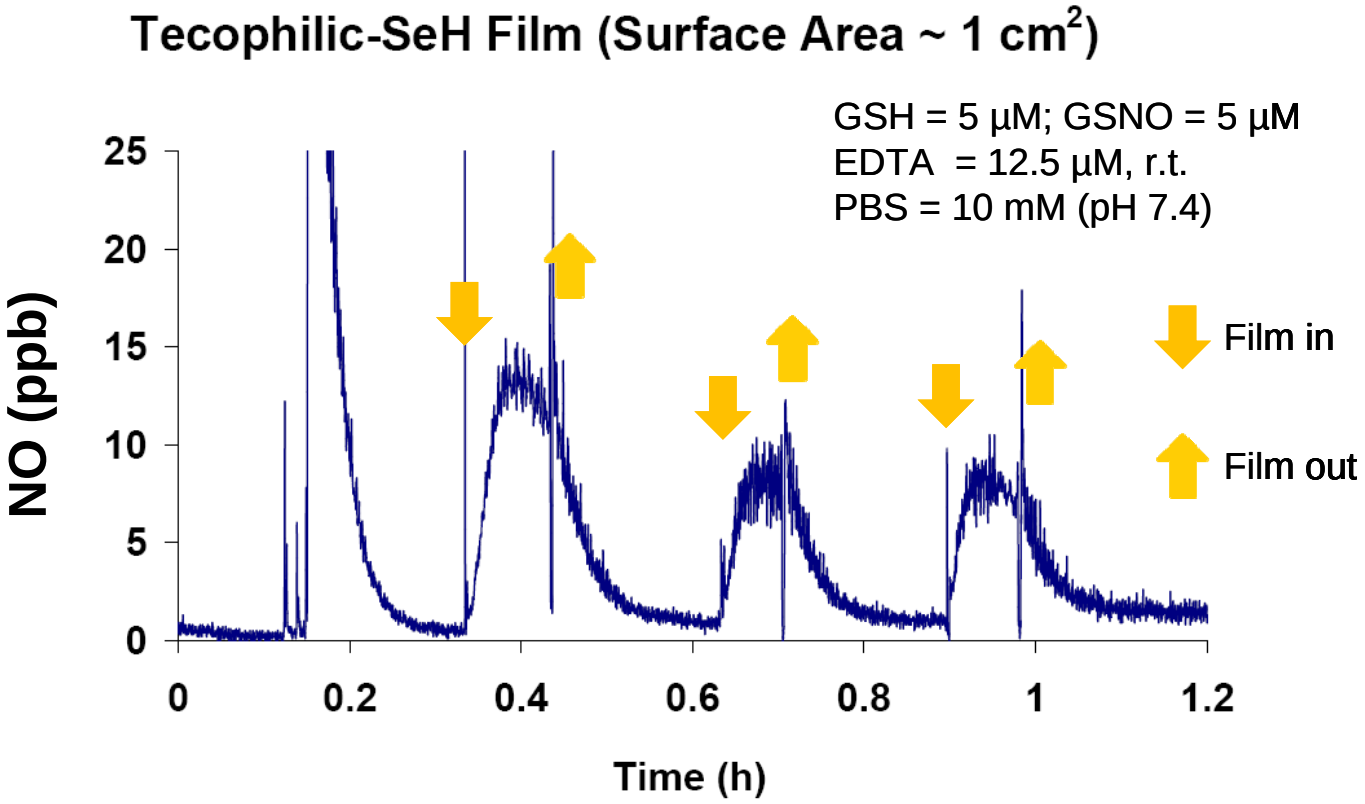

Figure 5.5. Catalytic generation of NO from RSNO by PU-SeH.

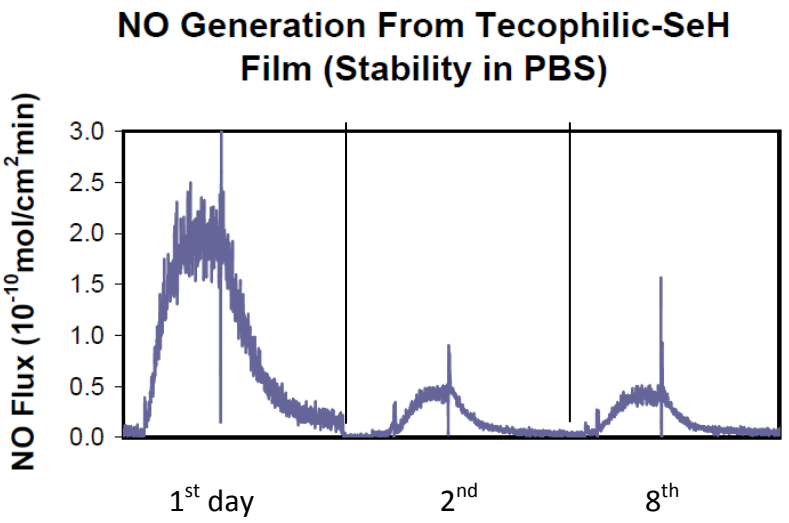

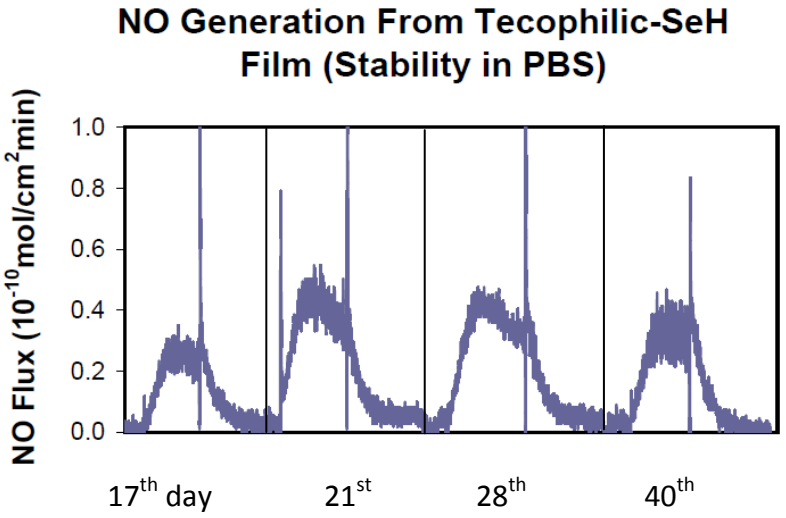

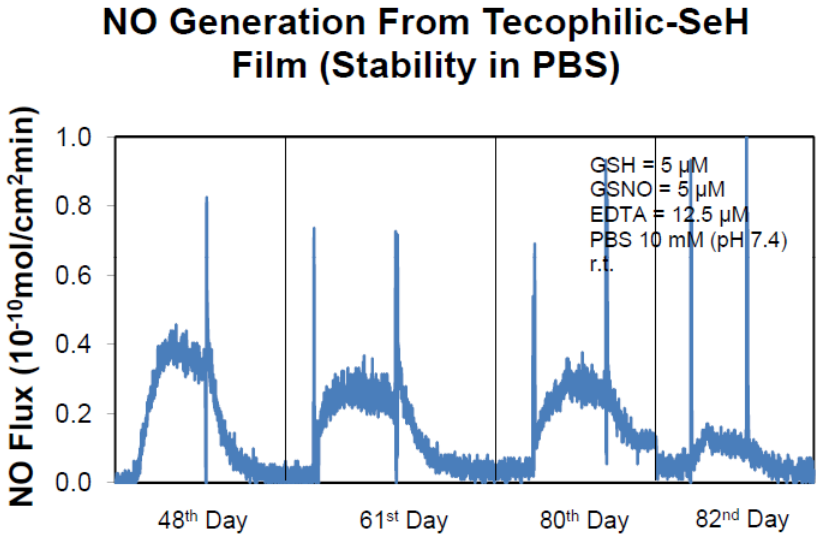

Figure 5.6. Nitric oxide generation capability was tested at specific time points.

In this study, the NO generating capability of the combined PU-SeH and sirolimus release polymer was tested. A piece of Tecophilic-SeH/Sirolimus polymer (ca. 3 mg with a surface area of 1 cm^2) was incubated in 4 mL PBS (pH 7.4, 10 mM) at room temperature. Nitric oxide generation capability was tested at specific time points (see Figure 5.6). It was found that the NO flux decreased quickly on the first day and stabilized starting from the second day. NOA testing was stopped at the 82nd day when the NO flux decreased to a level below 0.2 × 10^{-10} mol min^{-1} cm^{-2} (see Figure 5.7). The NO generating capability of the combined PU-SeH and sirolimus release polymer was also tested in air (see Figure 5.7).

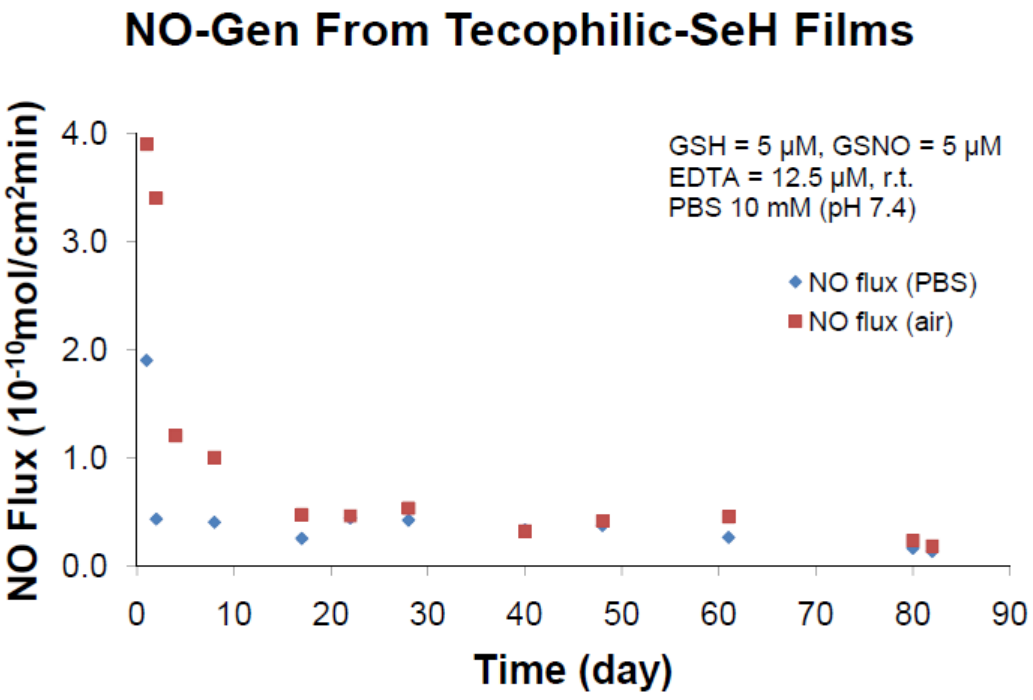

Figure 5.7. Stability of immobilized small organoselenium molecule catalyst in PBS (pH 7.4) and air at room temperature.

5.3.5. Sirolimus Release Studies

The pharmacological release kinetics of sirolimus was determined by immersing Tecophilic-SeH/sirolimus films in PBS at 37 °C. Samples taken at distinct time points were subjected to HPLC analysis. It has been found that sirolimus release rate slowly increased from approximately 0.4 to 0.6 μg cm^{-2} h^{-1} over the first 5 days and then slowly decreased to approximately 0.2 μg cm^{-2} h^{-1} over the following 3 weeks (see Figure 5.8). Methanol extraction solution was used to quantify the total releasable sirolimus and the total releasable sirolimus in the coating was estimated to be ca. 180 μg cm^{-2}. This is almost twice as much as the dosage of the sirolimus-coated BX Velocity stent (Cordis) (140 μg sirolimus cm^{-2})[1].

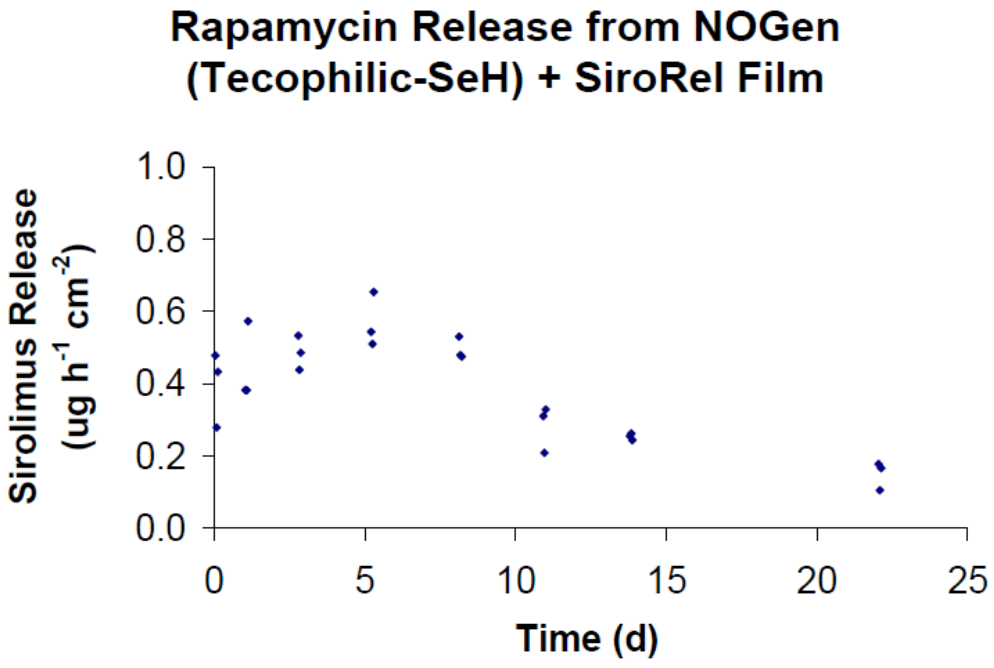

Figure 5.8. HPLC measurements of sirolimus release from polymeric coatings in PBS (pH 7.4) under 37 °C with intermittent sampling.

5.4. Conclusions

Organoselenium-derivatized medical-grade polyurethanes have been prepared. These NO generating materials were mixed with sirolimus to make dual-functional polymeric coatings that both generate NO from endogenous RSNO species and release sirolimus. Such composite polymeric coatings may be useful for preparing DESs that can potentially reduce the occurrence of late stent thrombosis as well as thrombosis on other intravascular biomedical devices. While, in principle, the generation of NO at the blood/polymer interface could be infinite in duration, it is likely that some leaching and/or fouling of the catalytic sites may limit the length of time that physiologically relevant levels of NO can be continuously generated when such polymers are in contact with blood. To address this issue, further studies are required.

5.5. References

1. Sousa, J.; Serruys, P.; Costa, M. 'New frontiers in cardiology: Drug-eluting stents: Part I.' *Circulation* **2003**, 107, 2274-2279.

2. Marx, S.; Marks, A. 'Bench to bedside: The development of rapamycin and its application to stent restenosis.' *Circulation* **2001**, 104, 852-855.

3. Curfman, G.D.; Morrissey, S.; Jarcho, J.A.; Drazen, J.M. 'Drug-eluting coronary stents – Promise and uncertainty.' *N. Engl. J. Med.* **2007**, 356, 1059-1060.

4. Shuchman, M. 'Trading restenosis for thrombosis? New questions about drug-eluting stents.**'** *N. Engl. J. Med.* **2006**, 355, 1949-1952.

5. Feelisch, M.; Stamler, J.S. *Methods in Nitric Oxide Research* West Sussex: John Willey and Sons Ltd. **1996**.

6. Jun, H.W.; Taite, L.J.; West, J.L. 'Nitric oxide-producing polyurethanes.' *Biomacromolecules* **2005**, 838-844.

7. Cha, W.; Meyerhoff, M.E. '*S*-Nitrosothiol detection via amperometric nitric oxide sensor with surface modified hydrogel layer containing immobilized oganoselenium catalyst.' *Langmuir* **2006**, 22, 10830-10836.

8. Cha, W.; Meyerhoff M.E. 'Catalytic generation of nitric oxide from *S*-nitrosothiols using immobilized oganoselenium species.' *Biomaterials* **2007,** 28, 19-27.

9. Zhou, Z.R.; Meyerhoff, M.E. 'Preparation and characterization of polymeric coatings with combined nitric oxide release and immobilized active heparin.' *Biomaterials* **2005**, 26, 6506–6517.

10. Pittelkow, M.; Christensen, J.B.; Meijer, E.W. 'Guest-host chemistry with dendrimers: stable polymer assemblies by rational design.' *J. Polym. Sci. A1* **2004**, 42, 3792–3799.

11. Bello, D.; Streicher, R.P.; Woskie, S.T. 'Evaluation of the NIOSH draft method 5525 for determination of the total reactive isocyanate group (TRIG) for aliphatic isocyanates in autobody repair shops.' *J. Environ. Monitor*. **2002**, 4, 351–360.

12. 'Biological evaluation of medical devices – Part 11: Tests for systemic toxicity.' ANSI/AAMI/ISO 10993-11:**2006**.

13. http://www.lubrizol.com/EnginereedPolymers/ThermedicsPolymerProducts.html

14. 'Biological evaluation of medical devices – Part 12: Sample preparation and reference materials.' ANSI/AAMI/ISO 10993-12:**2006**.

15. Mugesh, G.; Singh, H.B. 'Synthetic organoselenium compounds as antioxidants: glutathione peroxidase activity.' *Chem. Soc. Rev.* **2000**, 29, 347–357.

16. Hou, Y.; Guo, Z.; Li, J.; Wang, P.G. 'Seleno compounds and glutathione peroxidase catalyzed decomposition of *S*-nitrosothiols.' *Biochem. Biophys. Res. Commun.* **1996,** 228, 88–93.

17. Vaughn, M.W.; Kuo, L.; Liao, J.C. 'Estimation of nitric oxide production and reaction rates in tissue by use of a mathematical model.' *Am. J. Physiol.* **1998,** 274, H2163-H2176.

18. Batchelor, M.M.; Reoma, S.L.; Fleser, P.S.; Nuthakki, V.K.; Callahan, R.E.; Shanley, C.J.; Politis, J.K.; Elmore, J.; Merz, S.I; Meyerhoff, M.E. 'More lipophilic dialkyldiamine-based diazeniumdiolates: Synthesis, characterization, and application in preparing thromboresistant nitric oxide release polymeric coatings.' *J. Med. Chem.* **2003,** 46, 5153-5161.

19. Wu, Y.D.; Zhou, Z.R.; Meyerhoff, M.E. 'In vitro platelet adhesion on polymeric surfaces with varying fluxes of continuous nitic oxide release.' *J. Biomed. Mater. Res. A* **2007,** 81A, 956-963.

20. Carver, J.; Doctor, A.; Zaman, K.; Gaston, B. '*S*-Nitrosothiol formation.' *Methods in Enzymology* **2005**, 396, 95-105, Nitric Oxide, Part E.

CHAPTER 6

Conclusions and Future Directions

6.1. Conclusions

The research in this dissertation has focused on the development of novel multifunctional polymeric coatings that incorporate multiple antithrombogenic and/or anti-proliferative bioactive agents. These polymers could potentially be employed within certain blood contacting medical devices as well as used to construct or coat a wide variety of biomedical devices that are in contact with blood to improve the hemocompatibility of the devices. The incorporated bioactive agents, such as endogenous small molecules (nitric oxide (NO)), polysaccharides (heparin), proteins (thrombomodulin (TM)), and drugs (sirolimus), are intended to function synergistically to prevent the formation of thrombus and the proliferation of smooth muscle cells (SMCs), which are considered to be the two major causes for the failure of various blood-contacting implantable devices.

In Chapter 2, the development of new multifunctional bilayer polymeric coatings was described. These polyurethane-based polymeric coatings were prepared so as to present both controlled NO release and surface-bound active thrombomodulin (TM) or combined TM and heparin. These new coatings combine the anti-platelet activity of NO

and the anticoagulant ability of immobilized heparin and TM so as to more closely mimic the nonthrombogenic properties of the endothelium by multiple complementary anti-thrombotic mechanisms. The anticoagulant activity of TM and heparin were evaluated by activated protein C and anti-factor Xa assays, respectively. The NO release rate could be tuned by controlling different loadings of NO donors as well as by changing the coating procedures. It was possible to control the NO fluxes of the films at ca. the physiological level by applying top coatings with different thicknesses. The immobilization of TM and heparin had little influence on NO release levels, and the NO release did not influence the activity of surface-bound heparin and TM.

In addition to thrombus formation, SMC proliferation is another important cause for the failure of various blood-contacting implantable devices, including stents and small-diameter vascular grafts. In Chapter 3, the first dual-functional polymeric coating that releases both sirolimus and NO was prepared. This was accomplished by doping an underlying polymer film with a lipophilic diazeniumdiolate NO donor, and the outer layer with a sirolimus impregnated PU coating. In a formulation with 16 wt % NO donor in the underlying layer and 23 wt % sirolimus in the outer layer, NO was released at physiologically relevant levels (from 10 to 1×10^{-10} mol min^{-1} com^{-2}) with simultaneous release of sirolimus (from 3.00 to 0.10 μg cm^{-2} h^{-1}) over a period of 2 weeks. The use of NO, in combination with an anti-cell proliferation agent may provide the ideal solution to reduce both clotting and restenosis risk for the blood-contacting implanted medical devices.

In Chapter 4, *in vitro* cell testing was carried out to assess the effects of the new dual functional polymeric coatings on cell growth. Surprisingly, it was discovered that

the borate additive (lipophilic anionic species), which was used in the polymer phase to sustain the NO flux by maintaining the organic phase pH at a level required to drive NO release from the diazeniumdiolate, was rather toxic to SMCs. As a result, the possibilities of using alternative borate sources were explored and it was found that the problems of degradation and leaching could be greatly reduced by using a more stable and lipophilic borate species (e.g. potassium tetrakis[3,5-bis(trifluoromethyl)phenyl]borate as was described in chapter 4). Furthermore, in order to completely eliminate the leaching and possible toxicity issue associated with small molecules, a sulfonated polyurethane (PU-SO_3) was synthesized with sulfonic anionic sites chemically tethered to the polymer backbones. *In vitro* EC and SMC studies were done in collaboration with Ms Diane Studzinski in Dr. Shanley's Surgical Research Lab at Beaumont Hospital (Royal Oak, MI) and have proved that such coatings indeed showed much improved cell compatibility.

In Chapter 5, another approach to achieve sustained NO release was explored by using *S*-nitrosothiol (RSNO) species, the endogenous NO donors circulating in our blood stream. Selenium-derivatized polyurethanes (PUs) were synthesized and coatings made from such polymers showed prolonged catalytic NO-generating capability from RSNOs compared to NO-release polymeric coatings. This is because the RSNO species are constantly generated in the blood stream and serve as a reservoir that is theoretically infinite. Compared to NO-release coatings, such NO-generating coatings can also decrease greatly in thickness which would make them more applicable to the polymeric coating matrices for preparing drug-eluting stents (DESs) and other medical devices in which thinner coatings are preferred. Indeed, the first dual-functional polymeric coating

that can both generate NO from endogeneous RSNO species and simultaneously release sirolimus at a controlled rate was prepared and characterized. The new coating can potentially suppress SMC proliferation and thrombosis, as well as facilitate endothelialization at a given implant site.

6.2. Future Directions

6.2.1. Alternative Non-Toxic pH Stabilizing Additives for Sustained NO Release

In Chapter 4, the use of more lipophilic borate species as well as chemically tethered sulfonate anionic groups have shown much reduced cytotoxicity towards EC and SMC while maintaining the continuous NO flux. Similar experiments could also be carried out using sodium cholate, a naturally occurring compound (see Figure 6.1). As a highly lipophilic anion, cholate will likely function similarly to borate anion and will extract protons from the surrounding solutions into the films to maintain the polymeric phase pH value low enough for sustained NO release from the *N*-diazeniumdiolate NO donors.

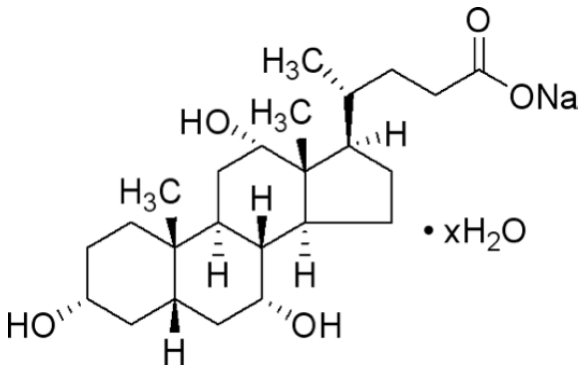

Figure 6.1. Structure of sodium cholate hydrate.

Indeed, a polymer coating has been prepared with sodium cholate as the additive and its NO release property has been characterized by NOA (see Figure 6.2). It has been shown that such film exhibits a sustained NO release for at least 20 d. The NO flux needs to be increased in future studies since the current flux is very close to the lower end of the endogenous NO flux on healthy endothelium ($0.5 – 4.0 \times 10^{-10}$ mol min^{-1} cm^{-2})[1]. Parameters for optimization should include hydrophilicity of the polymer matrices, thickness of the top coating, concentration of NO donor in the polymer, ratio between cholate and NO donor, solvent drying process, etc.

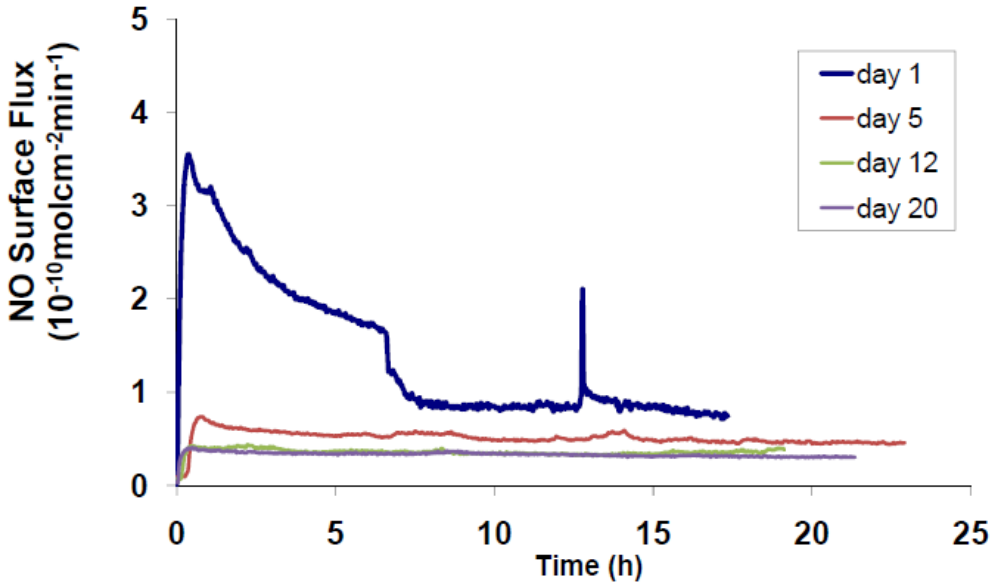

Figure 6.2. Nitric Oxide flux profiles of a PU catheter sleeve with sodium cholate as the pH-stabilizing additive. The underlying layer was loaded with equal molar of DBHD/N_2O_2 and sodium cholate (0.5 mmol DBHD/N_2O_2 and 0.5 mmol sodium cholate per gram PurSil). The top-coatings were made by dip-coating the catheter sleeves in 2 w/v % solution of PurSil in THF/DMAc (4:1, v/v). The PU catheter sleeve was incubated in PBS (pH 7.4, 10 mM) at 37 ºC and the released NO was purged with nitrogen flow and detected by a chemiluminescent NO analysizer (NOA™ 280, Sievers Instruments, Inc. (Boulder, CO)).

Another possibility is to use polymer additive that can release small acidic molecules upon degradation. A good candidate is poly(lactide-*co*-glycolide) (PLGA) since it is an FDA approved biodegradable polymer and has been widely used in bioabsorbable sutures[2], implantable vascular closure devices[3], etc. Lactic acid and glycolic acid are its degradation products (see Scheme 6.1). It is hypothesized that the presence of this continuous hydrolytic degradation will compensate for the increase in pH from generation of the free amines from NO release reaction, thereby maintaining a greater rate of NO release for longer periods of time[4].

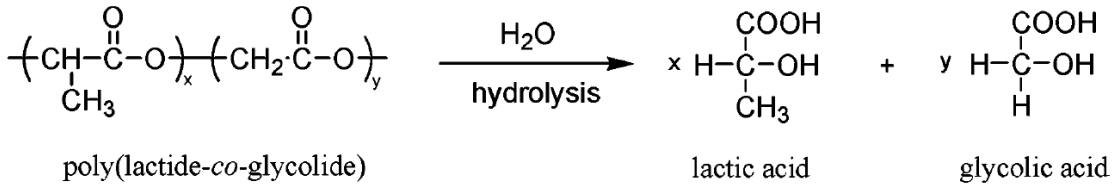

Scheme 6.1. Hydrolysis of PLGA in aqueous environment (adapted from Zhou, Z. and Meyerhoff, M. E. *Biomacromolecules* **2005**, 6, 780-789[4]).

By varying the types of monomers (D-lactide, L-lactide), the ratios between glycolide and lactide, molecular weight, the molecular weight of the copolymer, as well as the end groups, the degradation rate of PLGA can be tuned in a very wide range from 1-2 months to more than 24 months (see Table 6.1)[5]. This provides a full array of PLGA polymers to be tested to achieve the optimal NO release profile.

Table 6.1. Physical properties of selected PURASORB polymers (PLGA). Adapted from product data sheet[5] of Purac Biomaterials (Lincolnshire, IL).

Physical properties of selected PURASORB polymer families					
PURASORB polymers		**Tensile modulus of elasticity (GPa)**	**Tensile strength (MPa)**	**Elongation at break (%)**	**Degradation time* (months)***
PL	Poly(L-lactide)	3.1-3.7	60-70	2-6	> 24
PDL	Poly(DL-lactide)	3.1-3.7	45-55	2-6	12 – 16
PG	Poly(glycolide)	6.5-7.0	90-110	1-2	6 – 12
PDLG 50	50/50 DL-lactide/glycolide	3.4-3.8	40-50	1-4	1 – 2
PLG 85	85/15 L-lactide/glycolide	3.3-3.5	60-70	2-6	12 – 18
PLC 70	70/30 L-lactide/ε-caprolactone	0.02-0.04	18-22	>100	12 – 24

6.2.2. In Vitro Cell Studies of NO/Sirolimus Release Polymeric Coatings

In Chapter 4, *in vitro* EC and SMC viability tests have shown that the control polymeric coatings containing potassium tetrakis-(bis-3,5-trifluoromethylphenyl)borate (KTFPB) or PU-SO_3 had much improved biocompatibility. *In vitro* SMC proliferation and differentiation studies have also proved that such NO/siroliumus release coatings have decent efficacy towards the suppression of SMC proliferation and differentiation. Future work should be focused on testing whether these coatings are capable of enhancing endothelialization on the blood-material interfaces as had been observed on the NO-release coatings in the studies[6,7] reported by Dr. West's research group at Rice University. These experiments could be done in collaboration with Ms Diane Studzinski in Dr. Shanley's Surgical Research Lab at Beaumont Hospital (Royal Oak, MI), since she is already quite familiar with handling the NO/sirolimus release polymer materials.

6.2.3. Further Evaluation and Testing of Tecophilic-SeH and Tecoflex-SO_3 According to ISO (International Organization for Standardization) Standards

In Chapters 4 and 5, two new PU-based polymers have been synthesized, namely, Tecoflex-SO_3 and Tecophilic-SeH. They are intended to be used as matrices of hemocompatible polymeric coatings for blood-contacting medical devices. According to the categorization in ISO 10993-1[8], these polymers could ultimately be used in *External Communicating Devices* and *Implant Devices* with various duration of contact as indicated in the quoted text below:

4.2 Categorization by nature of body contact

……

4.2.3 External communicating devices

These include medical devices in contact with the following application sites:

……

c) circulating blood: devices that contact circulating blood; examples include intravascular catheters, temporary pacemaker electrodes, oxygenators, extracorporeal oxygenator tubing and accessories, dialyzers, dialysis tubing and accessories, hemoadsorbents, and immunoadsorbents.

4.2.4 Implant devices

These include medical devices in contact with the following application sites:

……

b) blood: devices principally contacting blood; examples include pacemaker electrodes, artificial arteriovenous fistulae, heart valves, vascular grafts, internal drug-delivery catheters, and ventricular assist devices.

In Chapter 5, the potential acute toxic adverse effects of the Tecophilic-SeH coatings within organs and tissues that are remote from the site of contact were tested in collaboration with Yang Wang in Dr. Roy-Chaudhury's internal medicine research lab in the University of Cincinnati according to ISO standard 10993-11[9]. While this preliminary result suggested good biocompatibility of this new NO-generating polymer, more tests need to be done to cover the full spectrum of chemical, toxicological and biological characterization and evaluation of this novel material. Indeed, tables 6.2 and 6.3 provide summaries of tests recommended in ISO 10993-1[8]. In fact, selected tests from this list must be preformed for both Tecophilic-SeH and Tecoflex-SO_3 if they are to be used in blood-contacting devices in the future.

Table 6.2. Summary of initial tests relevant to non-degradable blood-contacting materials recommended in ISO 10993-1[8].

Test	Description	ISO
Cytotoxicity	With the use of cell culture techniques, these tests determine the lysis of cells (cell death), the inhibition of cell growth, and other effects on cells caused by medical devices, materials, and/or their extracts.	10993-5[10]
Sensitization	These tests estimate, using an appropriate model, the potential of medical devices, materials, and/or their extracts for contact sensitization. These tests are appropriate because exposure or contact to even minute amounts of potential leachables can result in allergic or sensitization reactions.	10993-10[11]
Intracutaneous Reactivity	These tests assess the localized reaction of tissue to medical device extracts. These tests are applicable where determination of irritation by dermal or mucosal tests is inappropriate (e.g., medical devices having access to the blood path). These tests may also be useful where extractables are hydrophobic.	10993-10[11]
Systemic Toxicity (Acute Toxicity)	These tests estimate the potential harmful effects of either single or multiple exposures, during a period of less than 24 h, to medical devices, materials, and/or their extracts in an animal model. These tests are appropriate where contact allows potential absorption of toxic leachables and degradation products.	10993-11[9]
Subacute and Subchronic Toxicity	These tests determine the effects of either single or multiple exposures or contact to medical devices, materials, and/or their extracts for a period of not less than 24 h but not greater than 10 % of the total life span of the test animal (e.g., up to 90 days in rats).	10993-11[9]
Genotoxicity	These tests use mammalian or non-mammalian cell culture or other techniques to determine gene mutations, changes in chromosome structure and number, and other DNA or gene toxicities caused by medical devices, materials, and/or their extracts.	10993-3[12]
Implantation	These tests assess the local pathological effects on living tissue, at both the gross level and microscopic level, of a sample of a material or final product that is surgically implanted or placed in an implant site or in a tissue appropriate to the intended application (e.g., special dental usage tests). These tests should be appropriate for the route and duration of contact.	10993-6[13]
Hemocompatibility	These tests evaluate, using an appropriate model or system, the effects of blood-contacting medical devices or materials on blood or blood components. Specific hemocompatibility tests may also be designed to simulate the geometry, contact conditions, and flow dynamics of the device or material during clinical applications. Hemolysis tests determine the degree of red blood cell lysis and the release of hemoglobin caused by medical devices, materials, and/or their extracts *in vitro*.	10993-4[14]

Table 6.3. Summary of supplementary tests relevant to non-degradable blood-contacting materials recommended in ISO 10993-1[8].

Test	Description	ISO
Chronic Toxicity	These tests determine the effects of either single or multiple exposures to medical devices, materials, and/or their extracts during at least 10 % of the life span of the test animal (e.g., more than 90 days in rats). These tests should be appropriate for the route and duration of exposure or contact.	10993-11[9]
Carcinogenicity	These tests determine the tumorigenic potential of medical devices, materials, and/or their extracts from either single or multiple exposures or contacts during the major portion of the life span of the test animal. These tests may be designed in order to examine both chronic toxicity and tumorigenicity in a single experimental study. Carcinogenicity tests should be conducted only if there is suggestive data from other sources. These tests should be appropriate for the route and duration of exposure or contact.	10993-3[12]
Reproduction and Developmental Toxicity	These tests evaluate the potential effects of medical devices, materials, and/or their extracts on reproductive function, embryonic development (teratogenicity), and prenatal and early postnatal development. Reproductive/developmental toxicity tests or bioassays should only be conducted when the device has potential impact on the reproductive potential of the subject. The application site of the device should be considered.	10993-3[12]

6.3. References

1. Vaughn, M.W.; Kuo, L.; Liao, J.C. 'Estimation of nitric oxide production and reaction rates in tissue by use of a mathematical model.' *Am. J. Physiol.* **1998,** 274, H2163-H2176.

2. http://www.ecatalog.ethicon.com/sutures.absorbable/view/vicryl-rapide-suture

3. http://www.sjmprofessional.com/Products/US/Hemostasis-Management/Angio-Seal-Evolution.aspx

4. Zhou, Z.; Meyerhoff, M.E. 'Polymethacrylate-based nitric oxide donors with pendant *N*-diazeniumdiolated alkyldiamine moieties: Synthesis, characterization, and preparation of nitric oxide releasing polymeric coatings.' *Biomacromolecules* **2005**, 6, 780-789.

5. Purac Biomateirals 'PURASORB Data Sheet 04 – Physical Properties'.

6. Jun, H.W.; Taite, L.J.; West, J.L. 'Nitric oxide-producing polyurethanes.' *Biomacromolecules* **2005**, 838-844.

7. Taite, L.J.; Jun H.W.; Yang, P.; West J.L. 'Nitric oxide-releasing polyurethane-PEG copolymer containing the YIGSR peptide promotes endothelialization with decreased platelet adhesion.' *J. Biomed. Mater. Res. B* **2007**, 108-116.

8. 'Biological evaluation of medical devices – Part 1: Evaluation and testing.' ANSI/AAMI/ISO 10993-1:**2003**.

9. 'Biological evaluation of medical devices – Part 11: Tests for systemic toxicity.' ANSI/AAMI/ISO 10993-11:**2006**.

10. 'Biological evaluation of medical devices – Part 5: Tests for cytotoxicity, *in vitro* methods.' ANSI/AAMI/ISO 10993-5:**1999**.

11. 'Biological evaluation of medical devices – Part 10: Tests for irritation and delayed-type hypersensitivity.' ANSI/AAMI/ISO 10993-10:**2002**.

12. 'Biological evaluation of medical devices – Part 3: Tests for genotoxicity, carcinogenicity and reproductive toxicity.' ANSI/AAMI/ISO 10993-3:**2003**.

13. 'Biological evaluation of medical devices – Part 6: Tests for local effects after implantation.' ANSI/AAMI/ISO 10993-6:**2007**.

14. 'Biological evaluation of medical devices – Part 4: Selection of tests for interaction with blood.' ANSI/AAMI/ISO 10993-4:**2002** & A1:**2006**.